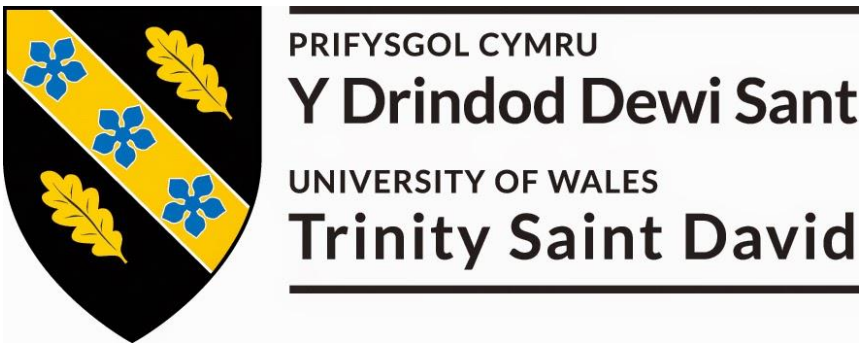

AN INVESTIGATION TO DETERMINE THE COMPLEXITY AND FEASIBILITY OF COMBUSTION & NOx MODELLING IN MODERN GTDI ENGINES.

University of Wales Trinity Saint David -

School of Engineering

MSc - Motorsport Engineering

Major Project - Dissertation

Author - Danny J. Richardson

Supervisor - Malcolm McDonald

Acknowledgments.

I would like to say thank you once again to my mother and father, Tina, and John Richardson, for all the support they have given me throughout my time at university and especially through this difficult MSc year.

I would like to say a massive thank you to my project supervisor, Malcolm McDonald, for aiding me with academic support and helping to obtain key data and methodologies that was used throughout this project and various other investigations I've conducted across my time.

Declaration of authenticity.

I, Danny J. Richardson, declare this dissertation is the result of my original research. It has been composed by the author and has not been previously submitted for examination which has led to the award of a degree.

Signed: Danny John Richardson *Date:* 03/09/2021

Abstract.

This paper has been written to demonstrate the common difficulties regarding achievement of respectable results when trying to predict NOx production in a GTDI engine using two zone combustion modelling and a variation of what is typically referred to as the “Zeldovich” model. The investigation assessed 3 collective data sets from two Ford Motor Company EcoBoost engines, their 4-cyl 1.5L and their 3-cyl 1L. With the data including various load conditions at induvial engine speed sites that correspond tabulated data reference sites that Ford produce to generate a map of calibration and combustion characteristics. The process began with the 1.5L because it was known to the be the ‘hardest’ to model because there was a lack of very specific data that is key to “accurately” predict production of NOx during combustion using the methodology discussed. That data included; EGR% in-cylinder, Lambda UEGO which is dynamometer measured and not PCM, and various other useful data like EOI, stated valve overlap, and CAC temperatures etc. Despite these issues the results for the 1.5L were shown to be able to predict production with some degree of accuracy, regarding trend and not value. The models of the 1L were then developed because the data that was seemingly missing of the 1.5L was available for the 1L and the effects on results were profound. The model immediately showed excellent modelling of trend, but also the values themselves considering the rate or decomposition wasn’t modelled, only the forward rate production.

Given the clear success of the 1L model the third data set was measured cylinder pressure over 500 cycles for each cylinder and this enable a very relevant study about how sensitive the techniques used are, especially when the conditions were apparently very similar through the testing, the prediction results vary a considerable amount. It did happen to over-predict production when averaged across the total, but it is within an acceptable margin of error considering only forward production is considered and given the multitude of other assumptions that need to be made. With this obvious effect on accuracy of results using the more accurately defined AFR, because it was measured in-cylinder on the 1L engine, it was thought best that a 1D simulation developed in Ricardo WAVE would be the most useful and logical next step to enhance influencing data of the 1.5L engine.

There were limitations encountered regarding ability to measure important components of the 1.5L engine because neither the full intake, nor exhaust system was available. Along with the constraints of “stripping” down engine parts, i.e. the turbo charger, to measure as accurately as possible to then influence the model exclusively again because the turbochargers pressure ratio dependence for mass air flow is extremely sensitive. As the model was developed it became clear that despite being able to show some correlation at lower engine speeds and controlling the model across all other aspects to be as similar as possible to Ford’s measured data, there is still issues in the model that result in incorrect MAF. This error was causing poor correlation of results and ultimately voided results of in-cylinder predictions trapped of AFR and internal EGR%. Ultimately the fundamental issue is more measurements of components are required, specifically the waste gate area because this is arguably the most influential element for controlling the turbocharger and therefore results.

Contents –

1. Introduction. 1

2. Literature Review. 4

2.1. History of the internal combustion engine – Four-Stroke. 4

2.2. Industry application and progression of the Atkinson cycle. 5

2.3. Industry application and progression of the Miller cycle. 7

2.4. Two-zone combustion & Emissions modelling. 9

3. Two-Zone Combustion Modelling Mathematics. 13

3.1. Logarithmic P-V graphs for polytropic indexes. 13

3.2. Mass Fraction Burnt Modelling. 15

3.3. Individual Zone's Temperature Modelling. 22

3.4. Dissociation Modelling. 27

4. 1.5L EcoBoost NOx Modelling Results & Discussion. 36

4.1. Mass Fraction Burnt profiles. 36

4.2. Unburned Temperatures. 41

4.3. Burned Temperatures. 50

4.4. NOx Modelling. 54

5. 1L EcoBoost NOx Modelling Results & Discussion. 68

5.1. Mass Fraction Burnt profiles. 68

5.2. Unburned Temperatures. 73

5.3. Burned Temperatures. 75

5.4. NOx Modelling. 76

6. 1L EcoBoost Cyclic NOx Modelling Results & Discussion. 80

6.1. Mass Fraction Burnt profiles. 81

6.2. Unburned Temperatures. 83

6.3. Burned Temperatures. 85

6.4. NOx Modelling. 87

7. Ricardo WAVE Modelling – 1.5L EcoBoost. 91

7.1. Known Areas of Concern and Errors. 92

7.2. Model Generation & Constants. 100

7.3. Final Model Results & Discussion. 104

8. Conclusion. 111
9. Further Work. 113
10. References. 114
11. Appendices. 119
Appendix A. 119
Appendix B. 120
Appendix C. 121

Table of Figures –

Figure 1 Average tailpipe emissions of passenger vehicles of the EU in g/km (EEA, 2020). . 2
Figure 2 Capability and accuracy of simulation software GT-SUITE (Gamma Technologies LLC, 2021). 3
Figure 3 Diagram of Nikolaus A. Otto's first four-stroke ICE (Sack, 2019). 4
Figure 4 Idealised Otto cycle where the combustion process happens during constant volume (Isochoric) (Left) (Proctor, 2003); Real cycle pressure data highlighting the issue with assuming the process abides the constant volume process (Right). 5
Figure 5 Comparison of the thermodynamic cycles, Otto (1-2-3-4O) and the Atkinson (1-2-3-4A). Where A is representing the pressure – volume [PV] diagram and B is representing the temperature – entropy diagram [TS] (Hou, 2007)**.** 6
Figure 6 Comparison between the PV diagram of the typical Otto cycle (a) and the over-expansion Miller cycle (b**)** (Mikalsen, et al., 2009)**.** 7
Figure 7 Visualisation of valve lift profiles when EIVC is utilised on an engine (Chen, et al., 2019). 8
Figure 8 Predicted combustion in-cylinder temperatures using both single-zone and two-zone modelling techniques, identifying the potential difference, and reiterating what could be cause for concern given the models temperature dependency (Xiang, et al., 2018). 9
Figure 9 Log PV diagram showing the values for the polytropic values of full load condition for the 1L EcoBoost engine. 14
Figure 10 ΔP within all four cylinders of the 1.5L EcoBoost @ 1000RPM Full Load. 16
Figure 11 Mass Fraction Burn (MFB%) through combustion for the 1500cc EcoBoost GTDI engine at 1000RPM and 150% relative load (Full Load). 17
Figure 12 MFB profile comparison based on the two methods used. 17
Figure 13 Comparison between MFB calculation methods and their accuracy against the stated points of 10, 50, and 90% burnt from Ford, including the bounds from standard deviation. 18
Figure 14 Burnt and Unburned percentages through combustion for the 1500cc EcoBoost GTDI engine at 1000RPM FL. 18
Figure 15 Burnt and Unburnt zone volumes at 1000RPM, Full load. 1.5L EcoBoost. 21
Figure 16 Specific heat ratio for an unburned stoichiometric mixture as a function of temperature (Klein & Eriksson, 2004). 22
Figure 17 Specific heat capacity at constant pressure for various species using the coefficients from the JANAF tables (Heywood, 2018). 24
Figure 18 Recreation of the calculated specific heat of species using MATLAB (Average accuracy, 100.3%). 24
Figure 19 Unburned temperature in cylinder at 1000RPM, Full Load. 1.5L EcoBoost. 25
Figure 20 Burnt and unburned temperature in cylinder at 1000RPM, Full Load. 1.5L EcoBoost. 26

Figure 21 Original JANAF Table results of equilibrium constants for $CO2$ through temperature, with the model's curve fitted results and accuracy of fit through temperature. Including polynomial exponents to the 9th degree. 28
Figure 22 Original JANAF Table results of equilibrium constants for $H2O$ through temperature, with the model's curve fitted results and accuracy of fit through temperature. Including polynomial exponents to the 9th degree. 29
Figure 23 'n' values of each species through crank angle at 1000RPM, FL. 1.5L EcoBoost. 31
Figure 24 Error between the guessed ratio of oxygen to total moles, Vs the calculated solve through crank angle at 1000RPM, FL. 1.5L EcoBoost. 31
Figure 25 Comparison of the reference [top] Vs modelled [bottom] values of $N5$ at various pressures through temperature at $\varphi = 1$. 32
Figure 26 NO formation and disintegration in a thermal reactor. p = 60 Bar, λ 1. (Merker, et al., 2006) 33
Figure 27 Calculated combustion period and average temperature during, for all full load cases. 1.5L EcoBoost. 33
Figure 28 Estimated NOx PPM per degree at 1000RPM, Full load. 1.5L EcoBoost. 35
Figure 29 MFB points through crank angle comparison between modelled and those stated by Ford. 1500 RPM, 20% Load – Best Case. 37
Figure 30 MFB points through crank angle comparison between modelled and those stated by Ford. 2000 RPM, 20% Load – Worst Case. 37
Figure 31 MFB points through crank angle comparison between modelled and those stated by Ford. 2500 RPM, 70% Load – Best Case. 38
Figure 32 MFB points through crank angle comparison between modelled and those stated by Ford. 1000 RPM, 70% Load – Worst Case. 38
Figure 33 MFB points through crank angle comparison between modelled and those stated by Ford. 1000 RPM, Full Load – Best Case. 39
Figure 34 MFB points through crank angle comparison between modelled and those stated by Ford. 4500 RPM, Full Load – Worst Case. 39
Figure 35 Effect of Air-Fuel ratio on typical maximum temperatures in the burned and unburned zone gases. (Blair, 1998) 42
Figure 36 Net IMEP Vs Spark for different IAT's - DI E20 @ 2000RPM & nominal boost. (Kasseris, 2011) 43
Figure 37 Maximum unburned temperatures at borderline knock Vs Engine speed (Kasseris, 2011). 43
Figure 38 Maximum unburned temperatures at knock Vs MAP for different fuels and fuelling methods. (Kasseris, 2011) 44
Figure 39 Maximum unburned temperatures at knock Vs IAT @ 2000 RPM, nominal boost condition. (Kasseris, 2011) 44
Figure 40 Unburnt gas temperatures predicted at Low load for all speeds. 1.5L EcoBoost. 45
Figure 41 Degrees of valve overlap at the lower load situations (20 – 50%) for the engine speeds typical of the drive cycle. 46

Figure 42 Unburnt gas temperatures predicted at Mid load for all speeds. 1.5L EcoBoost .. 46
Figure 43 Degrees of valve overlap for the mid load situations (60 - 100%) for all engine speeds typical of the drive cycle. 47
Figure 44 Boost pressure comparison for all speeds typical to the drive cycle for the mid load cases (70%). 47
Figure 45 Unburnt gas temperatures predicted at Full load for all speeds. 1.5L EcoBoost. . 48
Figure 46 Measured Oxygen content in exhaust gases [g/h]. 1.5L EcoBoost. 49
Figure 47 Measured Carbon Monoxide content in exhaust gases [g/h]. 1.5L EcoBoost. 49
Figure 48 Measured Nitric Oxides in exhaust gases [PPM]. 1.5L EcoBoost. 50
Figure 49 Measured cylinder pressure and predicted temperature at 6000 RPM, Full Load. 1.5L EcoBoost 50
Figure 50 Predicted burned zone temperatures for the low load cases, 1.5L EcoBoost. 51
Figure 51 Predicted Burned zone temperatures for the mid load cases, 1.5L EcoBoost. 52
Figure 52 Crank angle position of maximum HRR for load cases of 20 - 100% at the lower engine speeds. 1.5L EcoBoost – Measured. 53
Figure 53 Predicted Burned zone temperatures for the high load cases, 1.5L EcoBoost. 53
Figure 54 Results of NOx PPM predicted using alternate methods for φ for the load cases across 1000 RPM for the 1.5L EcoBoost. 55
Figure 55 Sensitivity study results of change in φ and EGR at 1000RPM Full load. 55
Figure 56 Contour map of results of NOx PPM predicted through the sensitivity study at 1000 RPM Full load for EGR % and φ. 56
Figure 57 Dependence of NOx modelling on temperature through combustion. 56
Figure 58 Percentage increase from previous result of NOx PPM calculated for temperature dependence study. 57
Figure 59 EGR percentage being recycled into each case taken from equivalent position of the 1L EcoBoost map. The cases are for each engine speed as load increase, so there's 3 for all up to 3000RPM after which there is only full load cases. 57
Figure 60 Predicted NOx PPM for the low load cases of the 1.5L EcoBoost (right hand axis) Vs the measured results from Ford (left hand axis). 60
Figure 61 Predicted NOx PPM for the mid load cases of the 1.5L EcoBoost Vs the measured results from Ford. 61
Figure 62 Valve overlap durations for the 1.5L EcoBoost engine. 62
Figure 63 Valve overlap durations for the 1L EcoBoost engine. 62
Figure 64 Predicted NOx PPM for the full load cases of the 1.5L EcoBoost Vs the measured results from Ford. 63
Figure 65 Difference between calculated fuel equivalency using either PCM, or Dyno Lambda, at low load 64
Figure 66 Difference between calculated fuel equivalency using either PCM, or Dyno Lambda, at mid load. 64
Figure 67 Difference between calculated fuel equivalency using either PCM, or Dyno Lambda, at full load. 65

Figure 68 Secondary method of fuel equivalency results for NOx PPM at low load. 65
Figure 69 Secondary method of fuel equivalency results for NOx PPM at mid load. 66
Figure 70 Secondary method of fuel equivalency results for NOx PPM at full load. 66
Figure 71 MFB profile points comparison for the lower load cases at various engine speeds on the 1L EcoBoost. 69
Figure 72 MFB points comparison at 4000 RPM, Low load. 1L EcoBoost. 70
Figure 73 MFB profile points comparison for various engine speeds at high load for the 1L EcoBoost. 71
Figure 74 MFB points comparison at 6000 RPM, Full load. 1L EcoBoost. 72
Figure 75 Combustion Durations [0 - 90%] using Ford's defined durations. 72
Figure 76 Unburned temperatures for the lower load cases of the 1L EcoBoost. 74
Figure 77 Unburned temperatures for the high load cases of the 1L EcoBoost. 74
Figure 78 Burnt temperatures for the lower load cases of the 1L EcoBoost. 75
Figure 79 Burnt temperatures for the higher load cases of the 1L EcoBoost. 76
Figure 80 NOx production predicted Vs stated measured for the lower load cases of the 1L EcoBoost. 77
Figure 81 NOx production predicted Vs stated measured for the higher load cases of the 1L EcoBoost. 77
Figure 82 Measured unburnt hydrocarbons in terms of PPM for the 1L EcoBoost. 78
Figure 83 Accuracy of the individual burn locations for 10, 50 and 90% modelled Vs stated in cylinder 1. 81
Figure 84 Accuracy of the individual burn locations for 10, 50 and 90% modelled Vs stated in cylinder 2. 82
Figure 85 Accuracy of the individual burn locations for 10, 50 and 90% modelled Vs stated in cylinder 3. 82
Figure 86 Peak cylinder pressures for cylinder 1 with the moving average (50) demonstrating the sine wave effect of timing changes. 83
Figure 87 Unburned temperatures for cylinder 1 – 500 Cycles. 83
Figure 88 Unburned temperatures in cylinder 2 – 500 Cycles. 84
Figure 89 Unburned temperatures in cylinder 3 – 500 Cycles. 84
Figure 90 Burned zone temperatures in cylinder 1 - 500 cycles. 85
Figure 91 Burned zone temperatures in cylinder 2 - 500 cycles. 86
Figure 92 Burned zone temperatures in cylinder 3 - 500 cycles. 86
Figure 93 Predicted NOx PPM for cylinder 1 of the 500 cycles study. 87
Figure 94 Predicted NOx PPM for cylinder 2 of the 500 cycles study. 88
Figure 95 Predicted NOx PPM for cylinder 3 of the 500 cycles study. 88
Figure 96 NOx PPM results throughout each cycle using the sum of the individual cycles, including the average across and the stated Ford measured NOx PPM. 89
Figure 97 Ricardo WAVE model generated to represent the Ford 1500cc EcoBoost GTDI Engine. 91

Figure 98 Compressor map generated by Ricardo WAVE using the measured data from BorgWarner. 98
Figure 99 Turbine map generated in Ricardo WAVE using the measured data from BorgWarner. 99
Figure 100 Smart Controller system layout for the wastegate boost controller. 100
Figure 101 Intake manifold modelled in Ricardo WaveBuild 3D containing the CAC and as accurate as possible volumes either side. 101
Figure 102 Valve Lift profiles calculated and used in the Ricardo model. 102
Figure 103 Port flow coefficients measured by (Englebrecht & Chapman, 2019). 102
Figure 104 MAF comparison from Ford and the final Ricardo model. 105
Figure 105 Comparison of BMEP from Ford and the final Ricardo model. 105
Figure 106 Comparison of FMEP from Ford and the final Ricardo model. 105
Figure 107 Comparison of PMEP from Ford and the final Ricardo model. 106
Figure 108 Brake specific fuel consumption comparison of Ford's measured and the Ricardo models predicition. 106
Figure 109 Evidence that the Ricardo model is correctly controlling the degrees of valve overlap. 106
Figure 110 Pressure ratio comparison for the compressor between Ford's measured pressures either side of the compressor and Ricardo's calculated pressure ratio. 107
Figure 111 Comparison of the modelled and measured pressures at both the inlet and exit of the compressor. 107
Figure 112 Comparison of the modelled and measured temperatures at both the inlet and exit of the compressor. 107
Figure 113 Comparison of the modelled and measured pressures at both the inlet and exit of the turbine. 108
Figure 114 Comparison of the modelled and measured temperatures at both the inlet and exit of the turbine. 108
Figure 115 Exhaust back pressure comparison, assuming the location is somewhere post-catalyst. 108
Figure 116 Manifold absolute pressure comparison. 109
Figure 117 Inlet Manifold temperature comparison. [Highlighting the fact that the wall temperature multiplier and initial temperature can't be changed with speed]. 109
Figure 118 Apparent trapped exhaust gas percentage through engine speed as predicted by Ricardo WAVE. 109
Figure 119 Predicted MFB profile comparison from Ricardo WAVE using the Wiebe function and the validated MFB modelled in MATLAB. 1000RPM and the best result of the model. 110
Figure 120 Predicted MFB profile comparison from Ricardo WAVE using the Wiebe function and the validated MFB modelled in MATLAB. 4000RPM and the worst result of the model. 110
Figure 121 Maximum cylinder pressure comparison between the Ricardo model and Ford's measured data. 110

1. Introduction.

Throughout history the internal combustion engine has be a fundamental instrument of revolutionary progression for various industries, from construction to military, to aviation and energy production. It's versatility and unique construction has given mobility and access to countless numbers of individuals across generations.

And as history has shown us, change is inevitable, and the change of combustion is of the utmost importance given current climate conditions. With the number of vehicles on the roads of the world being some 1.32 billion (Chesterton, 2018), with around 300 million of those vehicles being in Europe alone (ACEA, 2018). Considering there was an estimated production 3.3 billion tonnes of CO_2 across Europe in 2019 (Tiseo, 2019), and knowing that the transport industry accounted for 1.1 billion tonnes of those greenhouse emissions (EEA, 2020), meaning our industry alone accounted for 33.42%, more than all other sectors bar energy supply (EEA, 2019). After recent reports and projections, current legislation suggests that new registration of petrol (58.9% of market) and diesel (30.5% of market) (ACEA, 2019) vehicles will no longer be distinct options by the year 2030, at least in the UK, in a bid to rapidly decrease the greenhouse gases (GHG) (GOV.UK, 2020).

Although this statement suggests that the internal combustion engine is reaching its end, the key point of this net-zero statement is that it's new petrol and diesel, it doesn't mitigate the use of new fuels or fuel blends that will still be fundamentally reliant on an ICE of sorts.

"Because it is not combustion that is the problem, but the fuel" (Müller, 2021).

Using these methods of enhancement, the carbon dioxide emission output of passenger vehicles had been on a steady decline since at least the year 2000, but we've now began to plateau, and if anything, increase average output.

With this unfortunate turn in emission output and the clear pressing of new regulations coming to the industry, the ability to optimise engine design and operation using simulation tools is now the most all-round effective manner of design. Simulation of combustion can save money for the manufacturer, save a significant period during research and development, but most importantly, reduce their net footprint by not requiring substantial physical testing.

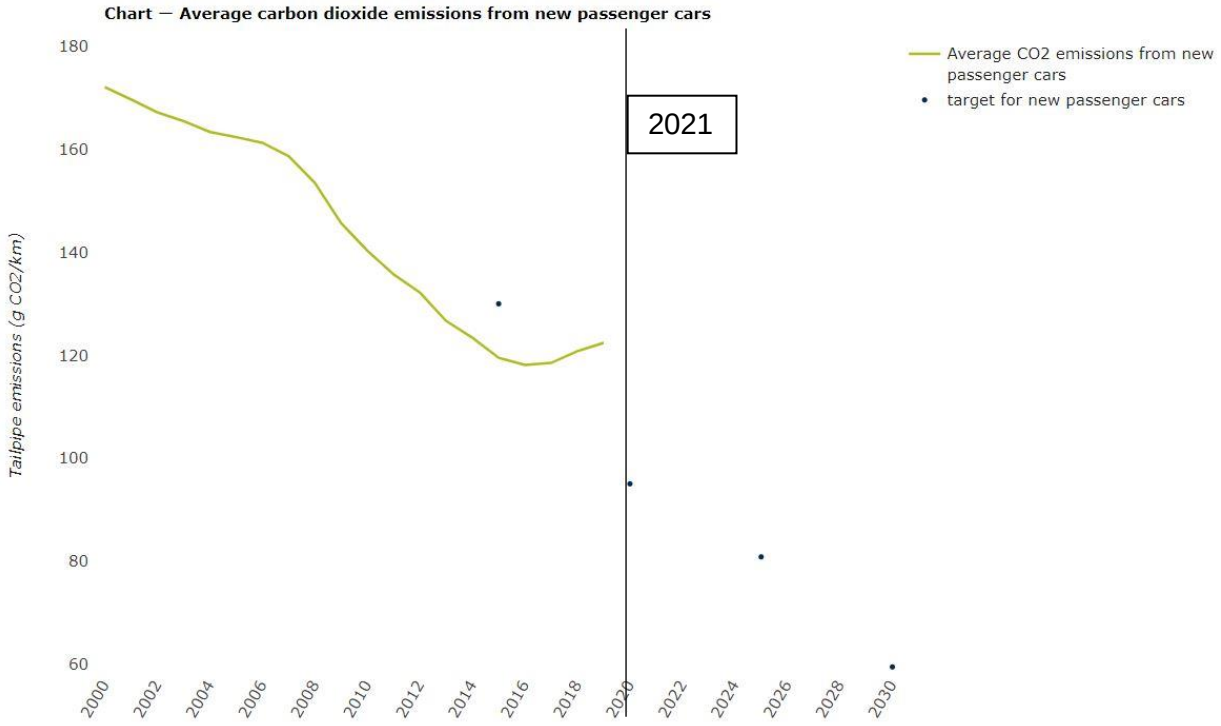

Figure 1 Average tailpipe emissions of passenger vehicles of the EU in g/km (EEA, 2020).

Using measured in-cylinder pressure data of an engine, along with the accompanying values for air and fuel mass, and EGR%, we can reveal a lot about the characteristics of combustion for the engine in question. This understanding of an engine can be used to inform that of another configuration upon validation, hence why industry giants like MAHLE powertrain have turned to using various simulation tools for up to 70% of their development process, where there is no physical testing required until the end of the project. This use of thermodynamic principles, laws of physics and computational fluid dynamics is paving the way for a new generation of rapid development of ICE's that utilise; new technologies, materials, designs, and fuels, with the hope that we can reduce emissions effectively until we have a new alternative, sustainable and cost-effective propulsion method.

Objectives –

- From first principles develop a correctly correlated **two-zone combustion model** of the Ford Motor Company, 1500cc & 1000cc GTDI EcoBoost engines across varied load conditions and engine speeds within MathWorks MATLAB.
- Upon validation of the model's mass fraction burnt (**MFB**) for these varied conditions, begin the development of a valid emissions model based on simplified **chemical kinetics**, again in MATLAB.
- Asses the level of correlation between the modelled results and measured by Ford and highlight reasonings for errors and perhaps no correspondence.
- Development of a model within **Ricardo WAVE** using measured values from the **1.5 GTDI** engine, and measured data from both Ford Motor Company and BorgWarner with the intention of identifying potential differences between the measured data and what should be used to model.
- Explain the reasoning behind why the expected areas of concern are of such importance and identify the extent of the issue when working with **limited data**.
- Assessment of the areas of concern for the model and produce an **analytical guide** for recreating a similar model for a forced induction engine within WAVE.

Although combustion simulations typical struggle to predict the exact erratic profiles of various characteristics, due to the nature of combustion, as seen in the figure below the definite trend can be modelled with a high level of accuracy. Hence the purpose of this research is to show both the importance, efficiency, and sensitivity of mathematical simulation within the industry of today. And to demonstrate that the evolution of the operating cycles, fuelling techniques, and fuels themselves, used within internal combustion engines, is still a viable option for reducing our net GHG footprint.

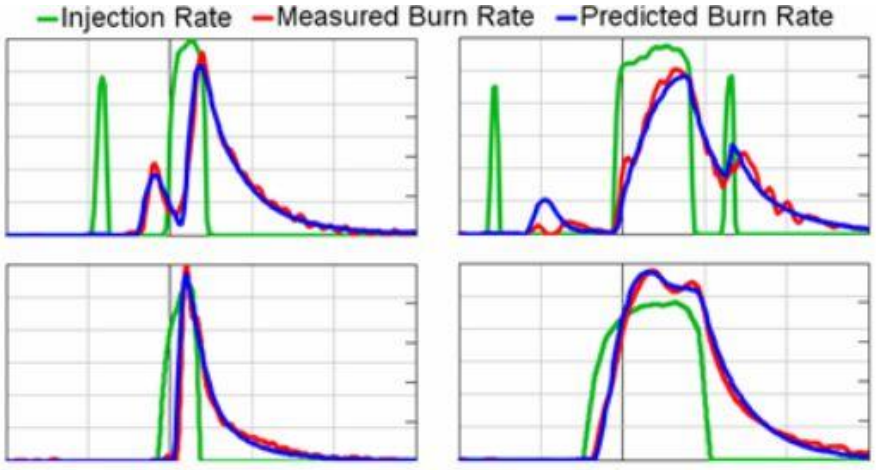

Figure 2 Capability and accuracy of simulation software GT-SUITE (Gamma Technologies LLC, 2021).

2. Literature Review.

2.1. History of the internal combustion engine – Four-Stroke.

The internal combustion engine owes itself to the extensive use of the steam engine during the 18th century because this allowed for a new stage of evolution for the iconic piston-in-cylinder system that is said to be traced back to 150BC and is still being utilised today. The first use of a steam “engine” in industrial application is accredited to one Jerónimo de Ayanz, who amongst many other things was regarded as a brilliant inventor who helped change the mining industry with his ideas of using the engine to drive a pump and remove excess water from the mines (Sandman, 2003). Despite its incredible range of application, issues pertaining to the steam engine were that the consumption of fuel was to happen externally, meaning even more time and surface contact where losses of heat energy that was being extracted could occur (Cromer & Proctor, 1999).

Because of this unfortunate problem, it was clear that to achieve higher efficiencies the two systems would have to become one, such that the combustion and expansion were to happen in the same cylinder. This concept was then theorised by Alphonse Beau de Rochas, in 1862, and this theory consisted of using of four consecutive cycles within a single cylinder to allow for the harmonious extraction of energy from a fuel. The four-stroke internal combustion engine was born.

However, because of financial limitations, it wasn’t developed past the point of being of a theorem by Alphonse. It took the intrigue of a German engineer; Nikolaus A. Otto to take the idea from paper to product and craft the first working engine in 1876. Upon its production it “rapidly” began to replace all other types of combustion engines, sparking the new revolution of propulsion and energy generation (Cromer & Proctor, 1999).

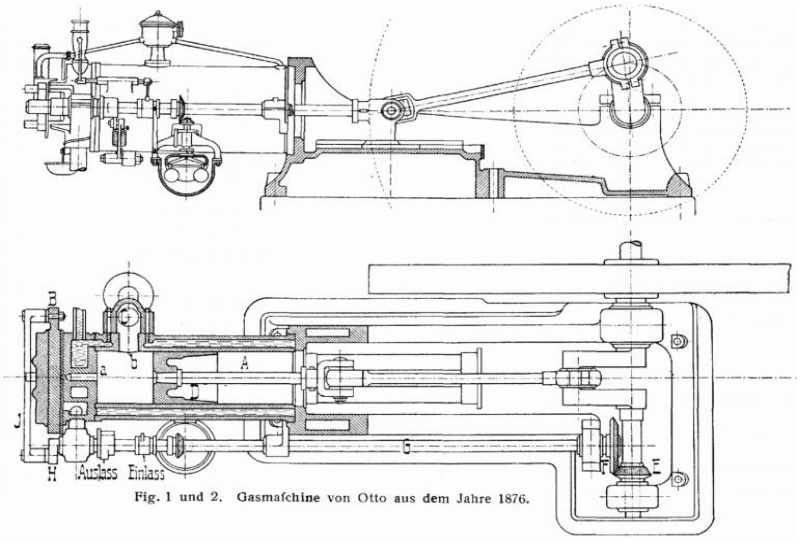

Figure 3 Diagram of Nikolaus A. Otto's first four-stroke ICE (Sack, 2019).

The standard operation of an internal combustion engine is renowned as the ‘Otto’ cycle. This cycle consists of four separate stages; intake, compression, combustion, and exhaust all of which are idealised across 180° of crankshaft rotation for each. The power stroke occurs once for every two revolutions of the crank, but most importantly the compression to expansion ratio is the same.

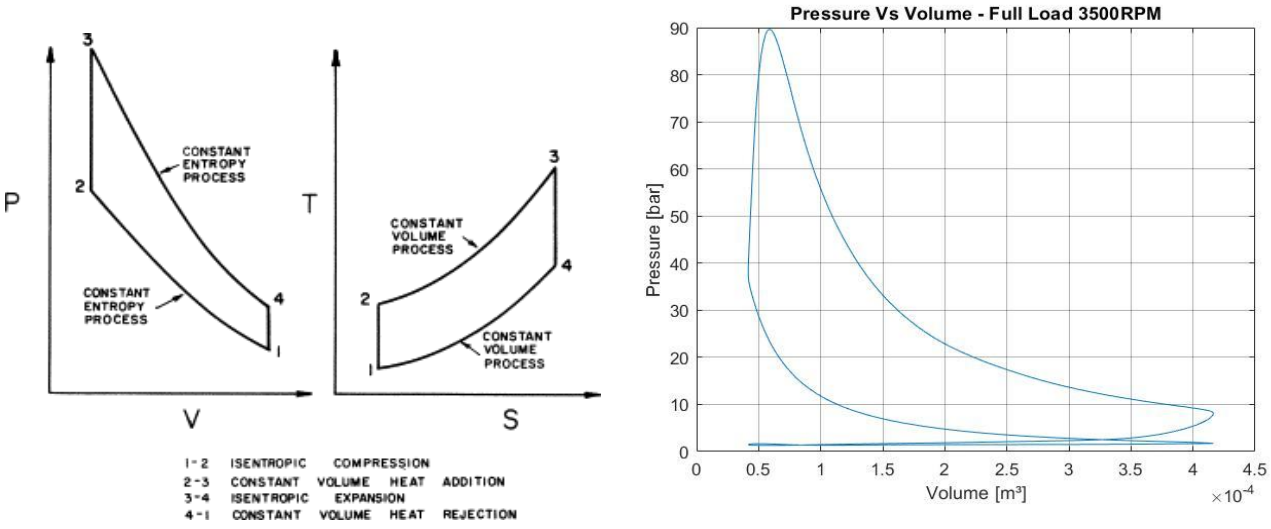

Figure 4 Idealised Otto cycle where the combustion process happens during constant volume (Isochoric) (Left) (Proctor, 2003); Real cycle pressure data highlighting the issue with assuming the process abides the constant volume process (Right).

2.2. Industry application and progression of the Atkinson cycle.

The Atkinson cycle is named unsurprisingly after its creator, James Atkinson (1864 – 1914). He was a British inventor that patented his design for an engine that operated over four-strokes, however the geometry of the engine allowed for longer time during the expansion cycle, increasing the time that work from the combusted fuel could be extracted and naturally increased the efficiency of the engine (Heywood, 1988). Advantages of Atkinson cycle were realised straight away, these can be categorised as;

- Higher thermal efficiency in comparison to the typical Otto cycle.
- Increased fuel efficiency.
- Potential for reduced pumping losses during operation.
- Ideal cycle to be used in harmony with an electric motor in hybrid applications.
- Potential for a reduction in emissions, without the addition of aftercare.

(Hou, 2007), (Li, et al., 2021), (Zhao, 2017), (Gahruei, et al., 2013).

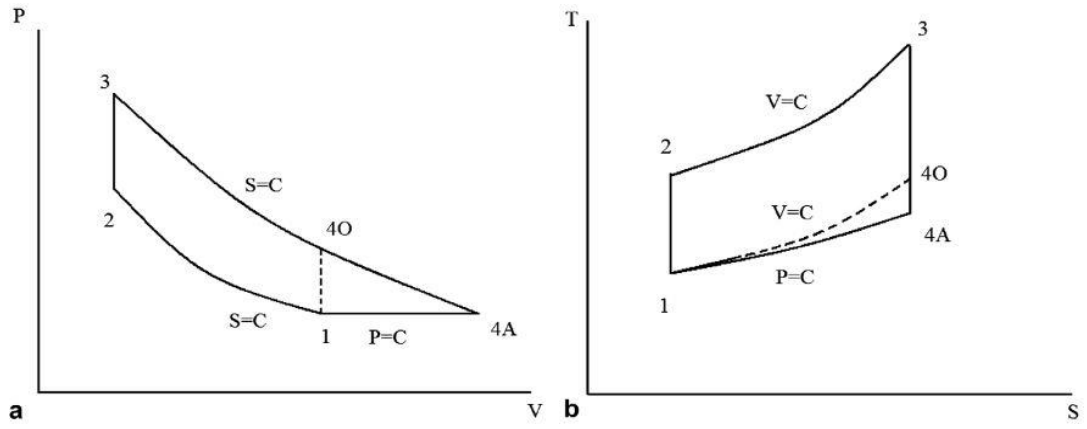

Figure 5 Comparison of the thermodynamic cycles, Otto (1-2-3-4O) and the Atkinson (1-2-3-4A). Where A is representing the pressure – volume [PV] diagram and B is representing the temperature – entropy diagram [TS] (Hou, 2007).

When James Atkinson first developed the cycle, his approach to cycle adjustment was to change the engines working geometry, meaning the compression ratio remained the same but the configuration allowed for further travel of the piston during the expansion cycle. This rather complicated system made the engine large and increased the mechanical losses through operation, hence why it was again adapted through the generations in such a way that now the valve timing is used to create the same effect. Late closing of the intake valve (LIVC) means that as the piston travels up the cylinder, there is less resistance (pumping losses) but does in turn reduce the compression ratio in doing so. This reduction is what then allows for the increase of expansion ratio (Li, et al., 2021).

$$OER = \frac{ER}{CR} = \frac{Vol_{\text{piston BDC after expansion}}}{\text{Vol}_{\text{piston BDC after intake}}}$$

(Yang, et al., 2020)

This adaptation of LIVC is used in industry engines today by manufactures such as; Ford Motor Company, Toyota, and Lexus. The most prominent of which is Toyota. They adopt the Atkinson cycle in many of their hybrid and some non-hybrid vehicles and in doing demonstrate effective use for a reduction in emissions and increased fuel efficiency (Clifford, 2015).

2.3. Industry application and progression of the Miller cycle.

The miller cycle is another adaptation of the traditional Otto cycle that Ralph Miller, an American engineer, filed a patent for on December 24th, 1957 (No. US2817322A). His approach was again to target an increase in thermal efficiency, achieved again with the use on an over-expansion type engine. The key difference between the Atkinson and Miller cycle is the idea for achieving this, being Atkinson initially used engine geometry and Miller targeted the valve timing (ATKINSON, 1886) (MILLER, 1957).

Miller choose initially to create the cycle to revolve around early intake valve closing (EIVC) on engines that utilised forced induction as not to impair the following combustion cycle because the volumetric efficiency could be kept high. As opposed to that of a naturally aspirated engine that requires that longest available opening time as possible, to increase volumetric efficiency to an adequate level, hence the typical association of cycles to that of Atkinson on NA engines, and Miller of FI engines (Jääskeläinen, 2019).

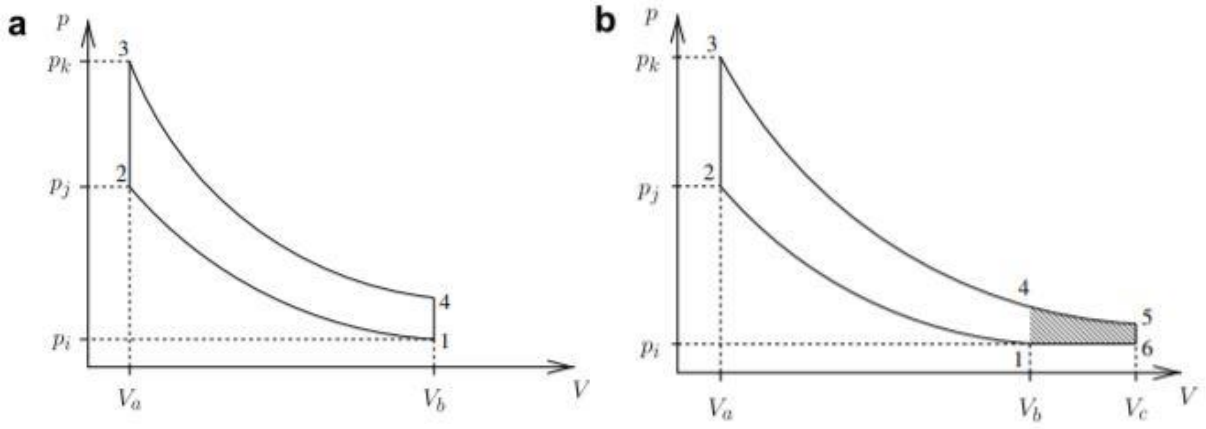

Figure 6 Comparison between the PV diagram of the typical Otto cycle (a) and the over-expansion Miller cycle (b**)** (Mikalsen, et al., 2009)**.**

As can be seen, the cycle is very similar to that of the Atkinson with respect to the 'increased' volume during the expansion cycle. However, because Miller's target was to use EIVC instead of LIVC, his idea was there would be a reduction in charge temperature because the system should abide by the ideal gas law. Showing that with the change in volume without an increase in pressure, the temperature would have to decrease.

Miller's cycle is commonly used in diesel applications, on larger typical supercharged engines, where the loading condition can be kept relatively similar and not of high demand, because the limitation of both these cycles is known to be the reduced power output due to the common reduction in compression ratio (Gonca, et al., 2015) (Wang, et al., 2007) (Li, et al., 2019).

However, there is development in cases where the power output reduction can be offset with an increase in boost pressure to effectively increase charge density, whilst adjusting the effective exhaust gas recirculation ratio and equivalency ratio (Li, et al., 2014) (Chen, et al., 2019).

Typical uses of an engine utilising the miller cycle are larger off-road diesel applications throughout the marine industry and some power generation. Considering road applications, Mazda are the most notable manufacturer to have implemented the idea with their 2.25L KJ-ZEM V6 supercharged engine back in the late 1990's (Ashdown, 2018) and again for the later generation Mazda 2 MZR 1.3L DOHC (MAZDA, 2007). Although other's have tried, none were seemingly as effective as the Japanese manufacturer.

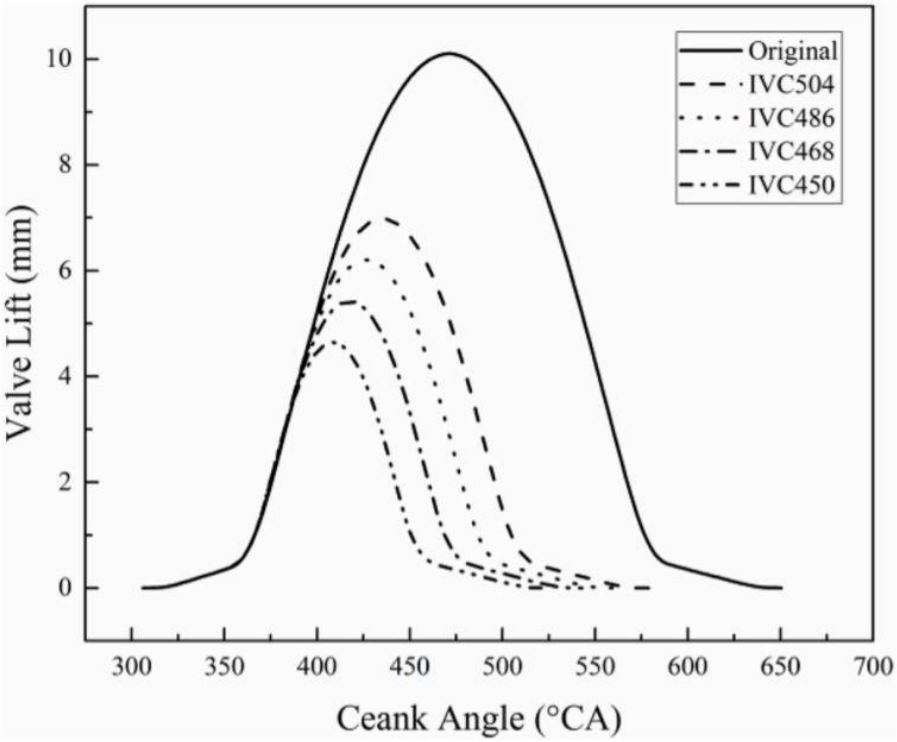

Figure 7 Visualisation of valve lift profiles when EIVC is utilised on an engine (Chen, et al., 2019).

2.4. Two-zone combustion & Emissions modelling.

Modelling combustion has become an integral part of technological, control and experimental advances for the internal combustion engine, because it “easily” allows for rapid development of knock, fuel consumption, and emissions modelling that can be used to influence how real-time control of the engine can be utilised (Guzzella & Onder, 2010). All of which are key targets for the industry at this point in history, given out current climate condition.

Two-zone combustion modelling is simply an advance from single-zone models, in which the combustion event isn’t treated as a single entity. Because the combustion process pertains more to a burnt and unburnt zone as the flame propagates through the cylinder, hence the use of the more accurate model that allows the calculation of these two zones independently of one another.

The advantage of using two-zone of single-zone modelling is identified in the following figures;

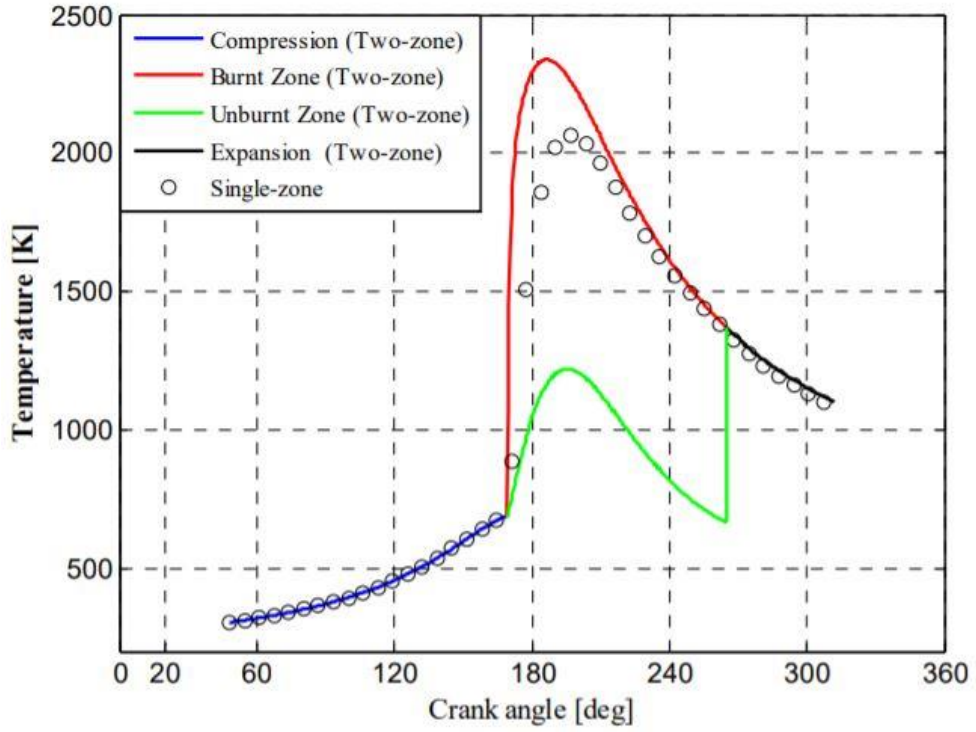

Figure 8 Predicted combustion in-cylinder temperatures using both single-zone and two-zone modelling techniques, identifying the potential difference, and reiterating what could be cause for concern given the models temperature dependency (Xiang, et al., 2018).

The fundamental equations used for this modelling format are those for mass conservation, energy conservation, and a pair of ideal gas equations;

$$M_b + M_u = M$$

$$V_b + V_u = V$$

$$\frac{d(m_u u_u)}{dt} = h_u \frac{dm_u}{dt} - P\frac{dV_u}{dt} - \dot{q}_u, L$$

$$\frac{d(m_b u_b)}{dt} = h_b \frac{dm_b}{dt} - P\frac{dV_b}{dt} - \dot{q}_b, L$$

Where M_b and M_u are the independent masses for the burnt and unburned zones, h_b and h_u and the enthalpies of these zones respectively, and V_b & V_u are the volumes associated to the zones. It's proposed that the term for heat transfer to the walls, $\dot{q}_u, L$ & $\dot{q}_b, L$ are to be model by experimental correlations. As for the gas laws of the zones;

$$P = \frac{m_u R_{un} T_u}{V_u} = \frac{m_b R_{bn} T_b}{V_b}$$

The pressure can be said to be equal across the burnt and unburned zones, and it's also assumed that there is no heat transfer between the zones (McAllister, et al., 2011).

This can then effectively be used to model emissions production because of the significant influence of pressure and temperature on the calculation of species production using the idea of partial pressures.

Typical approach to combustion product modelling is based around the idea that the reaction can go both forward and backwards. Under the impression that combustion operates as a closed compressible system, it can be said that the increase in entropy must always be greater than, or equal to zero. Also, because the system is commonly treated as one that abides by constant temperature and pressure, that every change in chemical composition will reduce the value of Gibbs free energy, to the point where at chemical equilibrium the following condition is met (Merker, et al., 2006).

$$dG_{T,p} = 0$$

It can be said that the change in Gibbs free energy, at constant pressure and temperature, as the gas composition changes is;

$$(\Delta G)_{T,p} = \sum \tilde{\mu}_i \delta n_i$$

Where Δn_i is the change in the number of moles of the species denoted, i. $\tilde{\mu}_i$ is the chemical potential (Heywood, 2018).

Using the principle of chemical potential means that the solution for the concentrations of the various species will have to be an iterative process. So, to save time and in industry, money, the idea of partial pressures is introduced.

$$\sum_i v_i \tilde{g}_i^{\circ} + RT \ln \prod_i \left(\frac{P_i}{P^{\circ}}\right)^{v_i} = 0$$

$$K_p = \prod_i \left(\frac{P_i}{P^{\circ}}\right)^{v_i}$$

Where K_p is the equilibrium constant and it's now in relation to the partial pressures for the species 'i'. This constant is only dependent on the temperature of the system, and using published data like the JANAF tables, the associated data between the constant and its associated temperature can be calculated and used to inform the model (Merker, et al., 2006). This is the method that'll lay the groundwork for emissions predictions throughout the research project.

The efficiency and validity of two-zone modelling can be seen across countless scholarly journals and papers; however, it should be noted that there is still assumptions to be made during this process that can lead to errors in predictions.

Throughout the industry the typical approach to predict the production of NOx during a combustion event is to use a form of what is usually referred to as the "Zeldovich Mechanism". And with the model we can predict the rate of production of NO which is generally accepted as the predominant form of nitric oxide created during combustion of typical fuel, and it can be written to include reverse reaction rates (decomposition) as well as the forward rates to try and further the accuracy of results. The two main reactions that result in the production of NO is that of the oxidization of atmospheric nitrogen and to some degree the oxidization of fuel-bound nitrogen (Blair, 1998).

$$O + N_2 \leftrightarrow NO + N \quad [1]$$

$$N + O_2 \leftrightarrow NO + O \quad [2]$$

Some consider an additional equation of,

$$N + OH \leftrightarrow NO + H \quad [3]$$

(Heywood, 2018), (McAllister, et al., 2011)

Each of these reactions have their own independent rate equations which are typically referred to as '$k_x =$'. These equations are only dependent on temperature and because of this they can easily be group together to generate one overall rate equation that covers the production of NO via all three reactions.

Depending on the researcher their version of the developed Zeldovich model will be different regarding the rate equations used, otherwise they typically maintain the same formation of;

$$\frac{d[NO]}{dt} = x \cdot 10^{x}[N_2][O_2]^{\frac{1}{2}} \exp\left(-\frac{x}{T}\right)$$

And depending on the author the units will be either '$\frac{mol}{cc \cdot s}$', or '$\frac{kmol}{m^3 \cdot s}$'. Naturally the results predicted by the model could be grossly out if the units are correct, so it is of the utmost importance that this is checked before use. Another note on the common construction of this equation is that the 'x' in '$-\frac{x}{T}$' will most likely be in the range of 60 – 70,000.

For example, the three most common adaptations of this equation are presented by Heywood, McAllister, et al., and Merker, et al. and are listed below in the order of the author.

$$\frac{d[NO]}{dt} = \frac{6 \text{ x } 10^{6}}{T^{\frac{1}{2}}} \cdot [N_2][O_2]^{\frac{1}{2}} \exp\left(-\frac{69{,}090}{T}\right), \qquad [mol/cm^3 \cdot s]$$

$$\frac{d[NO]}{dt} \cong 1.476 \cdot 10^{15} [N_2][O_2]^{\frac{1}{2}} \exp\left(-\frac{67{,}520}{T}\right), \qquad [mol/cc\ -s]$$

$$\frac{d[NO]}{dt} = 4.7 \cdot 10^{13} [N_2][O_2]^{\frac{1}{2}} \exp\left(-\frac{67{,}837}{T}\right), \qquad [kmol/m^3 \cdot s]$$

From the authors previous experience using these equations for production, albeit with far simpler combustion modelling, the equation proposed by Merker, et al. produces the best results and that's why it was chosen to be the fundamental equation in this study.

As mentioned, there is the possibility of reverse reactions that take place which naturally decrease the production of NOx during combustion and as is these are not specifically being accounted for in the modelling. Because the model is being treated as if it were in a state of equilibrium, meaning that the forward rate can be said to be equal to the reverse reaction rate and this is a fundamental assumption of this entire investigation, with one target being to assess the adequacy of this assumption and if the production of NOx across various load and speed cases can in fact be predicted with level of accuracy for both trend and value.

3. Two-Zone Combustion Modelling Mathematics.

Considering the approach for mathematical modelling, the traditional procedure of assessing the provided measured data for combustion characteristics will lay the groundwork for the investigations. All of which will be done within MathWorks MATLAB software.

Required characteristics are as follows;

- Polytropic index values for the order of change of pressure during compression and expansion.
- Starting position and delay of ignition helping to define the key point, the start of combustion.
- Duration time and end of combustion are also important for understanding the influence of the starting conditions; equivalency ratio, compression ratio, spark timing, etc.
- Volume and mass of the charge air and fuel mixture within the cylinder, to inform the chemical kinetics modelling.
- Burn rate of the mixture signifying the rate in which heat is added to the system.

(Merker, et al., 2006), (Heywood, 2018), (Heywood, 2018).

These characteristics inform the following model fundamentals:

3.1. Logarithmic P-V graphs for polytropic indexes.

In-cylinder pressure trace profile predictions that follow the assumption it's an isentropic process. With respect to the ideal gas law the pressure will be found per degree using;

$$PV^n = constant, \qquad or\ P_1{V_1}^n = P_2{V_2}^n$$

Where 'P' is pressure, 'V' is volume and 'n' is the polytropic index (Heywood, 2018).

To find this polytropic value that is intrinsic of the compression and expansion process, typical approach is to use a logarithmic pressure – volume diagram and using the leading component of the first order polynomial fit to log-pressure.

As seen in the following;

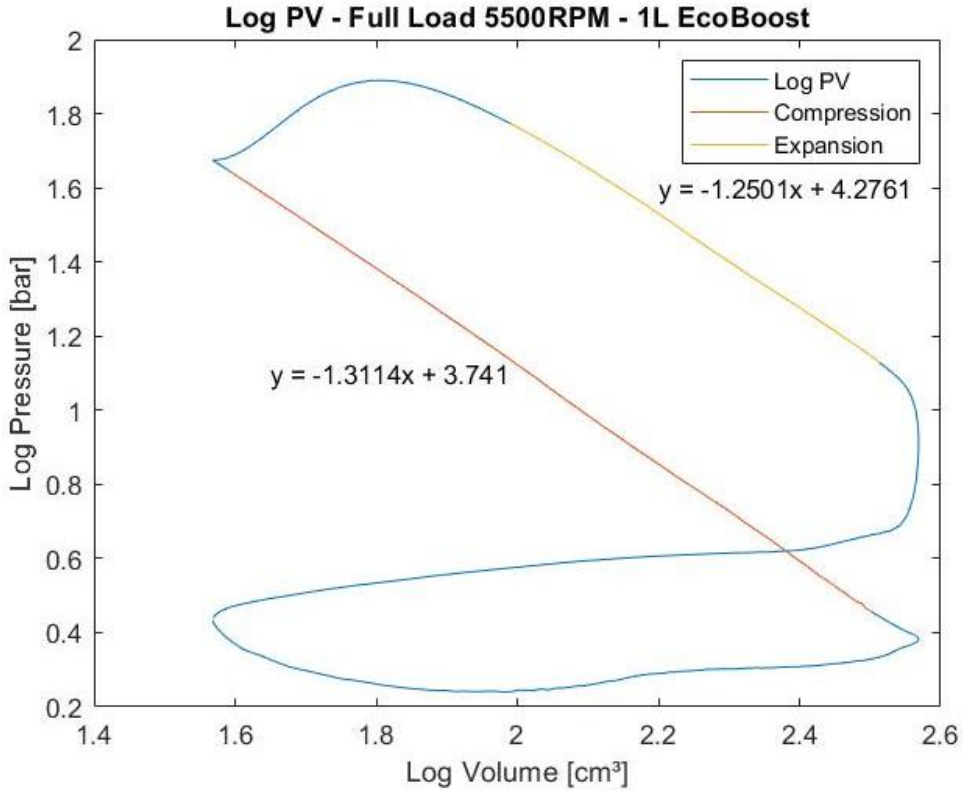

Figure 9 Log PV diagram showing the values for the polytropic values of full load condition for the 1L EcoBoost engine.

It is important to note that there is always potential for errors to occur in modelling, and one of those issues can start right from the off here. The issue is dependent upon how much of the curve is used to find the slope, and therefore the polytropic index. Because this value will be used to drive all subsequent modelling the removal of these errors is key, this is a simple process considering there is only a small data set of around 15 cases for each of the 1L & 1.5L varied load data sets, and when considering the modelled pressures during the compression and expansion sections of the measured pressure trace, it'll be obvious if the value of polytropic index is within bounds because these sections will match closely. If needs be, reassess the number of points on the curve used to fit, i.e. use less by reducing from the bottom of compression and the top of the expansion section, so the curve itself follows a more linear trend.

It should also be said that when deciding where on the curve to start and end the curve fitting, it can be useful to check the points of valve timing from measured data regarding the opening of the exhaust valve and the closing of the inlet valve. These are of great importance because when these are introduced, the system is no longer a "closed" system and the modelling technique no longer holds true.

3.2. Mass Fraction Burnt Modelling.

Considering the mass fraction burnt, this is modelled under the principal of a method proposed by the engineers Gerald M. Rassweiler and Lloyd Withrow after conduction an experiment to correlate the fraction of burnt mass to that of measured pressure data and photos of the combustion process (Rassweiler & Withrow, 1938).

$$\frac{V''_{tf}}{V_{tf}} = \frac{V'_t}{V_{tf}} \left(\frac{P_t}{P_{tf}}\right)^{\frac{1}{n''}}$$

Where 'V''' is the volume of the inflamed portion of the charge at the given time. ''V'' is the volume of the non-inflamed portion of the charge at the given time. 'P_t' is the absolute pressure (reduced to constant volume) at the given time and the notation of '$_f$' just defines the condition at EOC.

For the means of modelling in this investigation, there was two different variations of MFB used because it was found that the latter produced more accurate results regarding comparison to Ford's stated points of 10, 50 & 90% burnt within the data.

Initial methodology related to using the actual cylinder pressure that was measured and that predicted via the law of a polytropic process. Where the change in pressure is modelled as;

$$\Delta P = P_{2,m} - \left(P_{1,m} \cdot \left(\frac{V_2}{V_1}\right)^n\right)$$

The notation of '$_m$' is for identifying the use of measured cylinder pressure data.

It should be noted here that the value of '*n*' will be dependent on the change of section of cycle, i.e. before TDC (CA 0°) the value relates to the polytropic value during compression, and naturally after TDC it should be replaced by that found for the expansion cycle.

This calculation of the change in pressure within the cylinder will produce a figure that looks like the following and can then be used to identify the start and end of combustion (SOC & EOC respectively).

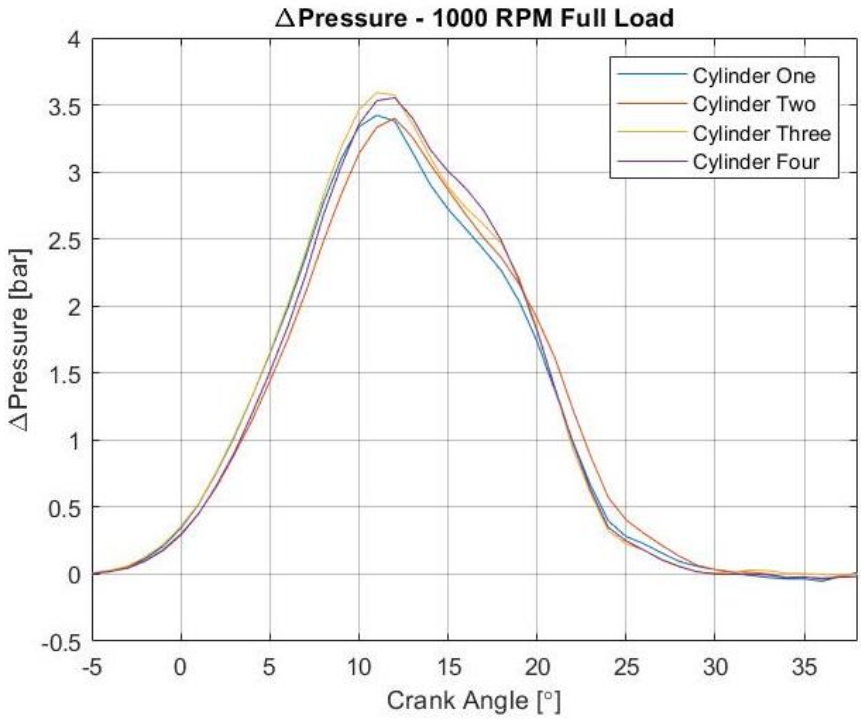

Figure 10 ΔP within all four cylinders of the 1.5L EcoBoost @ 1000RPM Full Load.

SOC and EOC with respect to crank angle was determined by finding the points of the curve that reached above, in this specific case, 0.02 Bar of pressure. This threshold did and should change/be adjusted for each individual load and engine speed situation because of the large differences in cylinder pressures and the rate of combustion itself.

Next step was to use the cumulative change in pressure to generate a the well-established 'S' shaped curve the is typical to mass fraction burnt. This is done simply by;

$$\Delta P_{C,i} = \Delta P_{C,i-1} + \Delta P_i$$

Where the subscript of 'c' is used to show it is the cumulative change in pressure, not the change in pressure previously calculated.

With this, MFB is found using the following relationship;

$$MFB_i = \frac{\Delta P_{C,i}}{\Delta P_{C,EOC}}$$

Using this methodology produces the MFB shown in the following figure and as can be seen in this, there is variation within each cylinder, and this can cause discrepancies within modelling if the averages were to be used. But this is not the intention, therefore each cylinder is calculated independently in the hope to retain errors to a minimum.

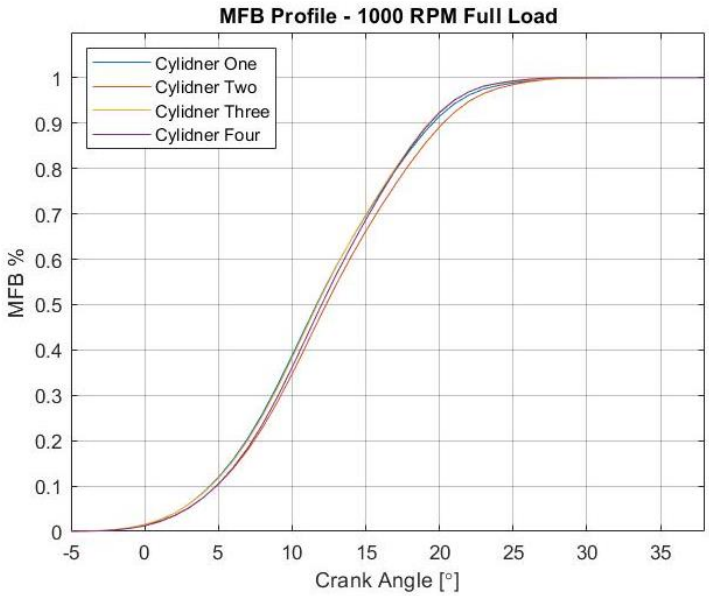

Figure 11 Mass Fraction Burn (MFB%) through combustion for the 1500cc EcoBoost GTDI engine at 1000RPM and 150% relative load (Full Load).

As for the secondary method the principals are relatively similar, however the key difference is using the mean value of the unburned zone's ratio of specific heats (discussed in 3.3), from SOC to EOC, along with the change in pressure previously calculated.

$$MFB_{1,i} = \frac{\Delta P_i \cdot V_i}{\gamma_{un,\ avg}}$$

Again, upon generating a cumulative profile like before, the new mass fraction burnt profile can be found by dividing the current point of the cumulative profile by that at EOC. A comparison of the profiles calculated via both options can be seen below, and then a validity comparison of the induvial points for 10, 50 and 90% burnt is shown under that, with the points stated by Ford and the upper and lower bounds coming from the standard deviation found be Ford.

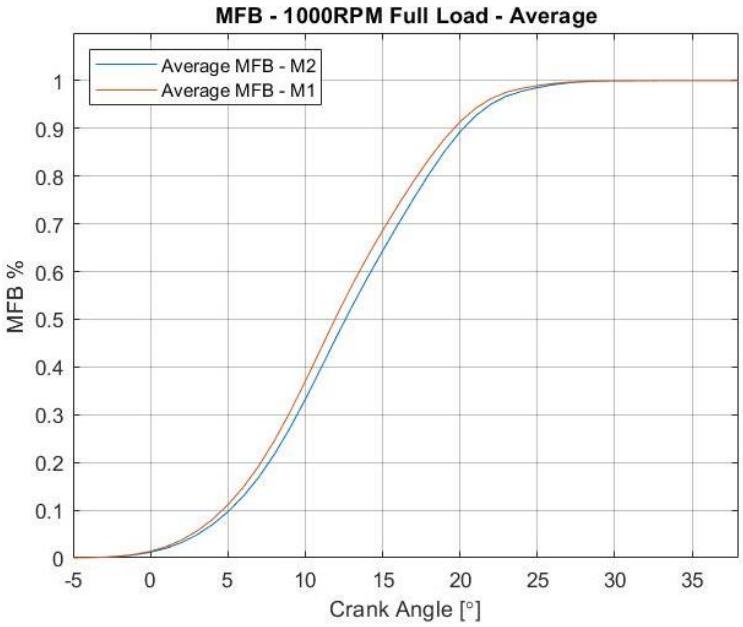

Figure 12 MFB profile comparison based on the two methods used.

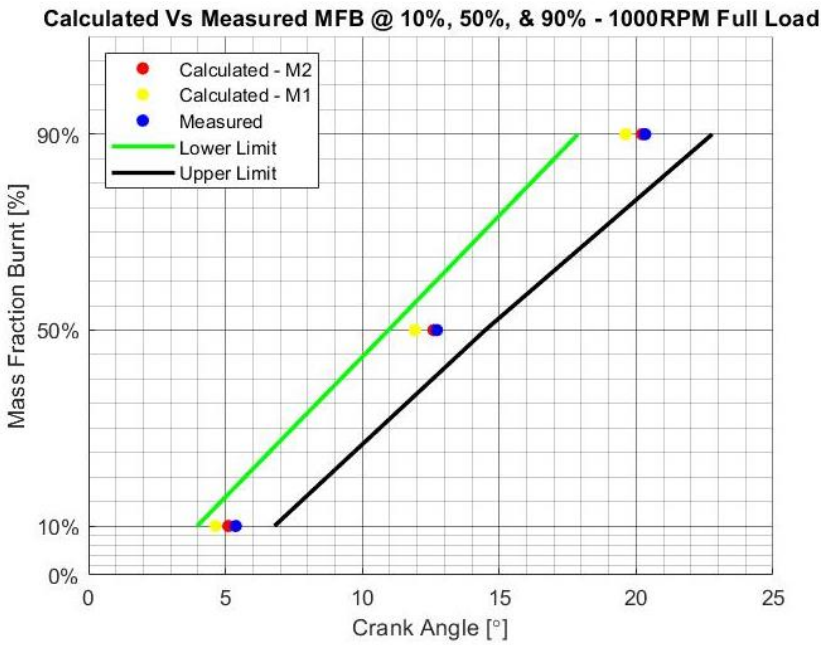

Figure 13 Comparison between MFB calculation methods and their accuracy against the stated points of 10, 50, and 90% burnt from Ford, including the bounds from standard deviation.

Although only a slight difference can be seen in the two methods of MFB calculation, that difference is important because it changes the volume of the burnt and unburned zones that will be used later in the dissociation modelling of emission. And this change is only slight at the full load situations, at part load the deviation in results is “far” more prominent, making it more obvious that the secondary method is better for accuracy in modelling.

As the for the unburnt zone, it’s simply; $Unburnt = 1 - MFB$

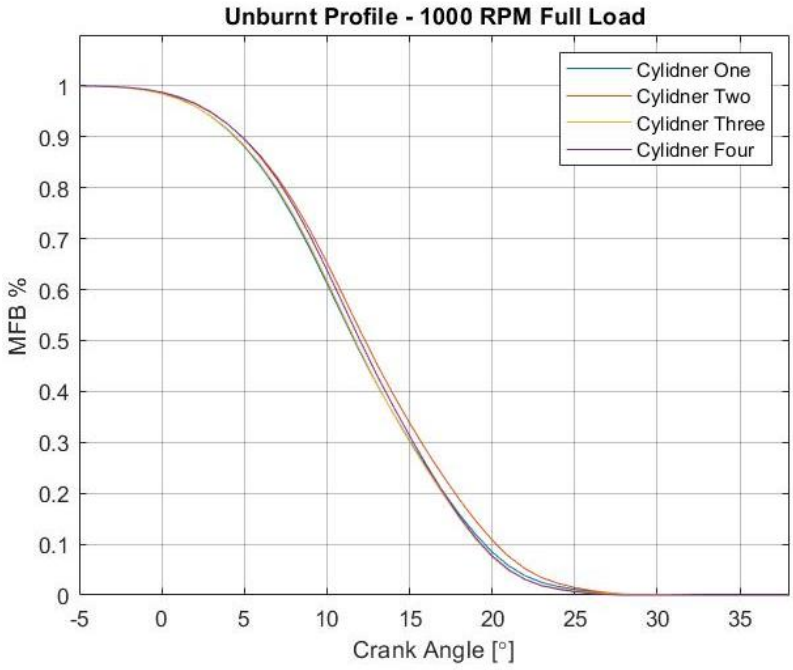

Figure 14 Burnt and Unburned percentages through combustion for the 1500cc EcoBoost GTDI engine at 1000RPM FL.

Considering the zones volumes, this is a simple relationship, again, that is calculated from the universal gas law;

$$PV = nR_uT$$

$$V_i = \frac{nR_uT_i}{P_i}$$

Where 'R_u' is the universal gas constant, and 'R' is the gas constant for the air trapped in the cylinder, '*n*' is the mass of that mixture trapped in-cylinder, and '*T*' is the temperature of the unburned zone. However, for the purposes of finding the specific gas constant of the gas in cylinder, we rearrange this relationship to have a direct corelation between the universal gas constant and the specific.

If we say that '$n = 1\ Kmol$',

$$PV = nR_uT = mRT$$

$$nR_u = mR$$

With '$n = 1$' and 'm' being the molecular weight in kilograms, we get;

$$R = \frac{R_u}{m}$$

'R' unburned is found using the following principals;

$$Average_{mol.w,\ un} = \frac{(Fuel_{Mass} + Air_{Mass})}{\varphi + 12.5 \cdot (1 + 3.773)}$$

Where the fuel mass is calculated based on the molecular weight of fuel type, in this case Iso-Octane (C_8H_{18}). So the mass equates to;

$$Fuel_{Mass} = \big((8 \cdot 12.011) + (18 \cdot 2.016) + (0 \cdot 15.99)\big) \cdot \varphi$$

And the same principle for the mass of air also, and this is kept as a constant through all situations because it is the fuel mass that is varied against it because of the fuel equivalency 'φ'.

$$Air_{Mass} = 12.5 \cdot \big(31.99 + 3.773 \cdot (28.013)\big)$$

The 12.5 used is the standard multiplier for Iso-Octane fuel based off the stoichiometric chemical balance of complete combustion, with R_u being the universal gas constant.

$$R_{un} = \frac{R_u}{Average_{mol.w,\ un}}, \qquad R_{un} = \frac{8314.5}{Average_{mol.w,\ un}}$$

As for the burnt zone, 'R_b', the method is slightly different in that the values of species aren't known at the time, so there is an assumption made of it being close to the equivalent of stoichiometric chemical balance. McAllister, et al., states that when considering the stoichiometric combustion of a general hydrocarbon fuel, the chemical balance can be written as;

$$C_\alpha H_\beta O_\gamma + \left(\alpha + \frac{\beta}{4} + \frac{\gamma}{2}\right) \cdot \left(O_2 + 3.773 \cdot (N_2)\right) = \alpha CO_2 + \frac{\beta}{2} H_2O + 3.773 \cdot \left(\alpha + \frac{\beta}{4} + \frac{\gamma}{2}\right) N_2$$

(McAllister, et al., 2011)

However, in essentially all cases investigated within this entire study, the fuel equivalency ratio is always greater than 1. Meaning that the mixture is rich and is therefore not stoichiometric and because of this, the equation needs adjusting to accommodate the additional species of carbon monoxide, '*CO*', when rich and oxygen when/if running lean.

Because all situations are apparently rich or stoichiometric, in the case of the 1.5L Ecoboost, only the adapted equation for the rich situations will be written.

$$\varphi(C_\alpha H_\beta O_\gamma) + \left(\alpha + \frac{\beta}{4} + \frac{\gamma}{2}\right) \cdot \left(O_2 + 3.773 \cdot (N_2)\right) = (\zeta - \alpha) CO_2 + \frac{\beta}{2} H_2O + (CO_2 - \alpha) CO + 3.773 \cdot \left(\alpha + \frac{\beta}{4} + \frac{\gamma}{2}\right) N_2$$

Where 'φ' is the fuel equivalency ratio, and 'ζ' for Iso-Octane is,

$$\zeta = \left(2 \cdot \left(\alpha + \frac{\beta}{4} + \frac{\gamma}{2}\right)\right) - {}_nH_2O. \quad Or, \qquad \zeta = 25 - {}_nH_2O$$

$$Average_{mol.w,\ b} = \frac{({}_nN_2 \cdot 28.013 + {}_nCO_2 \cdot 44.01 + {}_nH_2O \cdot 18.015 + {}_nCO \cdot 28.01)}{(\zeta - \alpha \cdot \varphi) CO_2 + \frac{\beta \cdot \varphi}{2} H_2O + (CO_2 - \alpha \cdot \varphi) CO + 3.773 \cdot \left(\alpha + \frac{\beta}{4} + \frac{\gamma}{2}\right) N_2}$$

$$R_b = \frac{R_u}{Average_{mol.w,\ b}}, \qquad R_b = \frac{8314.5}{Average_{mol.w,\ b}}$$

So to finally calculate the volumes of each zone, starting with the unburnt, using the relationship of the universal gas law, we can write it as;

$$V_{un,\ i} = \frac{(1 - MFB) \cdot M_{tot} \cdot R_{un} \cdot T_{un,\ i}}{P_i}$$

Where 'M_{tot}' is the total mass of the air and fuel in cylinder, and '$T_{un,\ i}$' is the unburned temperature, discussed in the next section.

As for the burnt zone's volumes, we can simply say that is equal to the volume of the cylinder minus the volume of the unburnt zone. This should result in a graph that looks similar to the following.

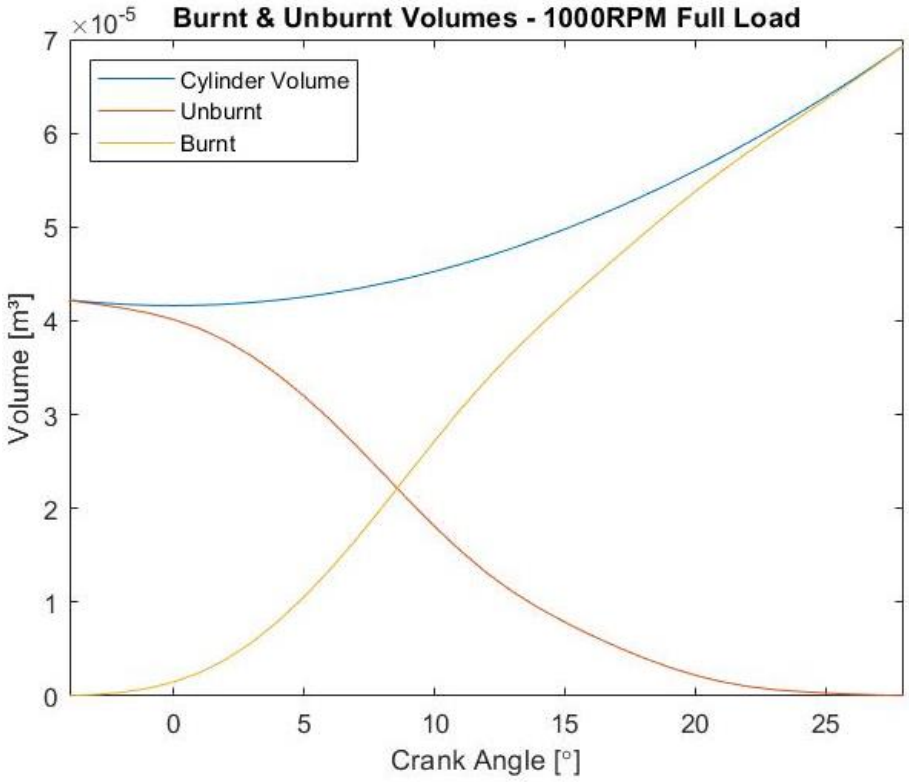

Figure 15 Burnt and Unburnt zone volumes at 1000RPM, Full load. 1.5L EcoBoost.

3.3. Individual Zone's Temperature Modelling.

The zonal temperatures are the most critical part of the modelling because of their influence on the prediction of emissions when considering partial pressure equilibrium. The first step of the model is the unburned zones temperature, found using the relationship of the effect of pressure on temperature during an isentropic thermodynamic process, such as;

$$T_2 = T_1 \cdot \left(\frac{P_2}{P_1}\right)^{\left(\frac{\gamma-1}{\gamma}\right)}$$

Where 'γ' is the ratio of specific heats;

$$\gamma = \frac{C_p}{C_v}$$

(McAllister, et al., 2011)

This ratio of specific heats will vary at each degree of crank rotation because of the change in temperature, as seen in the figure below. To account for this, we follow the process as described by John B. Heywood in his 2nd edition of Internal Combustion Engine Fundamentals, section 4.7.

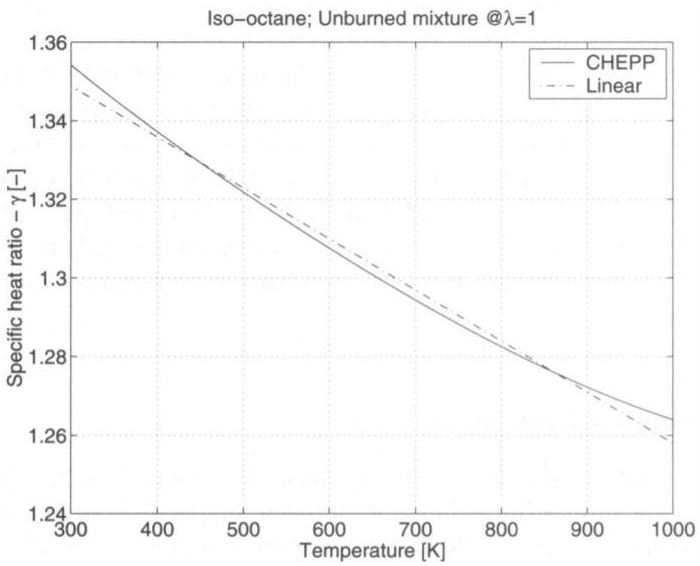

Figure 16 Specific heat ratio for an unburned stoichiometric mixture as a function of temperature (Klein & Eriksson, 2004).

The fundamentals of calculation process is by using experimentally fitted test data exponents, in a polynomial style curve fit, the specific heat capacity of the species at constant pressure can be estimated at the temperature calculated previously in an iterative process through the combustion period.

Calculating the zone's temperature up until the point of combustion initiation because the system is regarded as closed, we use the universal gas law again, with the previously calculated specific gas constant and mass trapped in the cylinder.

$$T_{un,\ i} = \frac{P_i V_i}{R_{un} \cdot M_{tot}}$$

Then to estimate the specific heat capacity at constant pressure of the species in the system (fuel & air, [Iso-Octane, $O_2 + N_2$]). Heywood states the curve fit equation for gaseous species as;

$$\frac{\tilde{C}_{p,i}}{R_u} = a_{i1} + a_{i2}T + a_{i3}T^2 + a_{i4}T^3 + a_{i5}T^4$$

And for fuels as;

$$\tilde{C}_{p,f} = A_{f1} + A_{f2}t + A_{f3}t^2 + A_{f4}t^3 + \frac{A_{f5}}{t^2}$$

Important to note that 'T' is actual temperature in kelvin, but 't' is temperature in kelvin divided by 1000, $t = T(K)/1000$. Also, with the specific heat of the fuel substance, the fit exponents and equation are relating to units of '$cal/gmol \cdot K$' and not the required, '$J/kmol \cdot K$'. So the conversion is to multiply the value by 4186.8.

Tables of the coefficients of fuel types and chemical species can be found in appendix B.

Results from the curve fits should generate a figure that is the same as the following, when considering all gaseous species through temperature.

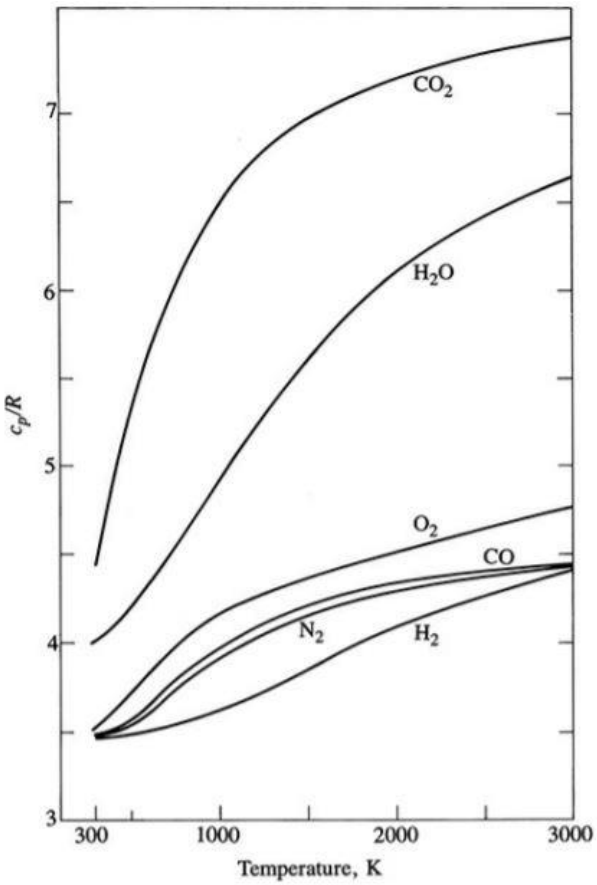

Figure 17 Specific heat capacity at constant pressure for various species using the coefficients from the JANAF tables (Heywood, 2018).

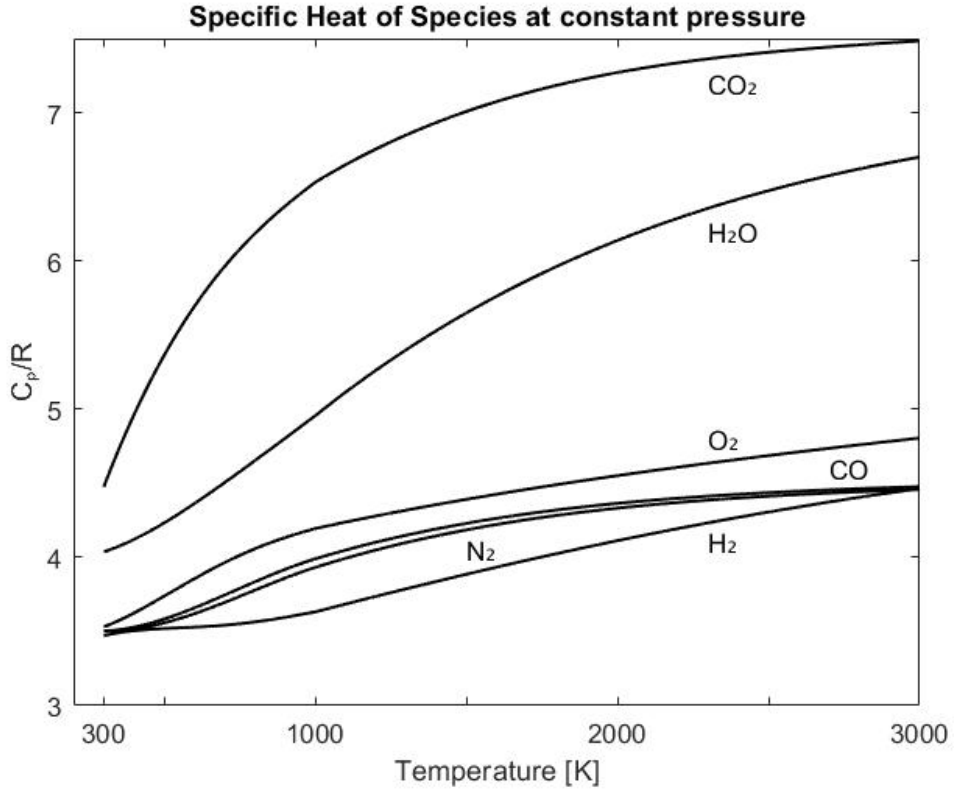

Figure 18 Recreation of the calculated specific heat of species using MATLAB (Average accuracy, 100.3%).

Using this method of calculation increases the ability for the prediction of combustion product species, per degree or crank rotation, and this will in turn help to corroborate the modelling techniques and the ability to predict combustion. Although there is variations of the process for combustion modelling techniques, it's thought that from both previous experience and influence of resources that this process is the best approach to a valid combustion model.

So with each iterative step, having calculated the ratio of specific heats at constant pressure, the next part is to find the average specific heat within the cylinder, done by;

$$\tilde{C}_{p,Avg,\ i} = \frac{\varphi \tilde{C}_{p,f,\ i} + 12.5\left(\tilde{C}_{p,O_2,\ i} + 3.773\left(\tilde{C}_{p,N_2,\ i}\right)\right)}{(\varphi + 12.5(1 + 3.773)) \cdot (1 - MFB_i)}$$

The relationship between the specific heat at constant pressure, to that at constant volume, is the universal gas constant 'R_u'.

$$\tilde{C}_{v,\ avg\ cyl} = \tilde{C}_{p,\ avg\ cyl} - R_u$$

Making 'γ',

$$\gamma = \frac{\tilde{C}_{p,\ avg\ cyl,\ i}}{\tilde{C}_{v,\ avg\ cyl,\ i}}$$

And we then calculate temperature of the unburned zone as,

$$T_{un,\ i} = \frac{P_i}{V_i}^{1-\frac{1}{\gamma}} \cdot T_{un,\ i-1}$$

This is now the calculated temperature at the next degree of crank and allows use to run through the iterative process through combustion.

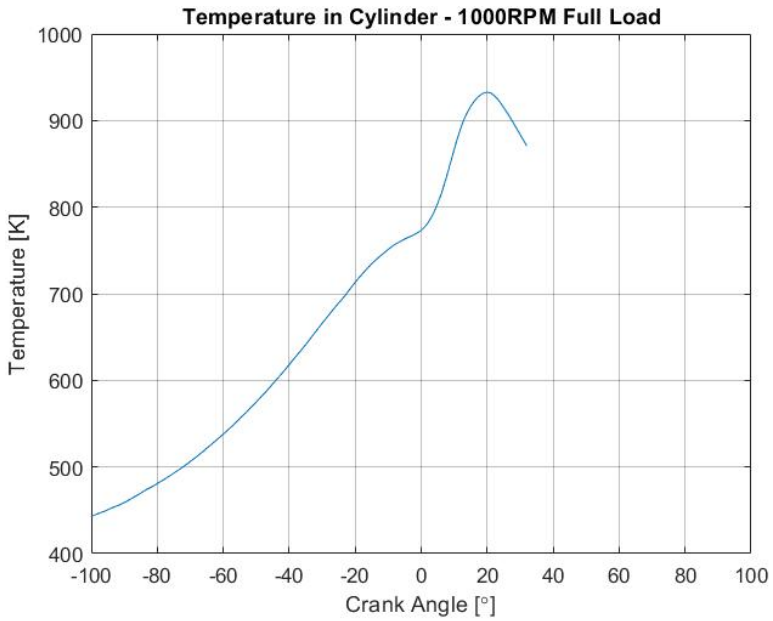

Figure 19 Unburned temperature in cylinder at 1000RPM, Full Load. 1.5L EcoBoost.

These temperatures shouldn't reach above 1000K because this is the typical area where knock will occur, this can therefore be used as a form of sanity check.

As for the burnt zone temperature, we consider the same process for the after-combustion section, however the species are different for here because they're treated as the right-hand side of the combustion stoichiometry equation, $CO_2, H_2O, N_2, O_2, N_2$.

During combustion the equation used is again using the gas law rearranged into,

$$T_{b,\ i} = \frac{P_i \cdot V_{b,\ i}}{(M_{tot} \cdot R_b) \cdot MFB_i}$$

Once the combustion event has finished, we use the previous process of calculating the specific heats of the species to then find the temperature as the cycle finishes its sections.

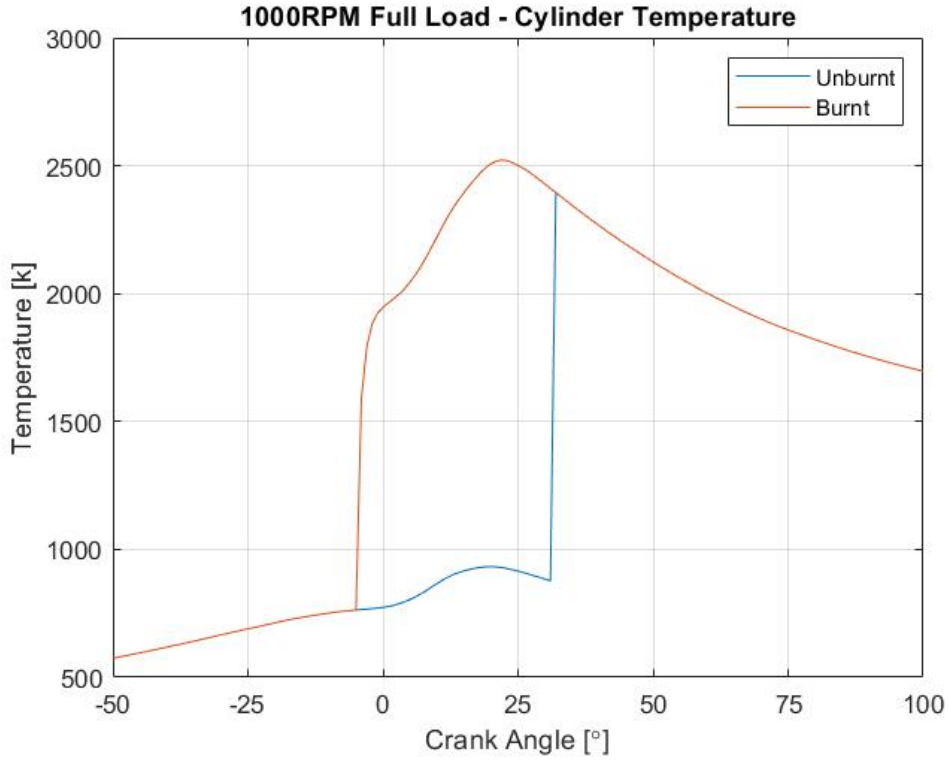

Figure 20 Burnt and unburned temperature in cylinder at 1000RPM, Full Load. 1.5L EcoBoost.

3.4. Dissociation Modelling.

Following into the calculation of the species produced during the combustion phenomenon the calculations will be done under the principal of combustion equilibrium. Using the known mass of fuel and air into the cylinder, this gives an initial value for the expected species of emissions, that will be found following the idea of their mole fraction based on their partial pressure constant in an iterative method (McAllister, et al., 2011). Naturally, these equilibrium constants will change with variation in temperature, so considering the validity of the model, combustion temperature calculation is of the utmost importance.

The modelling technique used in this investigation is as follows,

$$\varphi C_8H_{18} + 12.5(O_2 + 3.773N_2) = {}_{n1}CO_2 + {}_{n2}H_2O + {}_{n3}CO + {}_{n4}H_2 + {}_{n5}O_2 + {}_{n6}N_2 = N_t$$

Considering the species involved in the calculation of combustion emissions, the typical six of; $CO_2,\ H_2O,\ CO,\ H_2,\ O_2,$ & N_2. We can solve based on two different reactions to that will give us the required equilibrium constants,

$$CO_2 \leftrightarrow CO + \frac{1}{2}O_2, \qquad = reaction\ 1$$

$$H_2O \leftrightarrow H_2 + \frac{1}{2}O_2, \qquad = reaction\ 2$$

As can be seen, we cover five of the species from our initial equation. And although 'N_2' isn't covered, it is because we assume that the reaction to [NO] in terms of mole fraction is so small, it's negligible. Hence the value of 'n_6' is left constant.

Considering reaction '1', rewriting in terms of patrial pressure equilibrium we get,

$$K_pCO_2 = \frac{\left(\frac{n_1}{n_t} \cdot P\right)}{\left(\frac{n_3}{n_t} \cdot P\right) \cdot \left(\frac{n_5}{n_t} \cdot P\right)^{\frac{1}{2}}}$$

Transformed into a useable state of,

$$\frac{n_1}{n_3} = K_pCO_2 \cdot \left(\frac{n_5}{n_t} \cdot P\right)^{\frac{1}{2}}$$

Which we can title as *eq. 1*.

Regarding that of reaction 2, we rearrange into the form of;

$$K_pH_2O = \frac{\left(\frac{n_2}{n_t} \cdot P\right)}{\left(\frac{n_4}{n_t} \cdot P\right) \cdot \left(\frac{n_5}{n_t} \cdot P\right)^{\frac{1}{2}}}$$

$$\frac{n_2}{n_4} = K_pH_2O \cdot \left(\frac{n_5}{n_t} \cdot P\right)^{\frac{1}{2}}$$

Naturally, this is *eq. 2.*

In terms of finding the equilibrium constant 'K_p', for both 'H_2O' & 'CO_2', we introduce the concept of Gibbs free energy. This allows us to relate the value of the free energy from the reaction at a specific temperature and pressure, assuming constant and therefore at equilibrium, to what is termed as it's equilibrium constant. Because of this, we can say that;

$$-\Delta G^\circ = RT \ln K_p\,, \qquad K_p = \exp\left(\frac{-\Delta G^\circ}{RT}\right)$$

(Glassman & Yetter, 2008)

This relationship is very important because we now have the constant dependent only on temperature, again highlighting why in dissociation modelling, temperature is the key parameter.

To find the change in Gibbs free energy through temperatures in a system, the JANAF tables are used. Although they're common scriptures, Glassman, et. al. has them published in the appendices of their 'Combustion' book and these was the values referenced to determine the polynomial fit that is fundamental to the model.

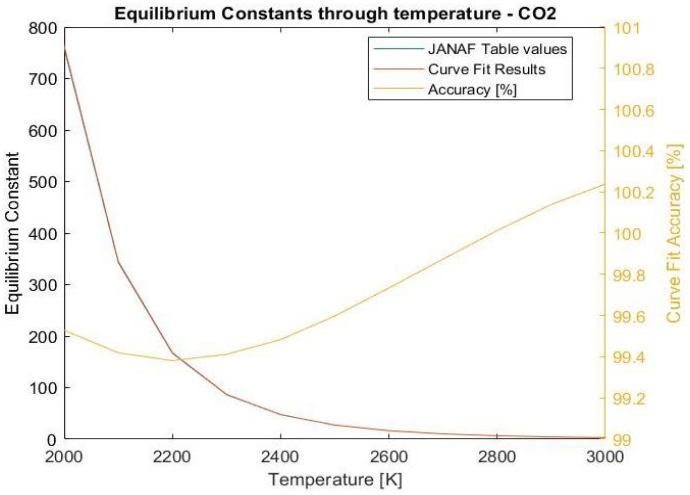


```
Linear model Poly8:
val(x) = p1*x^8 + p2*x^7 + p3*x^6 + p4*x^5 +
             p5*x^4 + p6*x^3 + p7*x^2 + p8*x + p9
  where x is normalized by mean 2956 and std 1794
Coefficients (with 95% confidence bounds):
  p1 =       0.438  (0.3138, 0.5622)
  p2 =     -0.5693  (-0.6764, -0.4623)
  p3 =      -1.745  (-2.419, -1.071)
  p4 =       2.013  (1.512, 2.514)
  p5 =       1.976  (0.8064, 3.145)
  p6 =       -1.28  (-1.975, -0.5845)
  p7 =      -3.607  (-4.304, -2.91)
  p8 =       147.1  (146.8, 147.4)
  p9 =      -31.15  (-31.25, -31.05)
```

Figure 21 Original JANAF Table results of equilibrium constants for CO_2 through temperature, with the model's curve fitted results and accuracy of fit through temperature. Including polynomial exponents to the 9th degree.

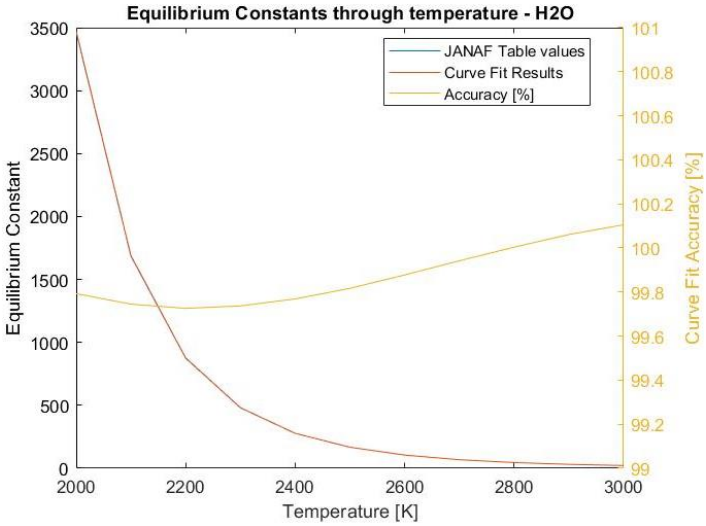


```
Linear model Poly8:
val(x) = p1*x^8 + p2*x^7 + p3*x^6 + p4*x^5 +
              p5*x^4 + p6*x^3 + p7*x^2 + p8*x + p9
  where x is normalized by mean 2956 and std 1794
Coefficients (with 95% confidence bounds):
  p1 =      0.2196  (0.157, 0.2823)
  p2 =     -0.3472  (-0.4011, -0.2932)
  p3 =      -0.664  (-1.004, -0.3242)
  p4 =      0.7997  (0.547, 1.052)
  p5 =       1.127  (0.5372, 1.716)
  p6 =          -1  (-1.351, -0.6497)
  p7 =      0.3264  (-0.02499, 0.6777)
  p8 =       105.3  (105.2, 105.5)
  p9 =       -79.7  (-79.75, -79.64)
```

Figure 22 Original JANAF Table results of equilibrium constants for H_2O through temperature, with the model's curve fitted results and accuracy of fit through temperature. Including polynomial exponents to the 9th degree.

There is two more relationships that need to be mentioned because they allow us to solve each species independently of each other, whereas they are currently ratios, i.e. '$\frac{n_1}{n_3}$'. As mentioned before, we can use the initial known value of carbon from the stoichiometric chemical balance to define the sum of '$n_1 + n_3$'.

$$\varphi C = n_1 + n_3 = n_3\left(\frac{n_1}{n_3} + 1\right)$$

We know already that '$\frac{n_1}{n_3}$' is equal to,

$$\frac{n_1}{n_3} = K_p CO_2 \cdot \left(\frac{n_5}{n_t} \cdot P\right)^{\frac{1}{2}}$$

Therefore,

$$\varphi C = n_3\left(K_p CO_2 \cdot \left(\frac{n_5}{n_t} \cdot P\right)^{\frac{1}{2}} + 1\right)$$

$$n_3 = \frac{\varphi C}{\left(K_p CO_2 \cdot \left(\frac{n_5}{n_t} \cdot P\right)^{\frac{1}{2}} + 1\right)}$$

This situation is the same for that of 'H_2O' in terms of solving for n_4.

$$\varphi H = n_2 + n_4 = n_4\left(\frac{n_2}{n_4} + 1\right)$$

$$\frac{n_2}{n_4} = K_p H_2O \cdot \left(\frac{n_5}{n_t} \cdot P\right)^{\frac{1}{2}}$$

Therefore,

$$\varphi H = n_4\left(K_pH_2O \cdot \left(\frac{n_5}{n_t}\cdot P\right)^{\frac{1}{2}} + 1\right)$$

$$n_4 = \frac{\varphi H}{\left(K_pH_2O \cdot \left(\frac{n_5}{n_t}\cdot P\right)^{\frac{1}{2}} + 1\right)}$$

Moving forward, the full set of equations in relation to each number of species, '*n*', can been seen below.

$$n_3 = \frac{\varphi C}{\left(K_pCO_2 \cdot \left(\frac{n_5}{n_t}\cdot P\right)^{\frac{1}{2}} + 1\right)}$$

$$n_4 = \frac{\varphi H}{\left(K_pH_2O \cdot \left(\frac{n_5}{n_t}\cdot P\right)^{\frac{1}{2}} + 1\right)}$$

$$n_1 = \varphi C - n_3$$

$$n_2 = \varphi H - n_4$$

Considering this set of reactions, if we say the oxygen in singular in each of them, we know the summed value to be, $O_{tot} = 12.5 \cdot (1 \cdot 2) = 25$. Therefore we can say that the sum of the total number of oxygen in each species containing it in the products is equal to that.

$$25 = 2n_1 + n_2 + n_3 + 2n_5$$

$$n_5 = \frac{25 - 2n_1 - n_2 - n_3}{2}$$

And we have already said that we are treating 'n_6' as if it remains constant, i.e. 47.163. The total, 'n_t', is obviously the sum of each of them and this is really where we start at in terms of the iterative solve process. We begin by guessing a value for the ratio of oxygen in the total number of those in the cylinder, '$\frac{n_5}{n_t}$' and using this we can then run through a solve and compare to the final value of '$\frac{n_5}{n_t}$' using the results calculated with the above equations.

Chances are the initial guess will be to low and the solve will require a new guess in terms of initial value and this is why the construction on an effective and efficient algorithm is important for computational time, because there will be a vast amount of iterations for each case and with this investigation, that number of cases is 1,533. For example, the loop generated in MATLAB for this solving mechanism assessed the difference between the guessed ratio to that of the calculated, to check if the error between them was within the confidence bounds set, on average, $x10^{-8}$.

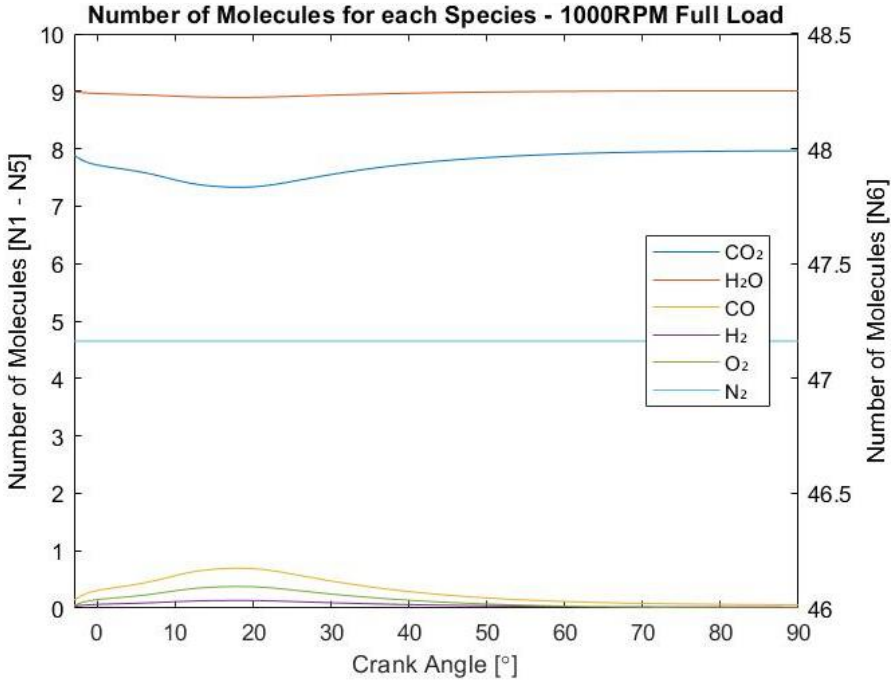

Figure 23 'n' values of each species through crank angle at 1000RPM, FL. 1.5L EcoBoost.

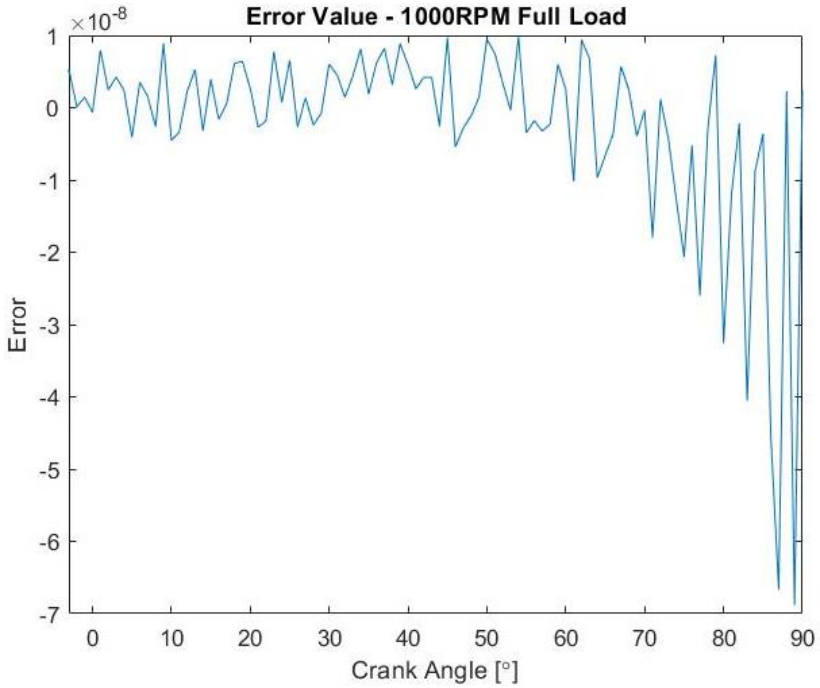

Figure 24 Error between the guessed ratio of oxygen to total moles, Vs the calculated solve through crank angle at 1000RPM, FL. 1.5L EcoBoost.

Considering the validity of the investigation, the modelling technique, and the effectiveness of the algorithm created, the results were compared to reference values of 'n_5' at individual pressures, as temperature increases from 2 – 3000K. Various values of φ were modelled, but because of the number of results in each, the values at $\varphi = 1$ are shown in a figure underneath to demonstrate the accuracy of modelling. Although not obviously comparable, the average accuracy between predicted and those in the reference values is 100.3% across all pressures and all temperature points.

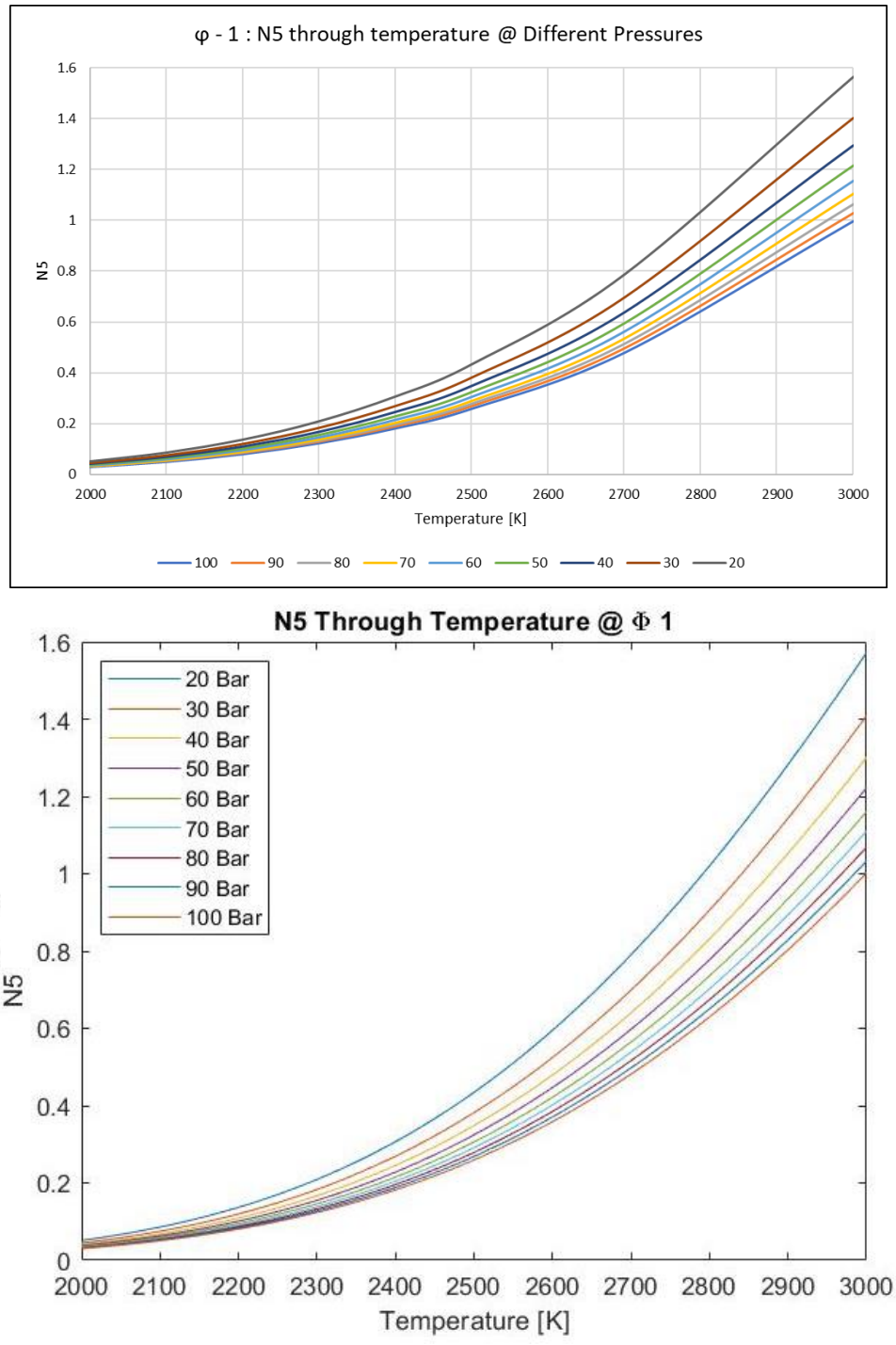

Figure 25 Comparison of the reference [top] Vs modelled [bottom] values of N_5 at various pressures through temperature at $\varphi = 1$.

As for modelling the actual values of nitric oxides production, the methodology and equation used for parts per million prediction are influenced by (Merker, et al., 2006), p. 136 – 138. And although the methodologies explained throughout this report are as accurate as can be, the time taken to reach equilibrium within a combustion reactor varies with temperature. And as can be seen by the following figure, unless the temperature is in the area of 2700 – 2800K, the time required for the system to reach equilibrium exceeds the standard time period that combustion will typically occur over. Hence why prediction of NOx in an internal combustion engine is often a factor out with respect to definite value, unless we use large species chemical reaction kinetics.

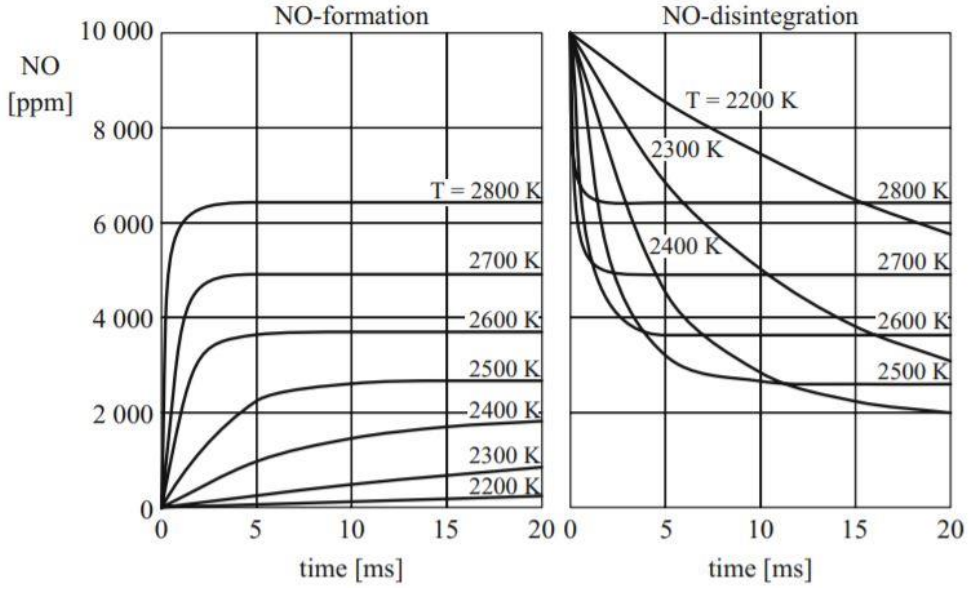

Figure 26 NO formation and disintegration in a thermal reactor. p = 60 Bar, λ 1. (Merker, et al., 2006)

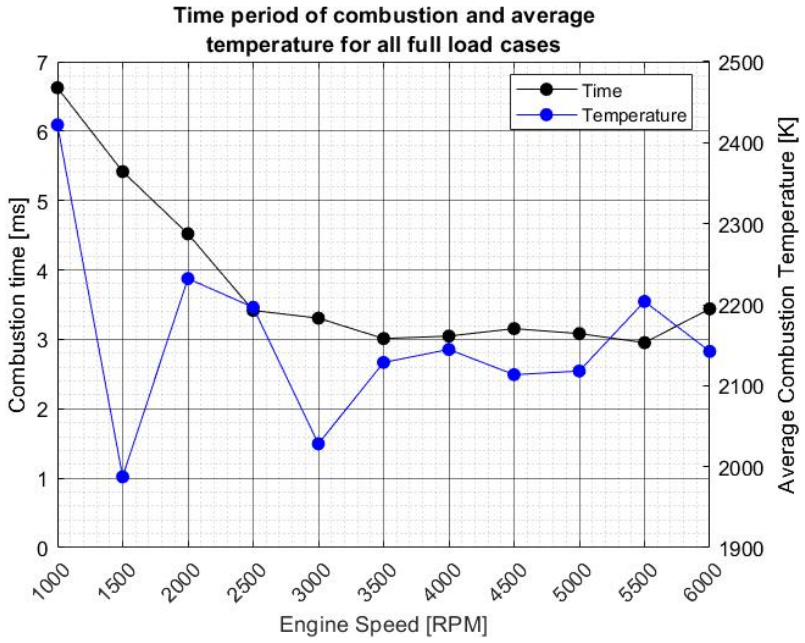

Figure 27 Calculated combustion period and average temperature during, for all full load cases. 1.5L EcoBoost.

Nevertheless, the procedure in which NOx parts per million [PPM] was calculated is explained below.

If we consider again the stoichiometry chemical balance written as;

$$\varphi C_8H_{18} + 12.5(O_2 + 3.773N_2) = {}_{n1}CO_2 + {}_{n2}H_2O + {}_{n3}CO + {}_{n4}H_2 + {}_{n5}O_2 + {}_{n6}N_2$$

We then multiply both sides of equation by alpha, 'α'.

$$\alpha\big(\varphi C_8H_{18} + 12.5(O_2 + 3.773N_2)\big) = \alpha({}_{n1}CO_2 + {}_{n2}H_2O + {}_{n3}CO + {}_{n4}H_2 + {}_{n5}O_2 + {}_{n6}N_2)$$

This multiplier is an equivalent method of finding the number of molecules in the cylinder to then convert the calculated values of oxygen 'n_5', and nitrogen 'n_6' into the correct units.

$$\alpha \cdot (\varphi \cdot Mass_{Fuel}) = Mass_{Fuel\ in\ cylinder}$$

$$\alpha = \frac{Mass_{Fuel\ in\ cylinder}}{(\varphi \cdot Mass_{Fuel})}$$

The fuel type in this case being Iso-Octane makes the '$Mass_{Fuel}$', 114.23 kg/kmol.

The reason for the conversion of 'n_5' & 'n_6' is so they can be used in the following equation proposed by (Merker, et al., 2006), to predict the formation of nitric oxides in the reactor.

$$\frac{d[NO]}{d\mathrm{t}} = 4.7 \cdot 10^{13}\,[N_2][O_2]^{\frac{1}{2}} \exp\left\{-\frac{67{,}837}{T}\right\}$$

$$\left(\frac{kmol}{m^3}\right), \qquad O_2 = \frac{\alpha \cdot n_5 \cdot MFB}{V_b}$$

$$\left(\frac{kmol}{m^3}\right), \qquad N_2 = \frac{\alpha \cdot n_6 \cdot MFB}{V_b}$$

Where 'V_b' is the burnt volume obviously in meters cubed and with the number of calculated species 'n_x', multiplied by alpha, this gives the correct units mentioned above.

$$NO/^\circ = \frac{d[NO]}{dt} \cdot \frac{1}{6 \cdot RPM}, \qquad \left(\frac{kmol}{m^3}\right)$$

$$NO/^\circ = \frac{d[NO]}{dt} \cdot \frac{1}{6 \cdot RPM} \cdot V_b, \qquad (kmol)$$

To calculate in terms of PPM, we need the ratio of 'NO' to the total number of kmol's in the cylinder and this is simply;

$$Total\ Exhaust\ Kmol = \alpha(n_1 + n_2 + n_3 + n_4 + n_5 + n_6) = Total_{Ex}$$

$$NO\ PPM/^\circ = \frac{NO/^\circ}{Total_{Ex}} \cdot 10^6$$

The argument from here on out is the difference between summing the PPM from SOC to EOC, or from SOC to maximum cylinder temperature. When considering the information above in figure 26, along with the reality that the maximum temperature is often not far from the point of $MFB = 1$. And then again on top of that, the equation used to predict formation of NOx from Merker, et al., is in it's their own words, "only to be seen as a crude estimation, as it predicts an excessively high NO concentration".

Because of all these various influencing factors and knowing that the system is most likely not at the point of equilibrium throughout, it was thought that summing to the point of maximum temperature would be the better approach. This is because for one that's the only point equilibrium could really happen in the time frame, plus when assessing various sources for results using chemical kinetic solutions, the reverse reactions that would occur, no matter how small, reduce the overall value of PPM anyway. Albeit these studies have different reference; reactors, speeds, pressures, etc., there is commonality in trend of results regarding the obvious difference between prediction via the assumption of equilibrium, and the use of chemical kinetic solutions when past the point of peak temperature. Therefore the sum of *NOx* PPM in this investigation is found by,

$$NO_x = \sum_{SOC}^{T_{Max}} NO\ PPM/°$$

Figure 28 Estimated NOx PPM per degree at 1000RPM, Full load. 1.5L EcoBoost.

4. 1.5L EcoBoost NOx Modelling Results & Discussion.

The study on Ford's 1500cc EcoBoost engine had complications from the beginning, because of an apparent lack of very important data, EGR% recycled (both internal and external), air to fuel ratio trapped in-cylinder, and UEGO lambda. All of which of fundamental to predicting the correct combustion temperature, and then play a big part in the dissociation model because of the dependence on phi to the number of species.

Results from all studies with be discussed in the same process as methodology is explained for both continuity and it allows for the discussion of sensitivity of each key stage of modelling.

The values inputted into all these models can also be seen below, i.e. fuel mass, air mass, EGR%, etc.

4.1. Mass Fraction Burnt profiles.

The data available for the Ford 1500cc EcoBoost contained the crank angles at which the points of 10, 50, and 90% burnt occurred. Along with the standard deviation of their test results across what is presumed to be 500 cycles, held at that load and speed condition, showing just how much variation that can occur in the engine despite the conditions being apparently identical. The extent of that variation will become more apparent later in the discussion of the 1000cc cyclic model, where despite atmospheric conditions remaining very consistent there can still be a difference in pressures of more than 30 bar. And that is extremely important to this model because we've already seen how much predictions can vary with the slightest change.

Because of the sheer number of results and the difficulty of presenting them as a collective at each load situation, low (20/30%), mid (70%), and high (full load), the best and worst of each case will be shown and discussed.

Low – Load Cases.

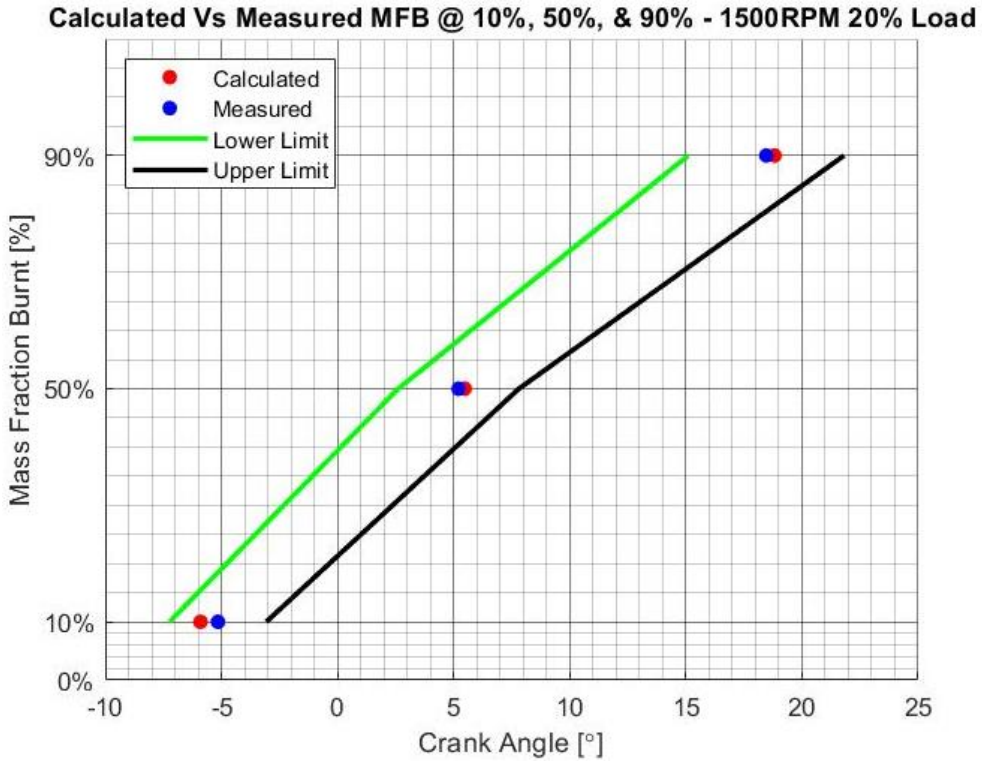

Figure 29 MFB points through crank angle comparison between modelled and those stated by Ford. 1500 RPM, 20% Load – Best Case.

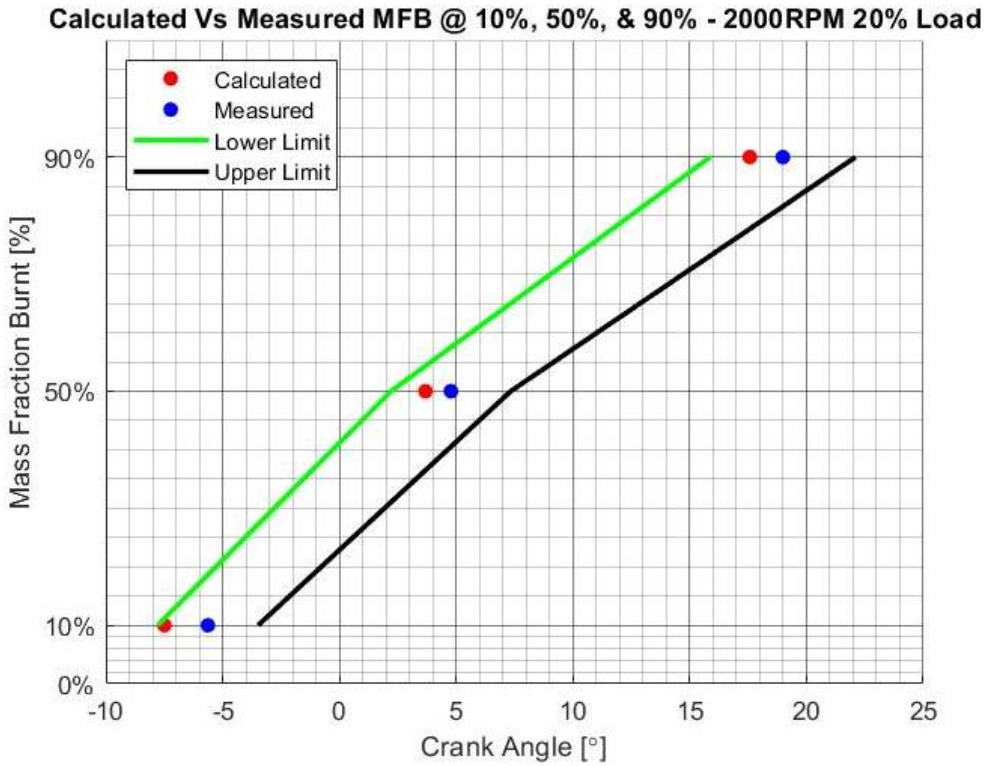

Figure 30 MFB points through crank angle comparison between modelled and those stated by Ford. 2000 RPM, 20% Load – Worst Case.

Mid – Load Cases.

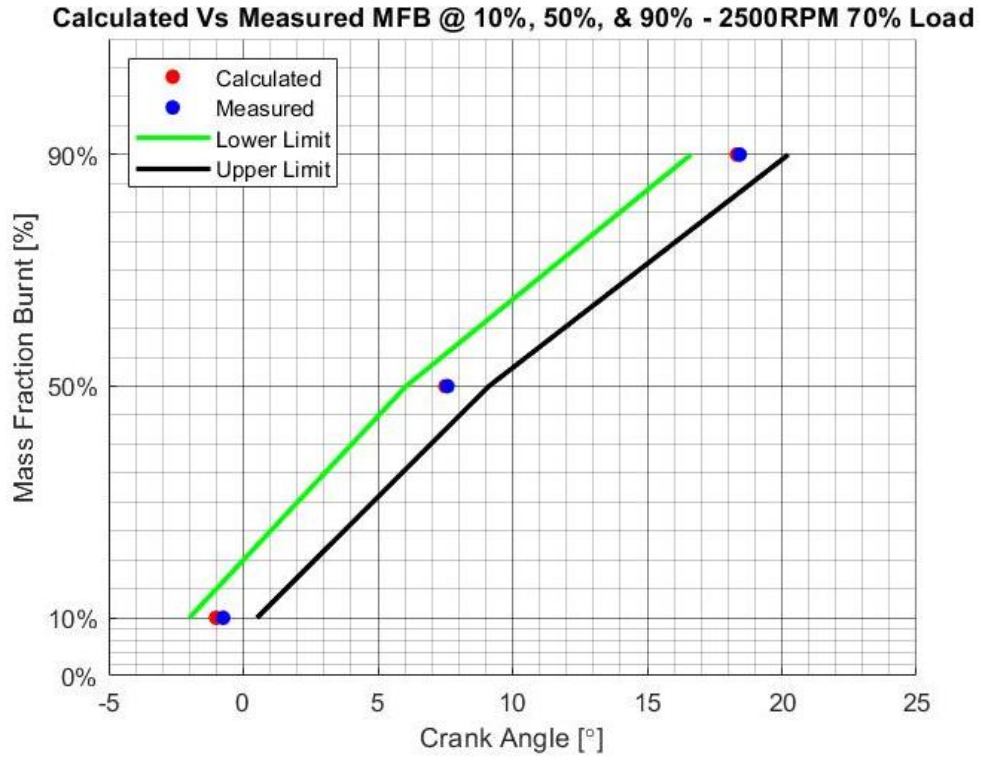

Figure 31 MFB points through crank angle comparison between modelled and those stated by Ford. 2500 RPM, 70% Load – Best Case.

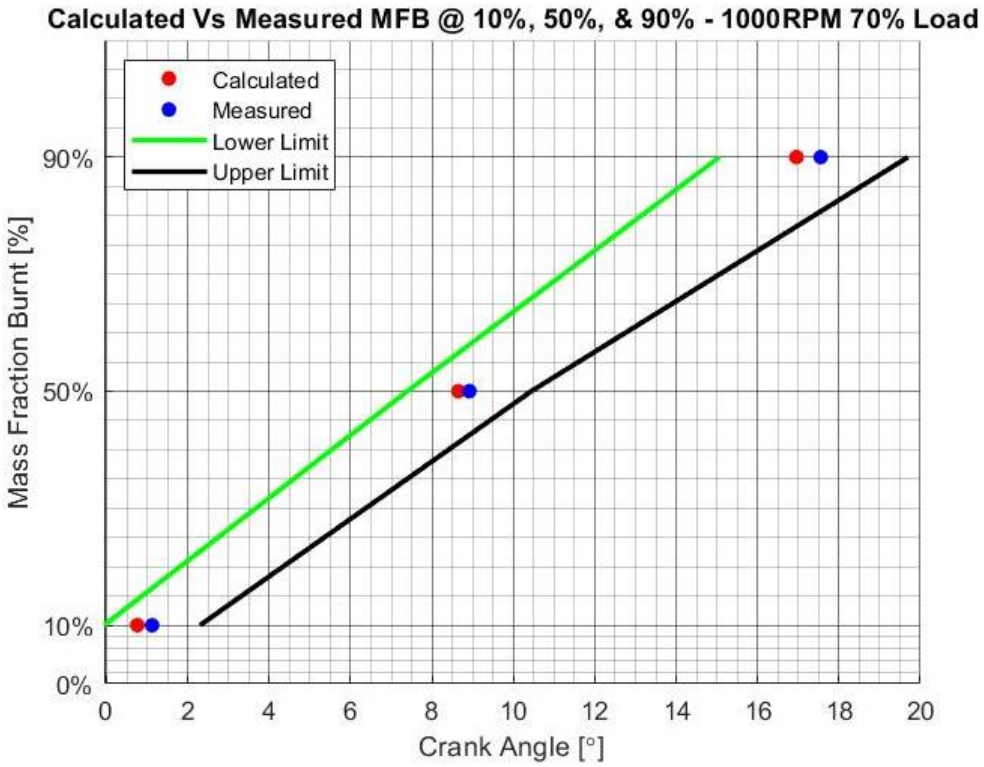

Figure 32 MFB points through crank angle comparison between modelled and those stated by Ford. 1000 RPM, 70% Load – Worst Case.

Full – Load Cases.

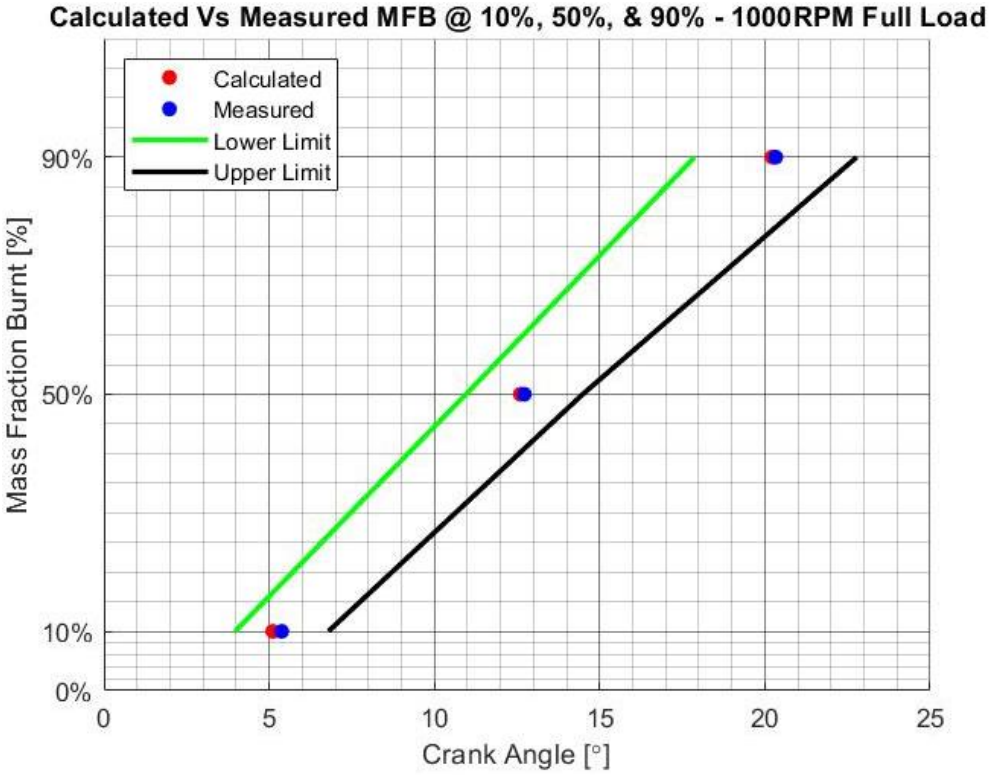

Figure 33 MFB points through crank angle comparison between modelled and those stated by Ford. 1000 RPM, Full Load – Best Case.

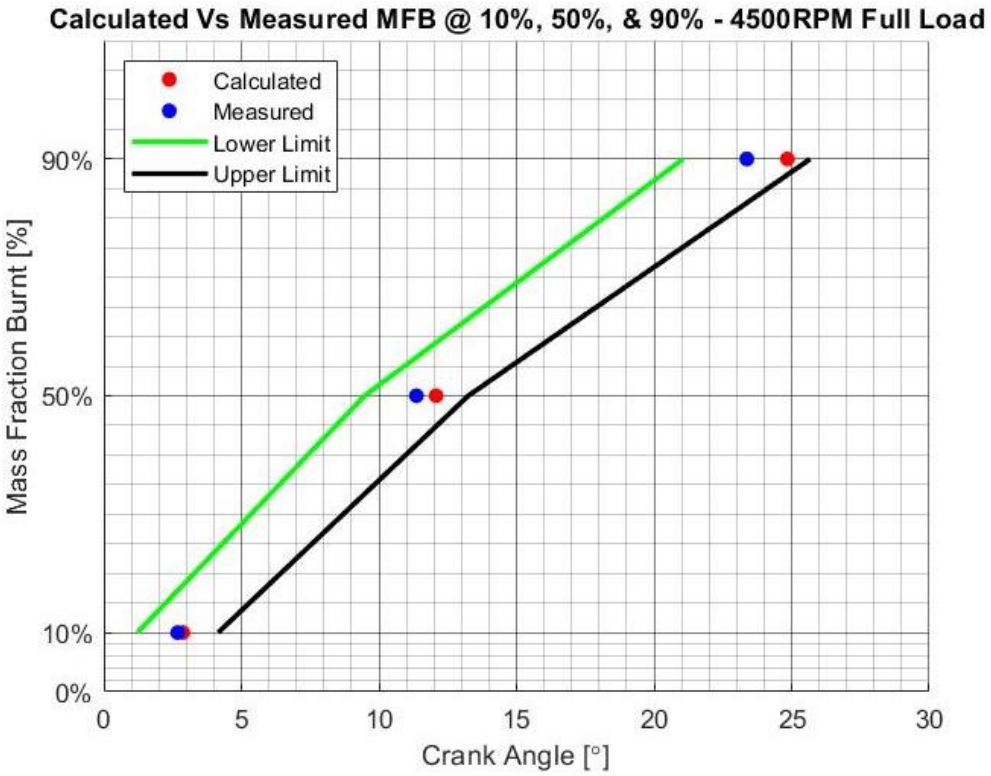

Figure 34 MFB points through crank angle comparison between modelled and those stated by Ford. 4500 RPM, Full Load – Worst Case.

With the points of mass fraction burnt, it is obvious that the modelled values are certainly all within the bounds that Ford also found which poses well regarding both the modelling techniques and values used to find them. And the key with the values inputted is the reliance on the ratio of specific heats for finding these points, and that ratio is found using the unburned temperatures which of course are driven from the collective masses in cylinder.

And although the fuel mass is known to be accurate, there is no guarantee for the air mass. In the sense that the trapped mass will be different to that measured by the MAF in the throttle valve, but also the supposed additional recirculated exhaust gas percentage that had to be estimated based on the torque output from the 1000cc EcoBoost engine. This assumption was made on the basis that with both engines being required to complete drive cycles and with both being fitted to vehicles of similar size and weight, the required torque from each should also be similar regardless of the actual percentage load [because that is displacement dependent]. With that, the high percentage EGR sections of the map, i.e. the low load cases, should be running roughly the same target recirculation, and then the higher load cases shouldn't really be running all that much EGR anyway because they're target is more for MBT than emissions. So it is believed that the masses at the mid load cases shouldn't deviate much from the measured MAF as is. And although the same could be said for the full load situations, with the high mass flow of air at these points joint with the rapidly reducing time available to complete the cycles as engine speed increases, the percentage of internal EGR is expected to increase. This pattern was evident in both the Ford 1000cc data and the Ricardo WAVE model for this engine in particular, the actual number for that trapped is hard to define. Because the valve timing for the smaller engine is vastly different in terms of overlap to that used on the 1500cc, and then there is the fact that the WAVE model has large error percentages at the high engine speed cases, so although the trend of more trapped internal EGR with increasing speed is predicted, the values are thought to be invalid and excessively high.

However, back to the comparison of modelled against stated MFB points, it is also unknown as how Ford have found and defined there points, be it through the typical Wiebe function which is the most common approach and alternative to the Rassweiler-Withrow that was used in this investigation. Or if they were perhaps using an alternative measurement process such as measuring the ionization occurring in the cylinder through the spark plug, as discussed by (Daniels, 1998), to then determine the development of the combustion process and highlight key milestones that relate to the MFB. But as shown with this method (ion measurement), the difference at the end of combustion between methods is considerable, and the point of 90% burn is typically the

one were the accuracy is the “furthest” out, i.e. over or under predicting it’s position. So this could be the method they used which of course changes the volumes of the sections and therefore will influence subsequent modelling, i.e. temperatures and NOx models.

Because of this there is of course always going to be a level of discrepancy between the results, however it has been proven that the techniques work and that the methodology approaches can provide an acceptable level of accuracy [averaged across all cases and all three points as 107.92%], independent of engine speed and load condition.

It should also be mentioned that these are representative of the averaged cylinder pressures from all four cylinders, in each case, which has discrepancies in terms of their peak pressures at that time of measurement, so again this is something to consider in the grand scheme because Ford would’ve had all required data for every run they use to average over. So in terms of validity of this method one could argue that more data at this time would be required, however this is another reason the cyclic data was analysed to mitigate this, along with countless amounts of publications that show this method of prediction works when compared to experimental data.

4.2. Unburned Temperatures.

The modelling of unburned temperatures is a difficult one because there’s no guarantee that the results are definite, because again there’s the potential of some reactions that could occur, additional/reductions of masses in cylinder which change the properties of associated with the gases. And then the knock-on effect here to the volume and temperature of the burnt zone, which then continues onto emissions model changes and could cause either inconclusive, or simply poor results.

However, there is some form of sanity check available in that the temperatures shouldn’t reach over 1000K [≈730 °C] because this will suggest knock occurring at that time, which should lead into a large increase in the maximum cylinder pressure, and or very abnormal combustion profile and this is not evident in any of the data used.

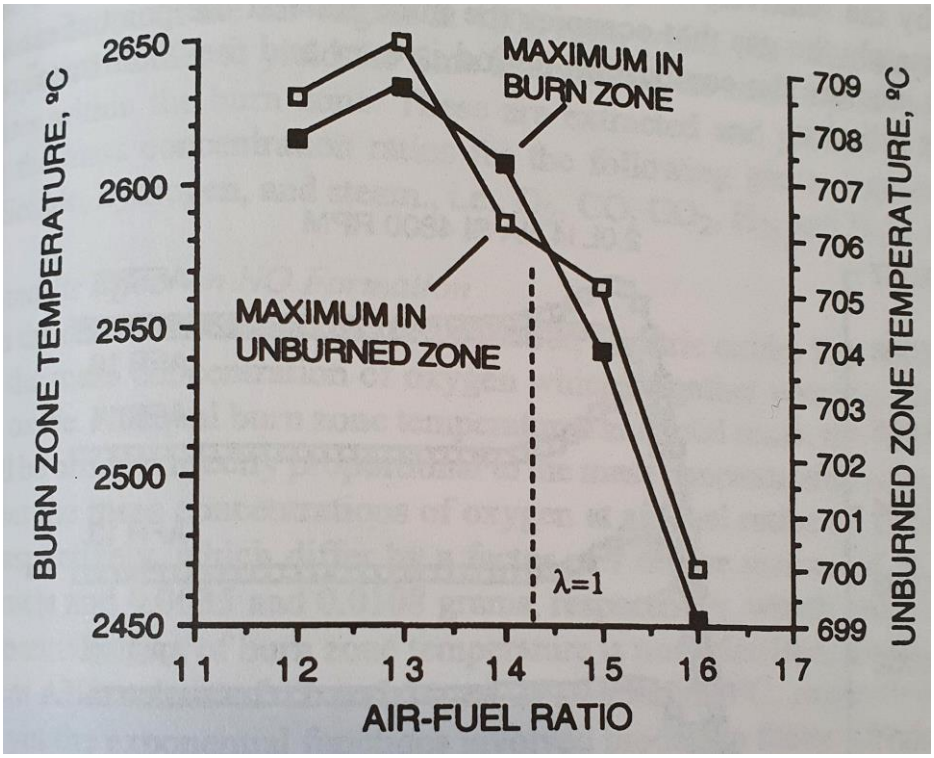

Figure 35 Effect of Air-Fuel ratio on typical maximum temperatures in the burned and unburned zone gases. (Blair, 1998)

Although this knock limit will change with; engine speed, manifold absolute pressure, and the intake air temperatures, as highlighted in the figures below (DI E0 is the most pertinent set of the results), the general rule of thumb is that with the increase of speed and maximum pressure [in a GTDI engine], the greater chance of knock at lower unburned mixture temperatures. This is because although the increased speed reduces time available to auto ignite, we have a reduction in time available for heat transfer to occur, and that naturally causes more chance to induce knock with speed, with the trade off point between the two and worst case scenario typically occurring in the bracket of 1500 – 2500RPM, when at full/high load situations, which is of course essentially at the bottom end of most engine speed ranges, and this is why controlling heat transfer in-cylinder is of such importance because it allows for more efficient operation of the engine in question (Gao, et al., 2021) (Khosravi, et al., 2017).

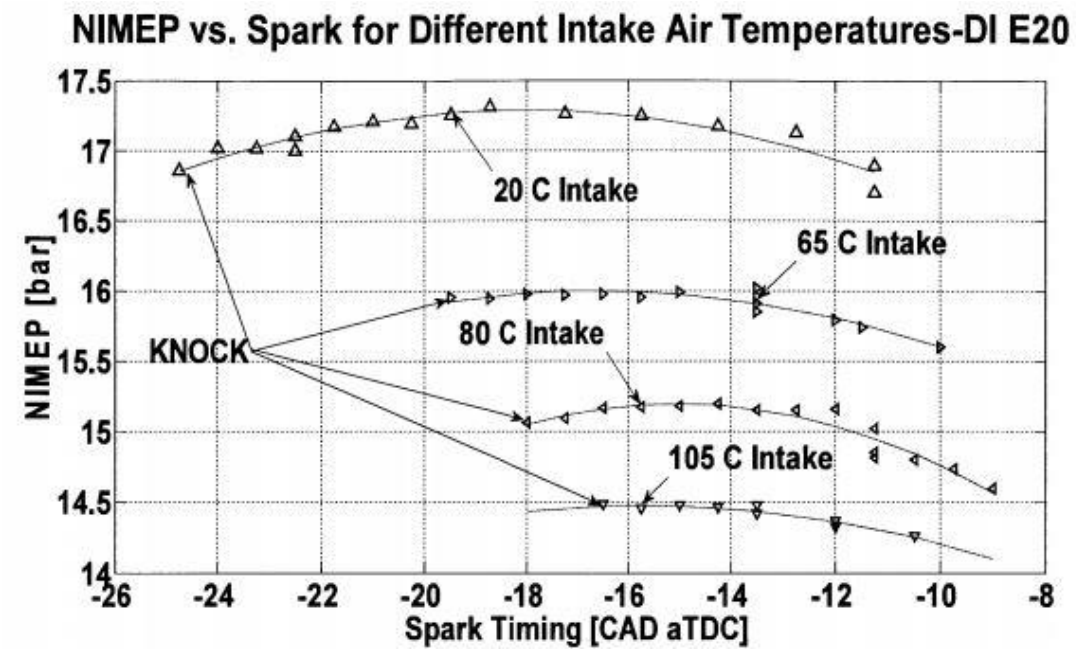

Figure 36 Net IMEP Vs Spark for different IAT's - DI E20 @ 2000RPM & nominal boost. (Kasseris, 2011)

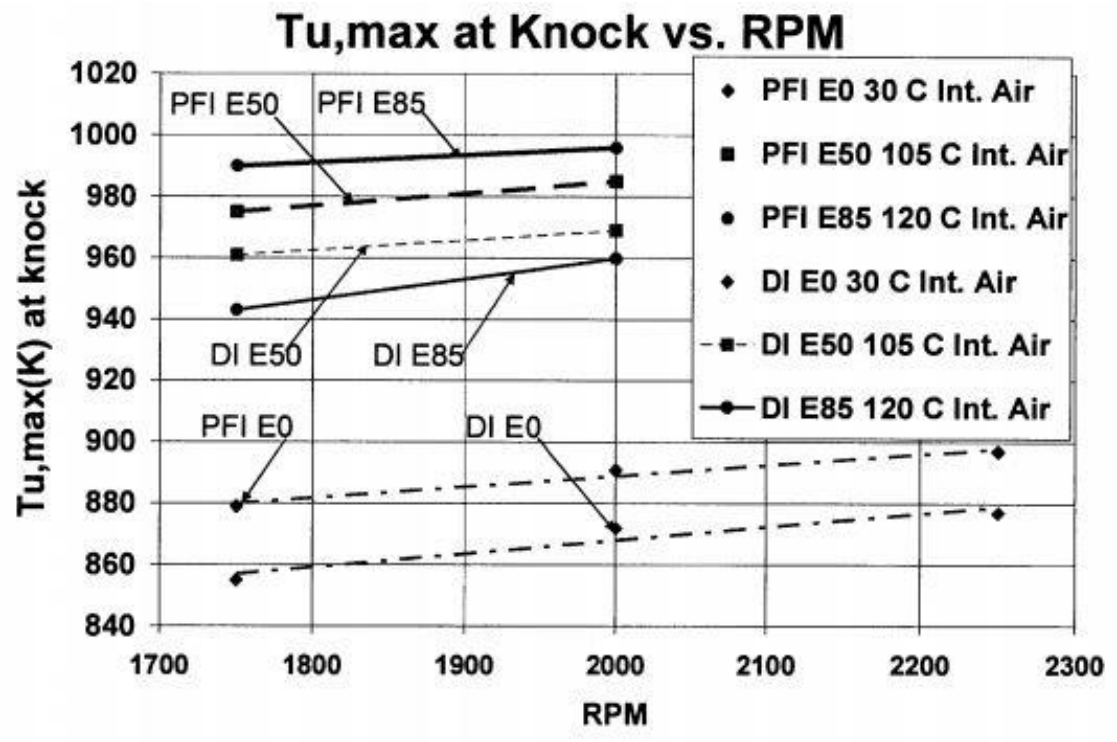

Figure 37 Maximum unburned temperatures at borderline knock Vs Engine speed (Kasseris, 2011).

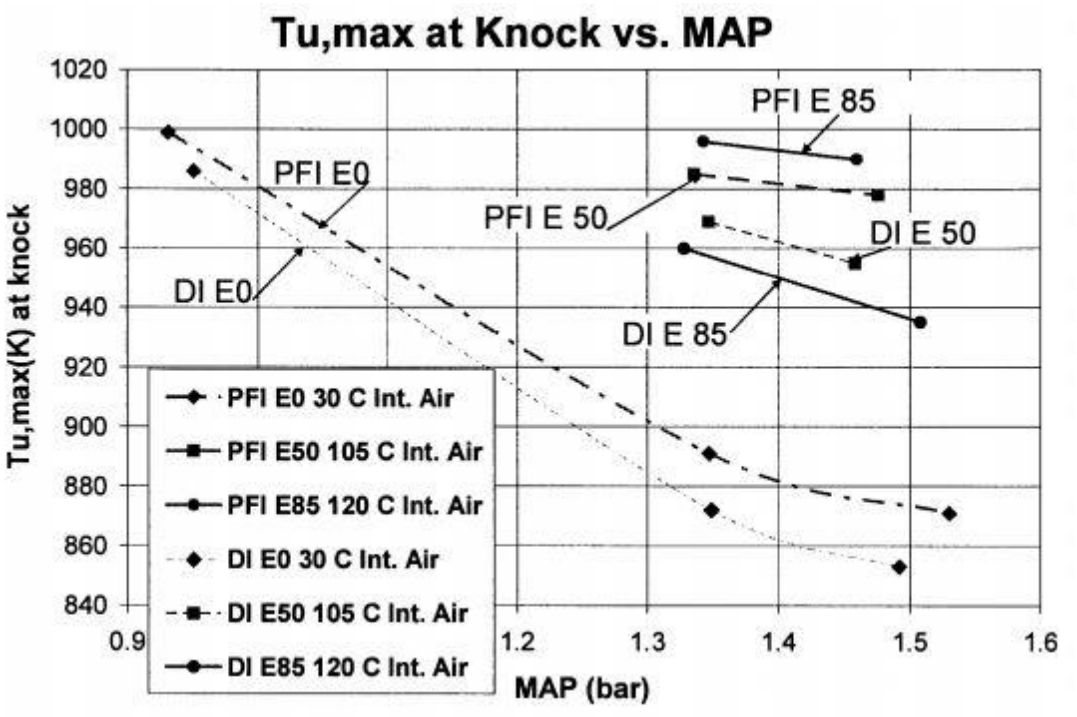

Figure 38 Maximum unburned temperatures at knock Vs MAP for different fuels and fuelling methods. (Kasseris, 2011)

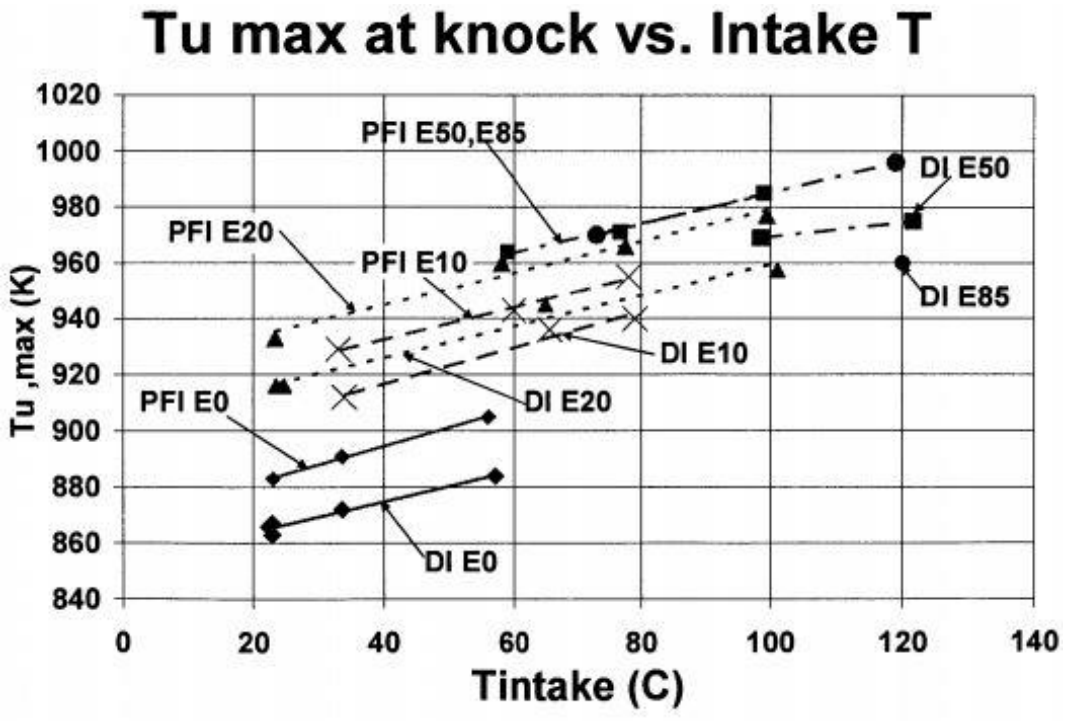

Figure 39 Maximum unburned temperatures at knock Vs IAT @ 2000 RPM, nominal boost condition. (Kasseris, 2011)

Nevertheless, the results for unburned temperatures predicted in-cylinder with the sets from each of the load cases (low-mid-high) are below.

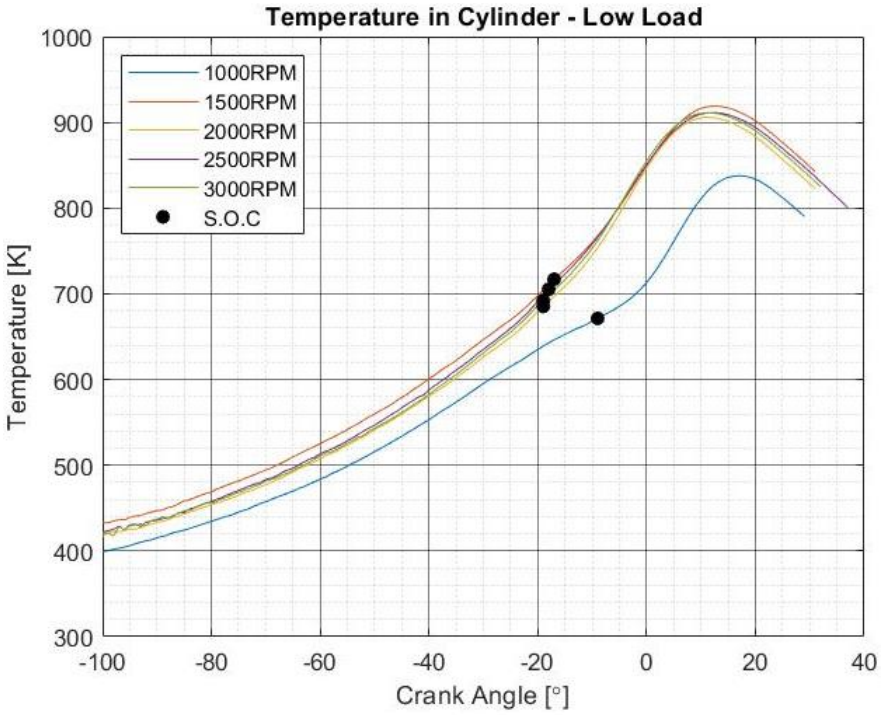

Figure 40 Unburnt gas temperatures predicted at Low load for all speeds. 1.5L EcoBoost.

It should be noted again that the situation for 1000RPM is at 30% load condition, not the 20% condition that all other cases are measured at and although it's not known why this is the case it does give a little more prospective on various points across the load map. It also strange as to how different the profile is considering the load situation isn't far from the others, however when considering the difference in EGR% added, initial boost pressure, and overall mass flow of fuel and air, the reasoning becomes clear. It's thought that Ford are considering this a typical area of operation regarding the slowing of the vehicle, and near idle situations when taking part in the drive cycle it was designed for (NEDC) where there is a considerable period spent on idle and would therefore be looking to bring peak combustion temperatures right down to avoid high levels of harmful emissions. You can also see from the valve timing that they run no real overlap at 1000RPM for the low load cases (up to 50%), and this is thought to be because yes they may incur "higher" pumping losses, but fuel consumption is already at its lowest at this point so the main concern really is the emissions control and by running no overlap, there is both no chance of exhaust gases reversing flow direction out the intake port (inlet gas pressure lower than exhaust because boost is very low), they can also retain exhaust gases and increase EGR% (internal) because there they can't raise the inlet

pressure adequately to entrap external EGR, which therefore drops the zonal temperature, as seen in the figure above, reducing emissions.

Immediately beyond this point, they begin to run a sizable amount of overlap for all speeds above this at the low load cases and this is presumed to be because it allows better “breathing” through the engine and in turn reduces the pumping losses incurred which is a crucial factor in reducing fuel consumption and in turn emissions.

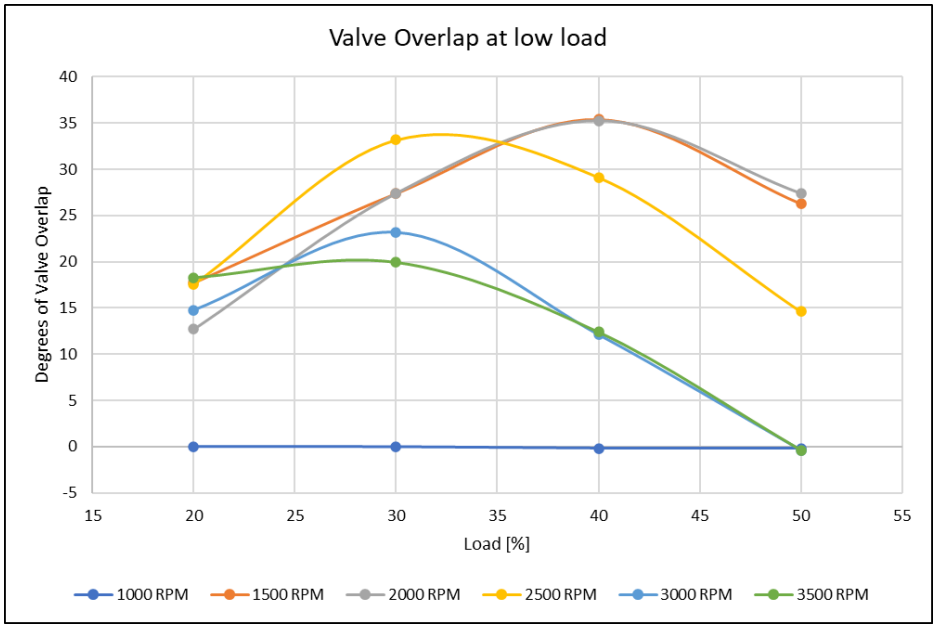

Figure 41 Degrees of valve overlap at the lower load situations (20 – 50%) for the engine speeds typical of the drive cycle.

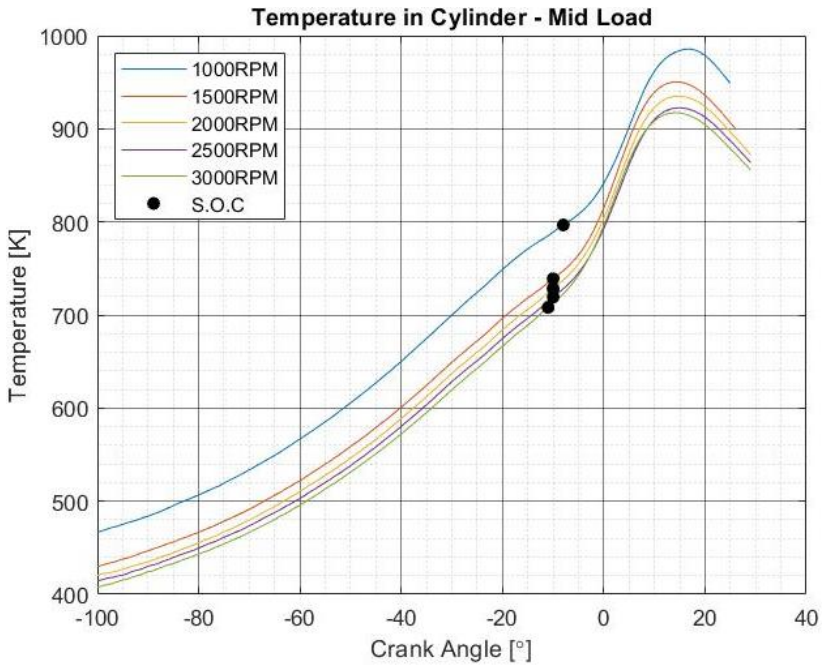

Figure 42 Unburnt gas temperatures predicted at Mid load for all speeds. 1.5L EcoBoost

Here with the mid load situations (70%), the situation is reversed in that 1000RPM is now the highest predicted temperature and this is thought to be because the boost pressures in comparison to all speeds above is “much” higher than that of 1000RPM and because of this the volumetric efficiency is lower and therefore the masses in-cylinder are not high enough to bring the temperatures down. We can see this again from assessing the boost pressures and the degrees of valve overlap for these case, shown in the figures below. Although again it should be mentioned that the temperature is thought to still be slightly too high, but this is only because the definite mass of exhaust gas recirculated is unknown and considering the strong chance that there is going to internal EGR at 1000RPM because the yes overlap is high, but inlet pressure is still relatively low, so further testing/modelling is required.

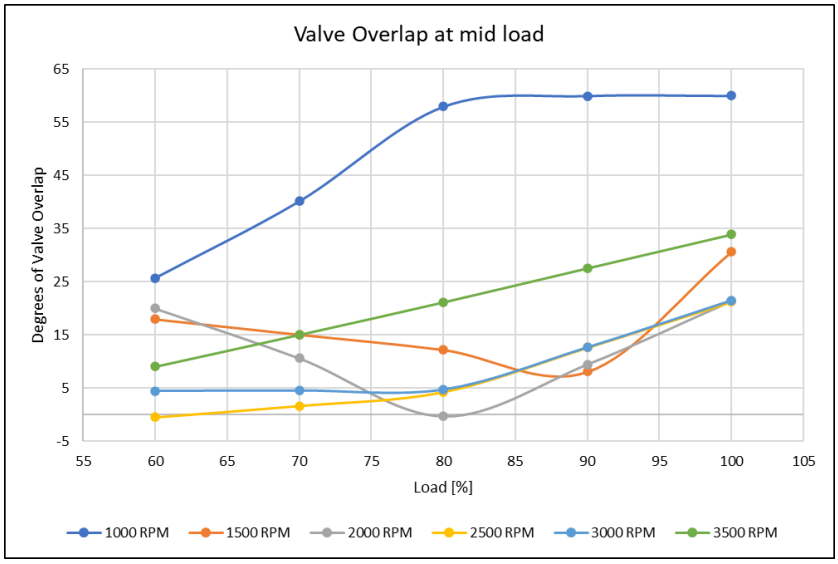

Figure 43 Degrees of valve overlap for the mid load situations (60 - 100%) for all engine speeds typical of the drive cycle.

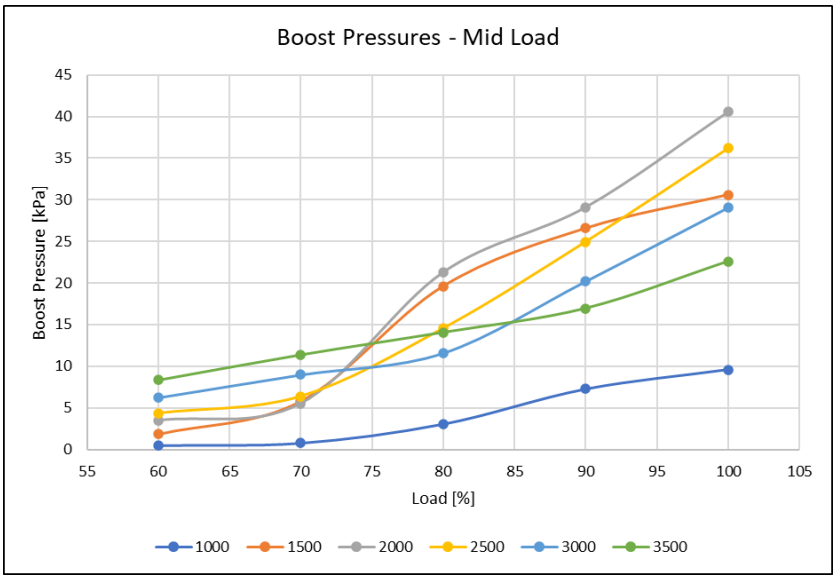

Figure 44 Boost pressure comparison for all speeds typical to the drive cycle for the mid load cases (70%).

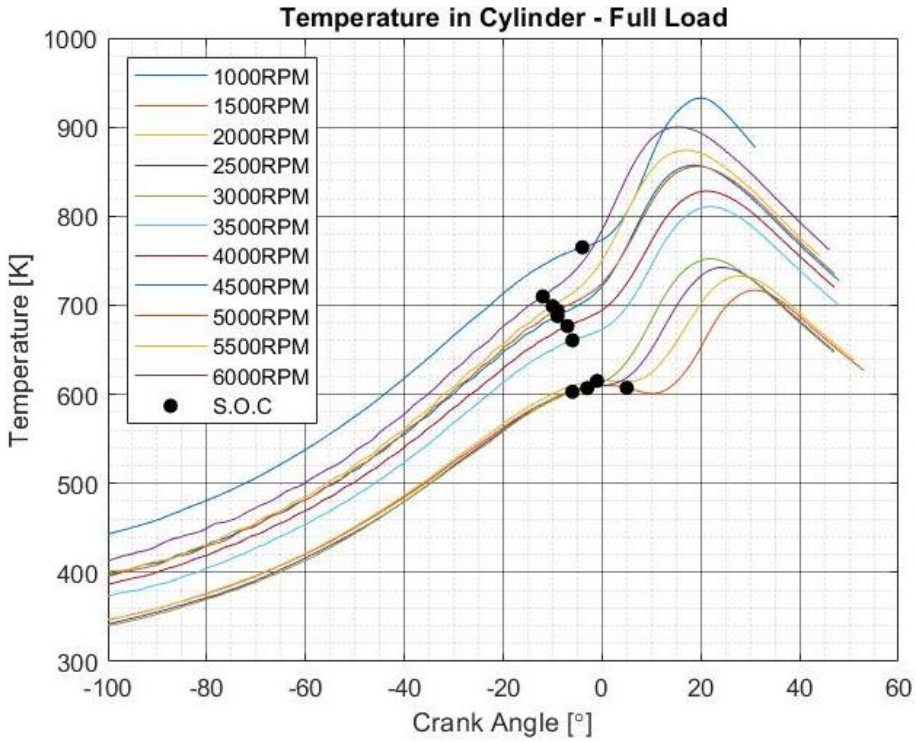

Figure 45 Unburnt gas temperatures predicted at Full load for all speeds. 1.5L EcoBoost.

With the full load situations the trend followed is believed to be as close to reality as possible considering all the assumptions made, because you can see that as the engine speed increases, the temperature goes up in relatively equal steps. As does the timing, spoken about earlier, where you see the lower speeds that are known to be areas of concern for knock the timing is moved forward (retarded), and then as the speed is increased the time available for combustion is reduced and there is going to be a point where there is a fixed speed that the flame can actually travel, so combustion as effectively as they can the SOC has to be moved back so they achieve peak pressure in the correct position relative to crank angle. Although the temperatures are increasing with engine speed, the mass of; fuel, air and EGR, along with fuel equivalency and pressures, also increase and this helps control the limit for knock. But regarding the effect on NOx parts per million, the fuelling ratio has increased enough to offset the exponential increase with temperature from speeds above 4000RPM because the chemical composition will generate more carbon monoxide than nitric oxides, so yes, the PPM does increase, the rate could be a lot worse. As opposed to the points below 4000RPM, the temperatures experienced against the composition in cylinder is not enough to offset the production of NOx compared to CO and this trend is seen in the actual measured data, results below.

It should be pointed out that the 1000RPM case considered here is titled “full load”, but in reality, it’s at a vastly different point of operation compared to the rest, because the engine isn’t capable of making it to the point of 150% equivalent load like the others, it stops at 100%. And as we’ve seen, the calibration techniques and requirements around this area are vastly different to the others and this is the area of the “map” where production of NOx PPM is at its highest, because the temperatures are high because there is next to no EGR used, joint with high pressures, a high enough AFR (closer to stoichiometric) that conversion to nitric oxides is more likely than that too carbon monoxides. And therefore the temperature profile for 1000RPM look’s considerably different and doesn’t follow the same pattern as the rest.

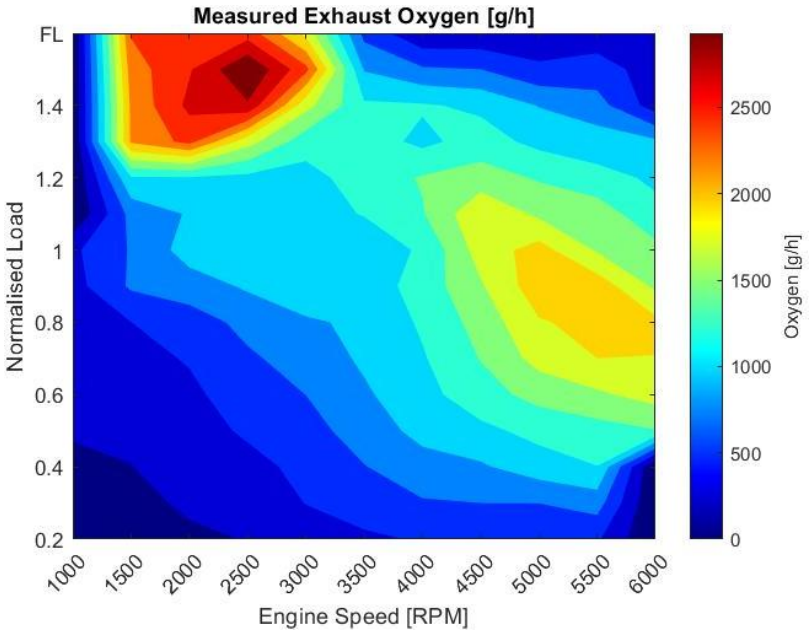

Figure 46 Measured Oxygen content in exhaust gases [g/h]. 1.5L EcoBoost.

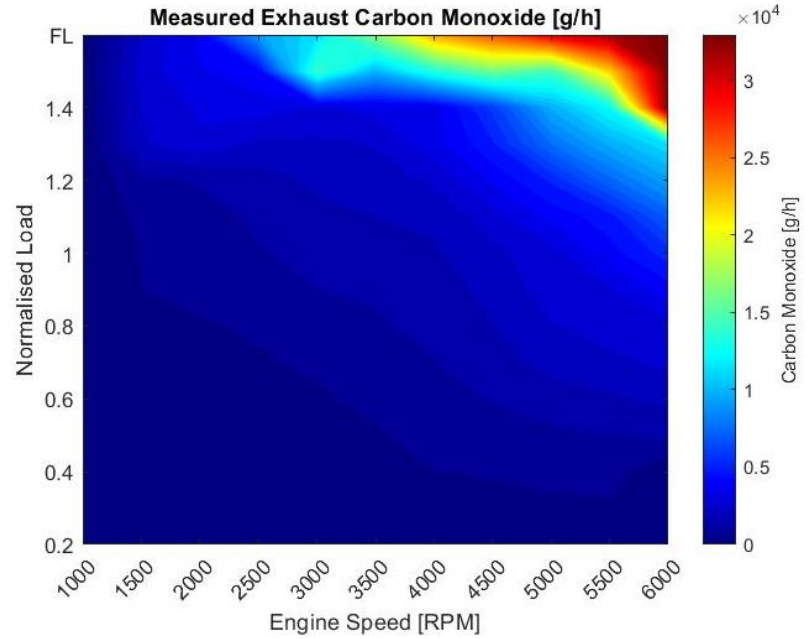

Figure 47 Measured Carbon Monoxide content in exhaust gases [g/h]. 1.5L EcoBoost.

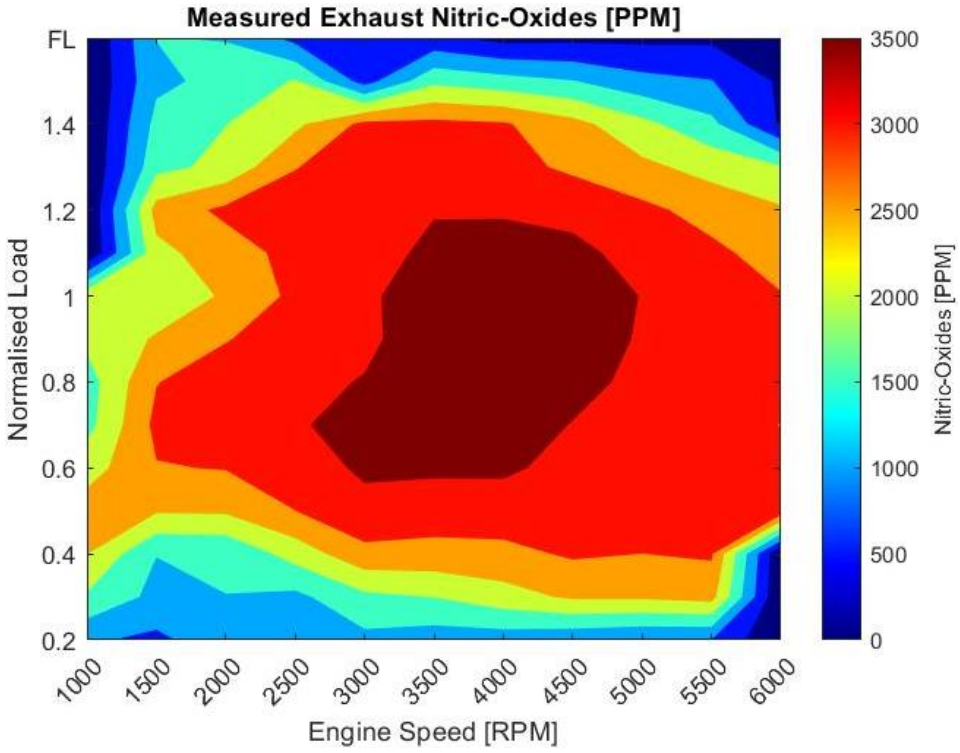

Figure 48 Measured Nitric Oxides in exhaust gases [PPM]. 1.5L EcoBoost.

4.3. Burned Temperatures.

With the burned zone temperatures, obviously the trends shown in the unburned are the same with respect to the position of the peaks and follow the expected trends of peaking a few degrees before peak cylinder pressure, and peak temperature rising as fuel equivalency increases (richer mixture) (Hershey & Paton, 1933).

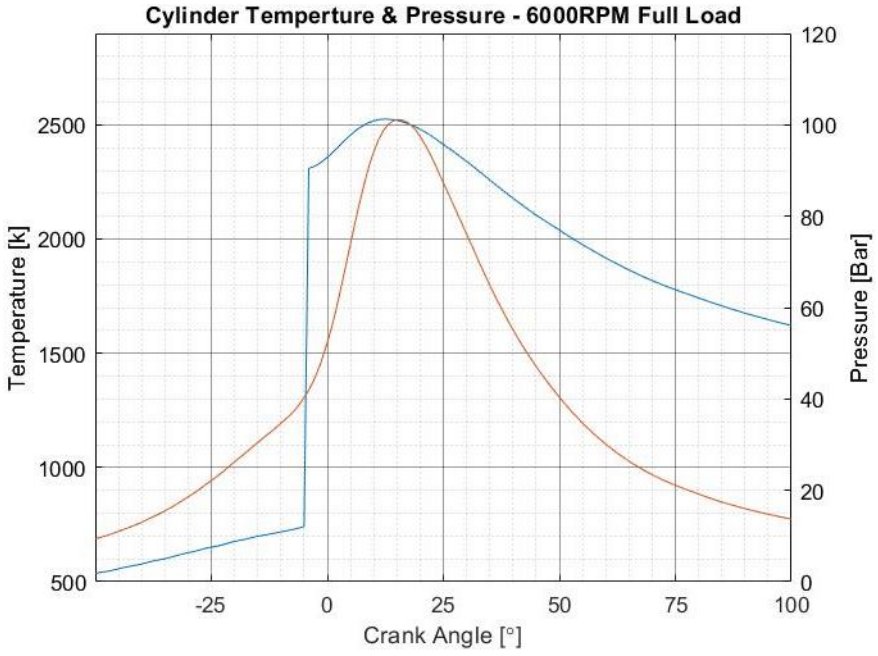

Figure 49 Measured cylinder pressure and predicted temperature at 6000 RPM, Full Load. 1.5L EcoBoost.

Only issue with the modelling found for the burnt temperatures is that at the very beginning of combustion, on occasion the temperature calculation was far from expected and reached unrealistic values and because of that, the position of SOC head to be moved forward to correct this. Often it was only a few degrees (1 – 4), but some of the full load cases were excessive, i.e. around 6 – 9, and this change makes a huge impact on the volume and pressure associated at the time, which is believed to be part of the reason there's issues with respect to trend in NOx PPM calculated and perhaps the value itself but in the grand scheme of things the predicted value is too far from the measured to really make an impact.

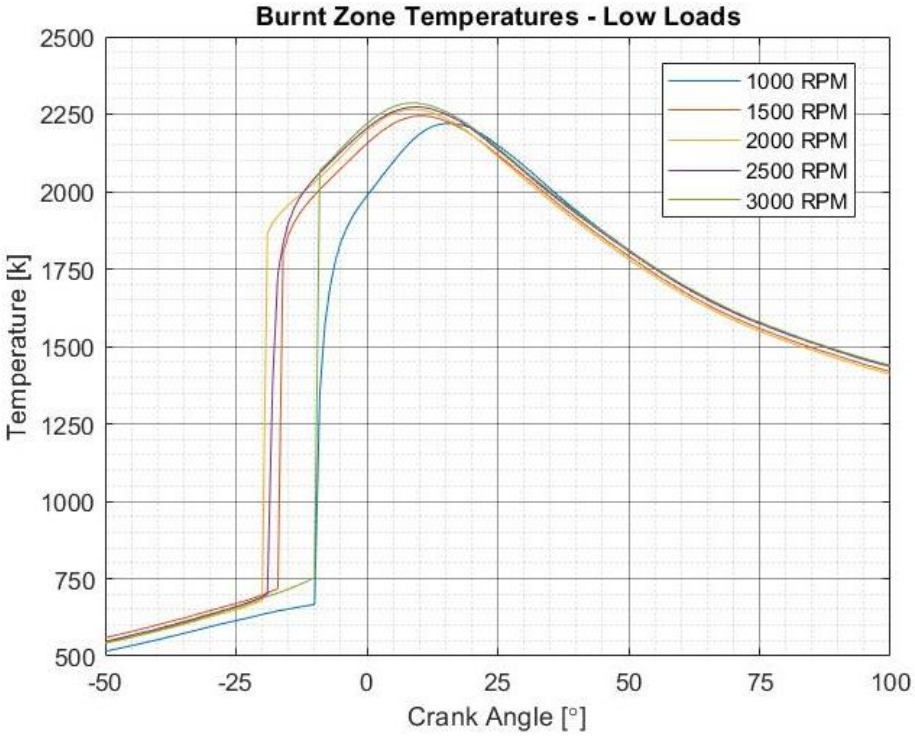

Figure 50 Predicted burned zone temperatures for the low load cases, 1.5L EcoBoost.

These temperatures are presumably a little low, but not inconceivable and are relatively consistent especially after combustion as the piston is moving back down towards BDC. However as mentioned above in terms of having to change the point of SOC forward for the calculation to work properly, the trend of getting worse as engine speed is introduced here as you can see, as the engine speed increases from 1000 – 3000 RPM, the beginning of the curve gets more aggressive and sharp, suggesting that the delay in combustion after initial SOC can cause issues when trying to model and it something that is suggested as further work regarding a proper investigation into perhaps modifying methodology used, or looking to incorporate a correction factor of sorts.

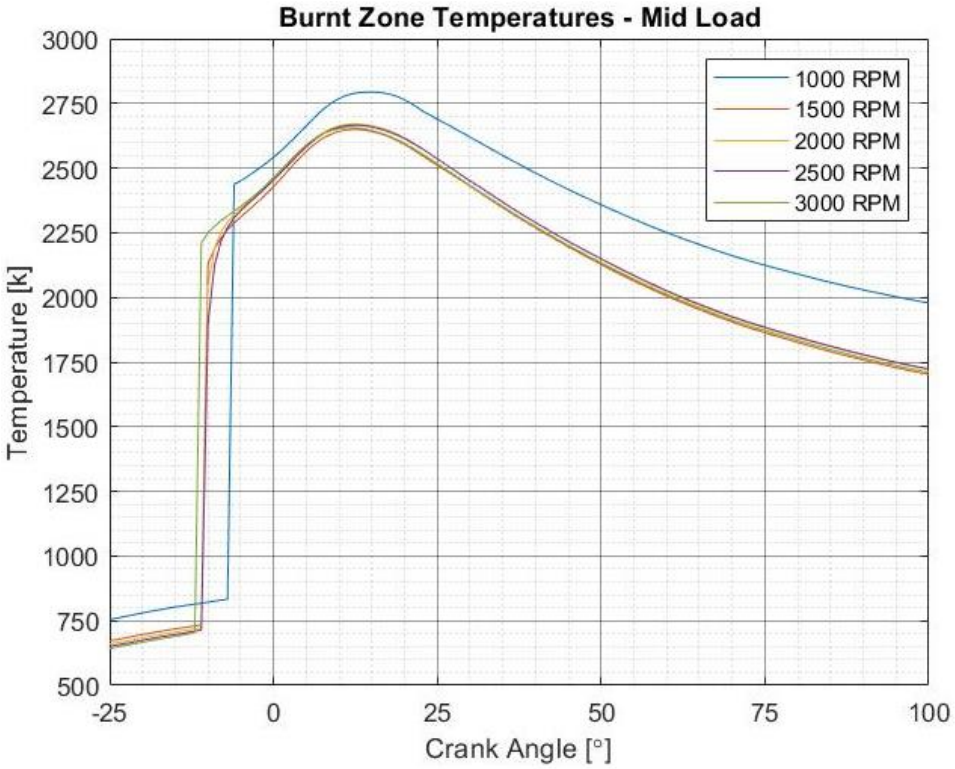

Figure 51 Predicted Burned zone temperatures for the mid load cases, 1.5L EcoBoost.

With the mid-load predicted temperatures, all cases above 1000RPM look exactly as expected considering all aspects of the influencing factors and when assessing parts of the measured data, each of those cases share a lot of similarities, bar 1000RPM that has clearly been calibrated to behave differently. One example of these similarities and differences is the maximum heat release rate crank angle position, where you can obviously see that nearly all the way through from 20% - 100% load, 1000RPM is burning faster causing the greater maximum HRR and this is shown in the calculated temperature profile in that starts later, and yet finishes roughly the same position as the rest, and still peaks higher. Perhaps a little too high, be again this is believed to only be because of the unknown EGR% at this time and considering the clearly different target for operation at 1000RPM, joint with the multitude of differences between the 1L & the 1.5L engines, only way to really know would be to run tests which of course wasn't an option at the time.

This higher peak in the heat release rate for 1000RPM is also believed to be the reason why NOx PPM is higher than various points at the same load at higher engine speeds, specifically the range of 20 – 50% load.

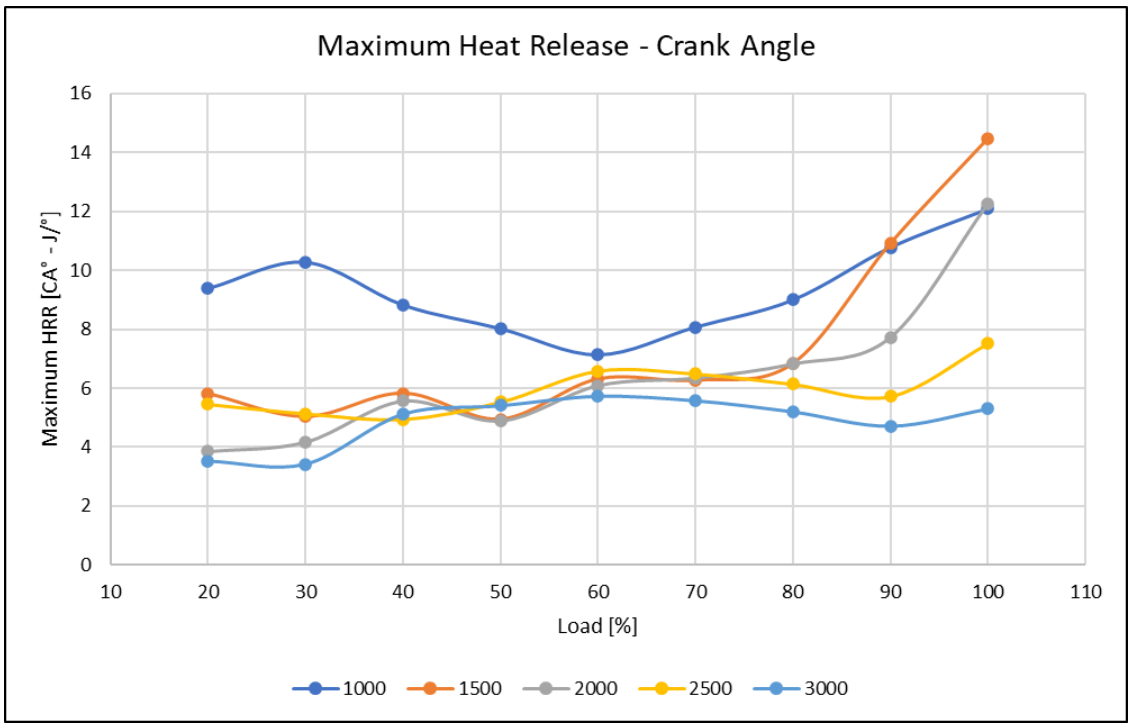

Figure 52 Crank angle position of maximum HRR for load cases of 20 - 100% at the lower engine speeds. 1.5L EcoBoost – Measured.

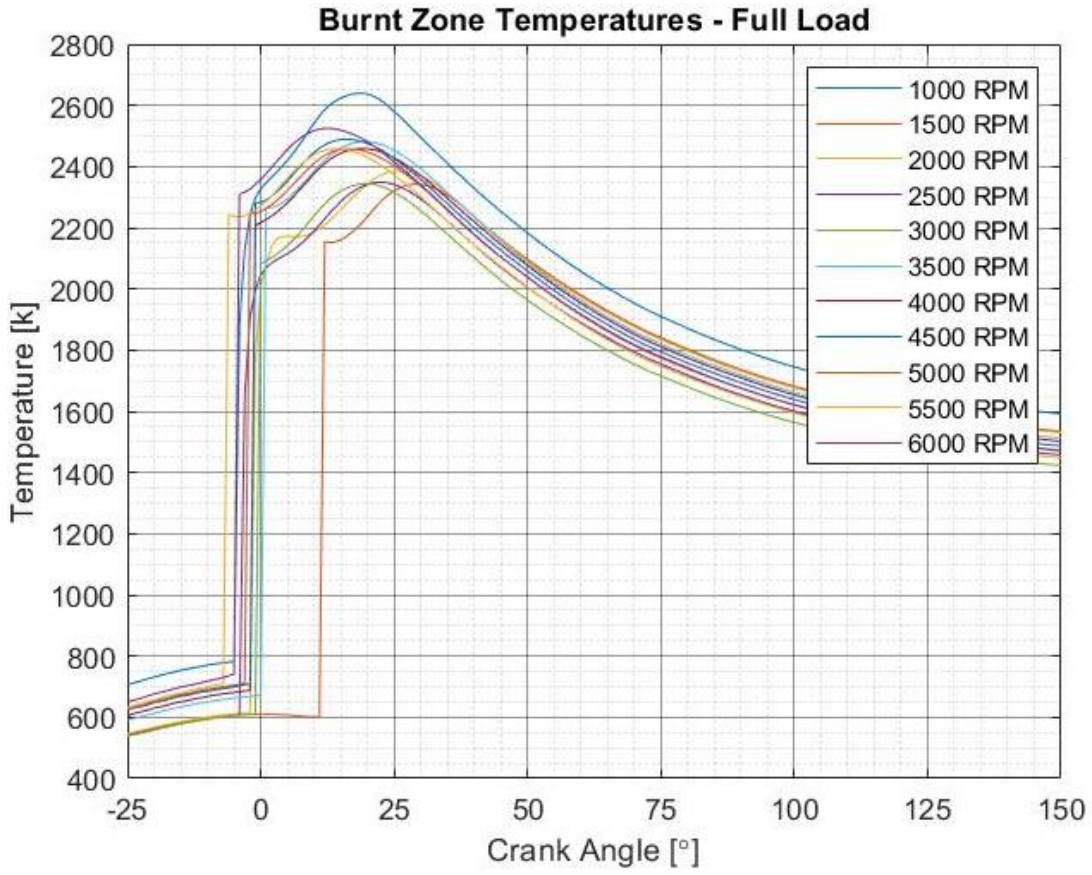

Figure 53 Predicted Burned zone temperatures for the high load cases, 1.5L EcoBoost.

With the full load cases we can see the issues of having to move forward the apparent SOC, which of course changes the volume at the time and the duration for production of chemical species up to the point of maximum temperature. Even more so at full load because heat release is high and combustion is happening fast, so the reduced period has a profound effect on the results trend, and this will be discussed in the following section.

Last note on these temperature profiles is that when at the higher end of the bracket expected, 2600K+, the effect on the calculated dissociation models relays very well with what (Merker, et al.) mention about how the predicted NOx values can be grossly high compared to actual measurements.

4.4. NOx Modelling.

The modelling of NOx PPM for the 1500cc EcoBoost engine proved to be very difficult and in none of the cases were the results close with respect to actual value, however trends were shown to match in the low load cases and a few of the higher load cases can be seen to show correlation. There is such a strong dependence of fuel equivalency for these models and because neither the AFR in cylinder, nor the more accurately measured UEGO (Universal Exhaust Gas Oxygen sensor) lambda are known, multiple variations of calculation were tried throughout the different loads at 1000RPM to find the most appropriate. The steps of the study can be seen below;

Calculation methods are as follows,

$$\frac{1}{\frac{\left(\left(\frac{Mass_{Air}}{Mass_{Fuel}}\right)\cdot\left(1+\left(\frac{EGR_{\%}}{1-EGR_{\%}}\right)\right)\right)}{14.35}}, \qquad [Eq\ 1]$$

$$\frac{1}{\left(\frac{\left(\frac{Mass_{Air}}{Mass_{Fuel}}\right)}{14.35}\right)}, \qquad [Eq\ 2]$$

$$\frac{1}{\lambda_{PCM}}, \qquad [Eq\ 3]$$

$$\frac{1}{\lambda_{Dyno}}, \qquad [Eq\ 4]$$

The 14.35 being used is what is being taken as the stoichiometric point for the 98RON fuel used during the test, as stated on the BorgWarner compressor data.

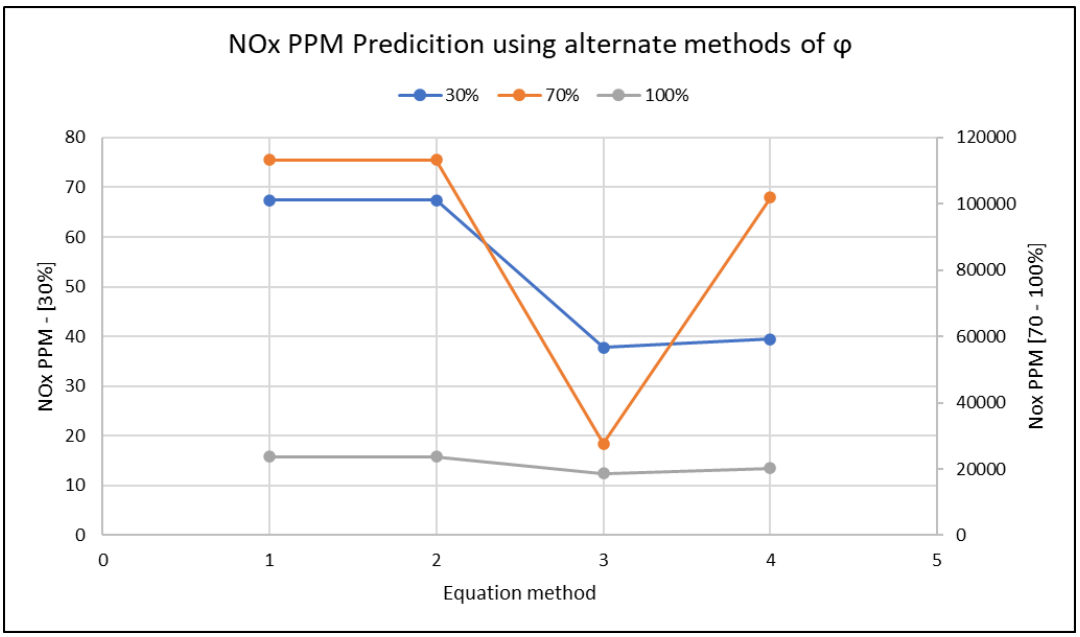

Figure 54 Results of NOx PPM predicted using alternate methods for φ for the load cases across 1000 RPM for the 1.5L EcoBoost.

The secondary method [*Eq 3*] is shown to be the "best" option to use because it brings the exponentially high results for 70% & 100% load down but does unfortunately result in a woefully low result for 30% load. The main reason for the change is the difference either side of stoichiometric and we can see from the table below that results for mid and high load are better when the fuel equivalency is rich, whereas all other equations change it to be apparently lean, with the opposite situation occurring at 30% load where the leaner equivalency provides better results. The effect of the addition of EGR, but really the dependency of fuel equivalency, can be seen in the small sensitivity study conducted using data from the full load case at 1000RPM where the change either side of $\varphi = 1$ to $\varphi = 0.95$ & $\varphi = 1.05$ change the predicted PPM from 18218.79 to 8110.29 respectively. Along with the addition of only 5% EGR that drops results dramatically which is massively important knowing at full load there's strong chance of internal EGR being trapped, up to around 7% at 6000RPM.

Fuel Equivalency		0.95	1	1.05	1.1	1.15	1.2	1.25
EGR [%]	0	18218.80	19967.80	8110.29	3176.97	1413.81	677.00	294.43
	5	4307.66	1961.42	1436.11	497.55	207.61	88.43	14.78
	10	1087.32	336.77	108.43	75.20	28.11	4.64	0.15
	15	257.88	58.93	16.14	3.53	1.91	0.22	0
	20	61.27	9.42	1.17	0.13	0	0	0
	25	14.58	1.39	0.01	0	0	0	0
	30	3.48	0.03	0	0	0	0	0

Figure 55 Sensitivity study results of change in φ and EGR at 1000RPM Full load.

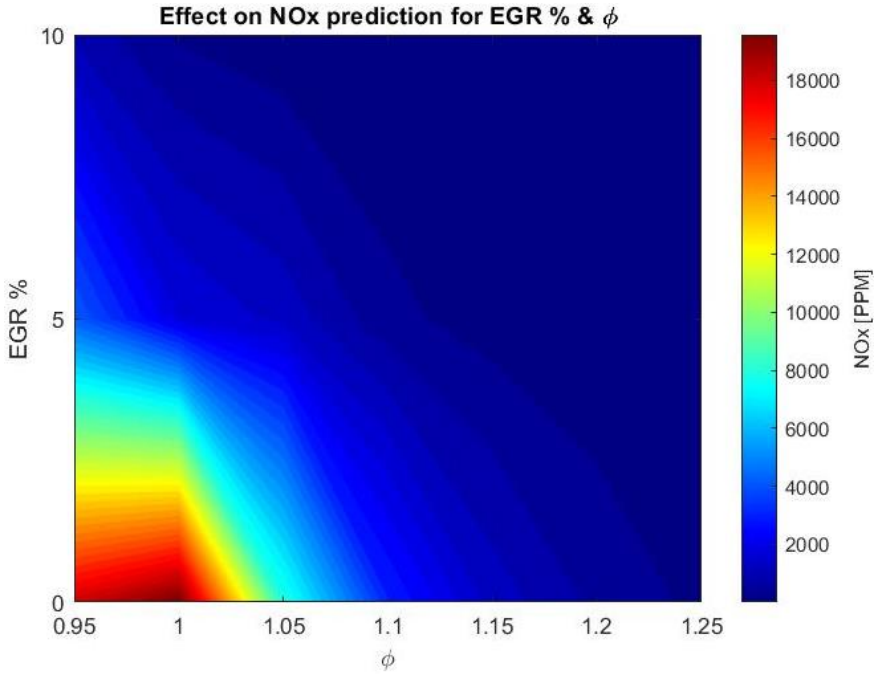

Figure 56 Contour map of results of NOx PPM predicted through the sensitivity study at 1000 RPM Full load for EGR % and φ.

Another small study was conducted again to show the modelling dependency on temperature and how important it is to have that correct during too. The study was set as if the temperature remains constant throughout combustion at $\varphi = 1$ and with no EGR added for the conditions attached to 1000RPM full load and as can be seen, the difference of even 50K on average through combustion can change the NOx PPM predicted by nearly two-fold.

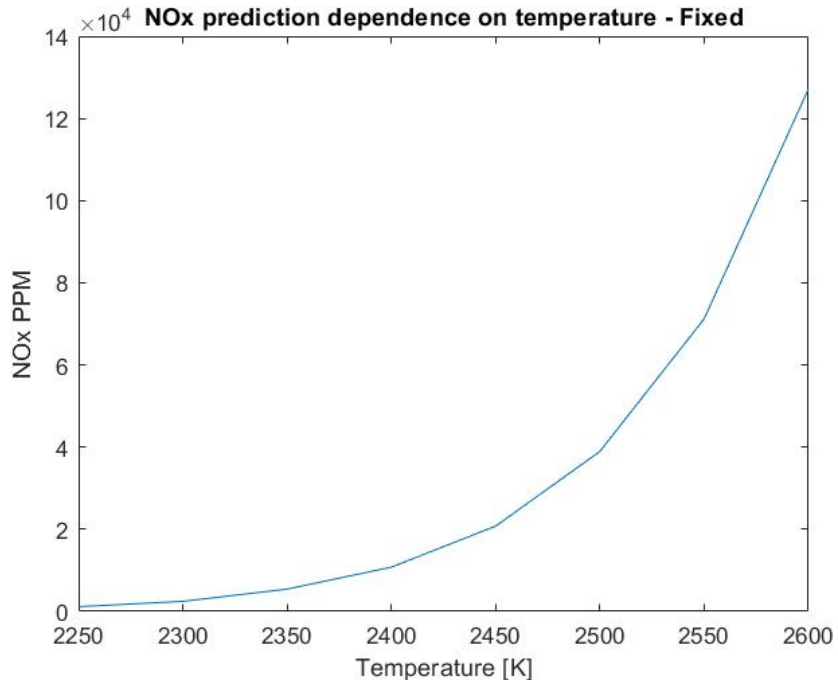

Figure 57 Dependence of NOx modelling on temperature through combustion.

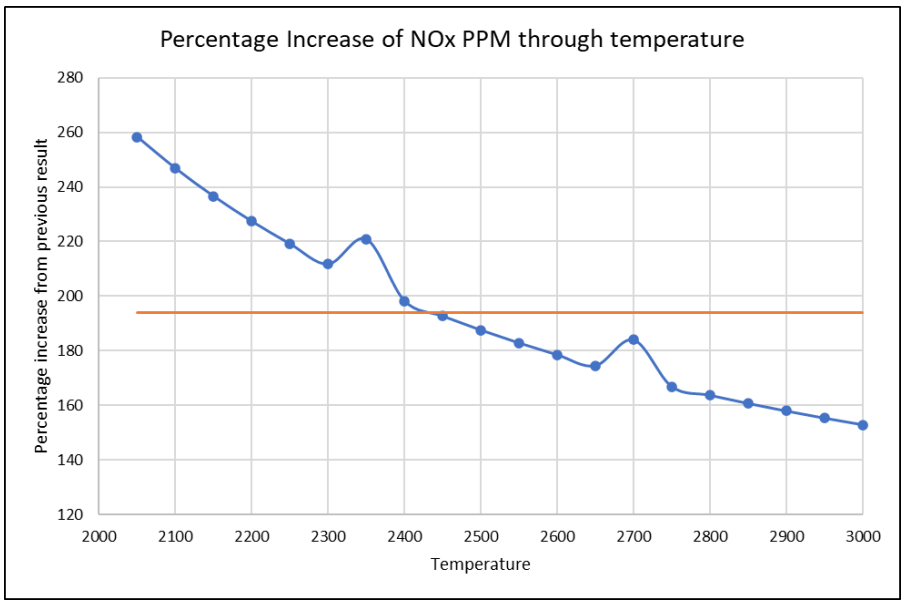

Figure 58 Percentage increase from previous result of NOx PPM calculated for temperature dependence study.

As we can see, the accuracy of this type of modelling is extremely sensitive to essentially every input and this is why it can be so difficult to get reliable, and more importantly useful results that could in turn be used in the real world, in real time, to run predictive combustion modelling in vehicles to help actively control emissions on the road. Either way, the results of the study on the 1.5L EcoBoost can be seen below.

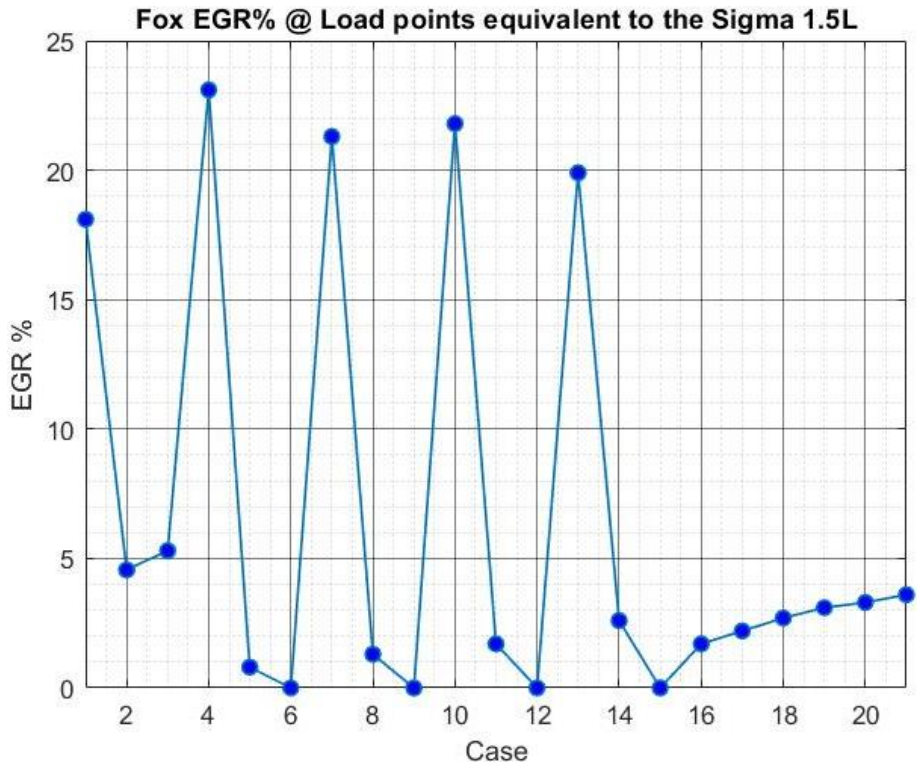

Figure 59 EGR percentage being recycled into each case taken from equivalent position of the 1L EcoBoost map. The cases are for each engine speed as load increase, so there's 3 for all up to 3000RPM after which there is only full load cases.

The point of “full” load at 1000 RPM [case 3], has been changed to 5.3% because the result was grossly high (order or 10^5) without any addition, which is clearly inconceivable when using the map from the 1L. And when using results from the sensitivity study, it showed that with the fuel equivalency for this case, the required EGR% was in the area of, hence the addition. It should also be mentioned that for future modelling the 1L has vastly different valve timing principals throughout the map, along with lower inlet pressures, higher temperatures, and different spark timing. So it’s believed that Ford are using a different philosophy at, at least 1000 RPM for the 1.5L than they do the 1L, specific reasons are unknown, meaning the percentage of exhaust gas they recirculate here has the definite potential to not follow the expected norm or the torque equivalent value.

The last addition before the results is a brief explanation of the algorithm created in MATLAB to run through the dissociation modelling for each of the cases. The principal is relatively straight forward and runs basically on a few different exit criteria for a series of “loops” that will assess the currently calculated value of ‘N_5’ and compare to the guessed to find the error percentage, if in the range deemed acceptable the loop moves to the next degree of crank angle, otherwise it changes the guess and runs again. A couple additions were required because it was easier to generate the code to run through the entire section of crank angle (720°), there is points where the calculated influences are widely out of correlation and result in a negative value of oxygen, hence these are skipped and left as zero. There is also some points where the either the calculated value, or the error percentage were independently in the correct range, hence there is another exit criterion under those mentioned to simply account for this and stop the occurrence of “infinite” loops.

```
while i < length(Crank_Angle) + 1

    while LeaveOKFL == 0

        N3_NTGOKFL(i,1) =
CNoLOKFL/((KpCCO2OKFL(i,1)*(N5_NTGOKFL(i,1)*AvgCYLPOKFL(i,1))^0.5)+1);

        N1_NTGOKFL(i,1) = CNoLOKFL - real(N3_NTGOKFL(i,1));

        N6_NTGOKFL(i,1) = NNoLOKFL;

        N4_NTGOKFL(i,1) =
(HNoLOKFL/2)/((KpCH2OOKFL(i,1)*(N5_NTGOKFL(i,1)*AvgCYLPOKFL(i,1))^0.5)+1)
;

        N2_NTGOKFL(i,1) = (HNoLOKFL/2) - real(N4_NTGOKFL(i,1));
```

```
        N5CalcOKFL(i,1) = (ONoLOKFL - (2*N1_NTGOKFL(i,1)) -
N2_NTGOKFL(i,1) - N3_NTGOKFL(i,1))/2;

        NtotalOKFL(i,1) = (N1_NTGOKFL(i,1) + N2_NTGOKFL(i,1) +
N3_NTGOKFL(i,1) + N4_NTGOKFL(i,1) + N5CalcOKFL(i,1) + N6_NTGOKFL(i,1));

        CalcN5NTOKFL(i,1) = real(N5CalcOKFL(i,1)/NtotalOKFL(i,1));

        errorOKFL(i,1) = real(CalcN5NTOKFL(i,1)) - N5_NTGOKFL(i,1);

        if N5CalcOKFL(i,1) < 1*10^-6 && N5CalcOKFL(i,1) > -1*10^-6
            LeaveOKFL = 1;

        elseif errorOKFL(i,1) > ecOKFLa

            N5_NTGOKFL(i,1) = N5_NTGOKFL(i,1) + 1*10^-8;
            LeaveOKFL = 0;

        elseif N5CalcOKFL(i,1) < 0

            N5CalcOKFL(i,1) = 0;
            LeaveOKFL = 1;

        elseif errorOKFL(i,1) < ecOKFLa && errorOKFL(i,1) > -1*10^-5
            LeaveOKFL = 1;

        else

            LeaveOKFL = 1;
        end
    end

    i = i + 1;
    LeaveOKFL = 0;
end
```

As mentioned, the calculation is run is a pair of 'while' loops that the external is made to run through each angle and the internal loop calculates the correct value of 'N_5' to within bounds and then exits to restart. The series of 'if' statements are the exit criterion checks which allow to move through the full data set within hindrances. With 'i' being used as a row counter, you can see the addition of 1 every time the internal loop is finished and the exit criterion of the internal loop, 'LeaveOKFL', is reset to zero to force the loop to run again. Throughout the loop it is running the series of equations laid out in the methodology section of this report that pertain to the equivalent relationships of one 'N' to the next.

It could be argued that the system could be made more computationally efficient regarding the number of degrees it calculates through, but with the exit criterion for below zero, it essentially immediately skips straight to SOC and works effectively as is.

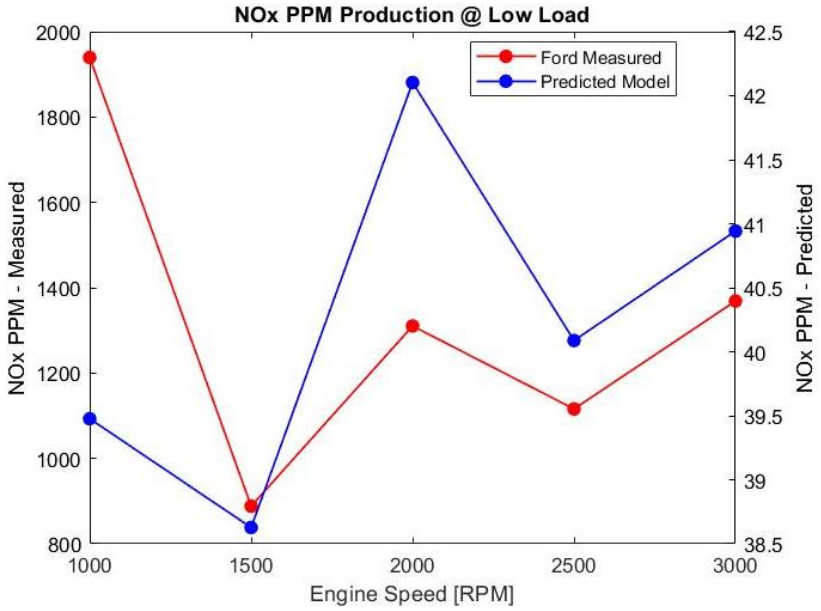

Figure 60 Predicted NOx PPM for the low load cases of the 1.5L EcoBoost (right hand axis) Vs the measured results from Ford (left hand axis).

We can see the results calculated at the low load situations are very far out with respect to actual value, with an average of 33 times below in fact. But with that said, we can see some following of trend in the results, for example with the rate of increase of 2500 to 3000 RPM following very closely to that of the measured results increase, along with 1500RPM calculating correctly as the lowest of the results. As for 1000RPM it is simply believed that the “measured” lambda value is incorrect causing a rich situation when it should be lean, this is backed up by the fact that when using the first, or second, method of calculation for fuel equivalency [*Eq. 1, Eq. 2*], the peak result occurs at 1000RPM just like the measured results because it is running slightly lean instead of rich. As for 2000RPM the case could be the same in terms of fuel equivalency, but the more probably situation is the percentage of exhaust gas recycled should be more here than is currently be modelled to change the magnitude. Again, it should be remembered that these are simply hypothesises because it would require more real-world testing, or Ford measured data to clarify.

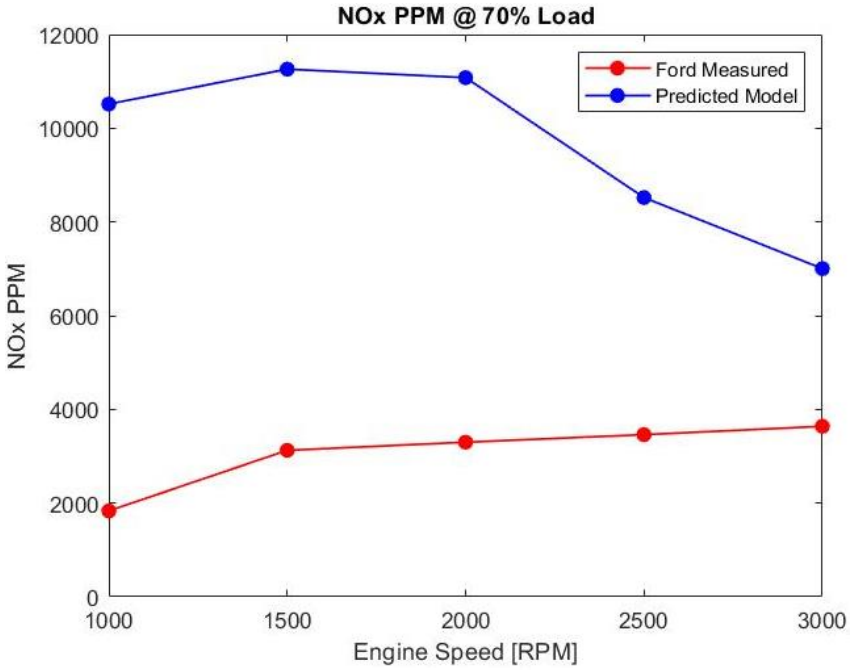

Figure 61 Predicted NOx PPM for the mid load cases of the 1.5L EcoBoost Vs the measured results from Ford.

The results for the mid load situations are certainly the highest predictions of all cases and unfortunately there isn't much correlation throughout, other than the trend of 1000 to 1500 RPM increasing at a similar rate. Because after which the other three cases seem to decline in production, and yes arguably that needs to happen so the predicted value is closer but given the reality that correct PPM calculations aren't going to happen, we are really after the trend. Reasons for this are thought to be again possibly fuel equivalency, but more so the EGR added because as mentioned the difference between valve timing for the 1L and 1.5L at this load is vast, shown in the figures below, and because of this the internal mass of EGR trapped in cylinder, along with the external added, is most likely different enough to cause the large trend difference. Another reason why it is believed that the EGR is the issue, is because at this point of the engines calibration map, they should be targeting toward MBT, which should more often than not result in "complete" combustion situations which therefore should mean the reading of lambda is at its most accurate.

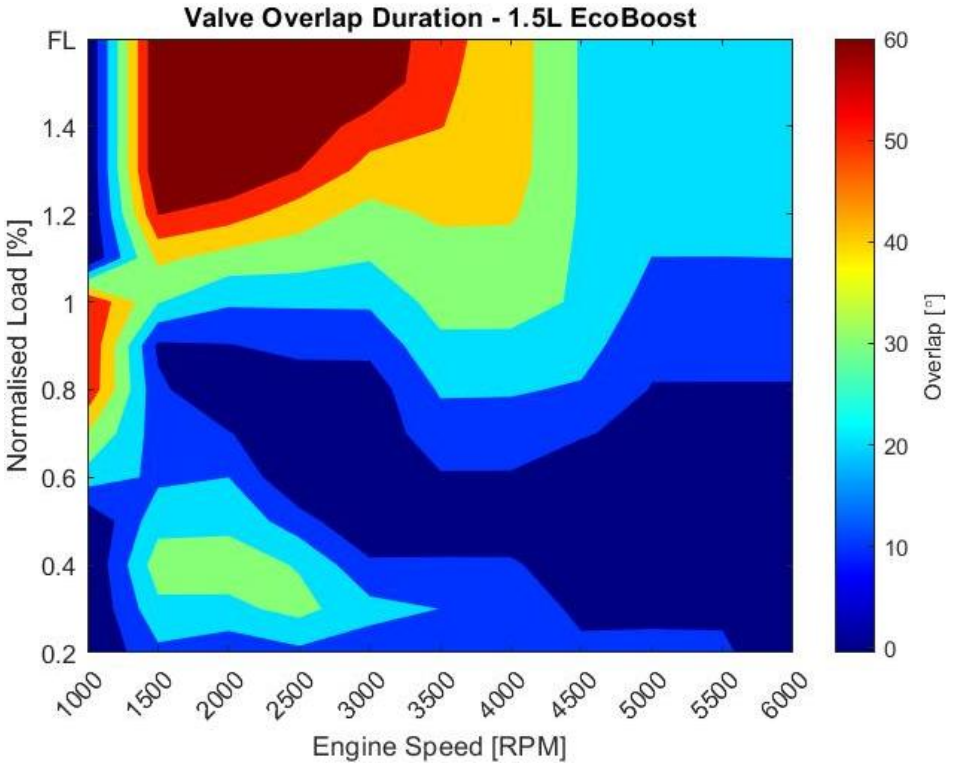

Figure 62 Valve overlap durations for the 1.5L EcoBoost engine.

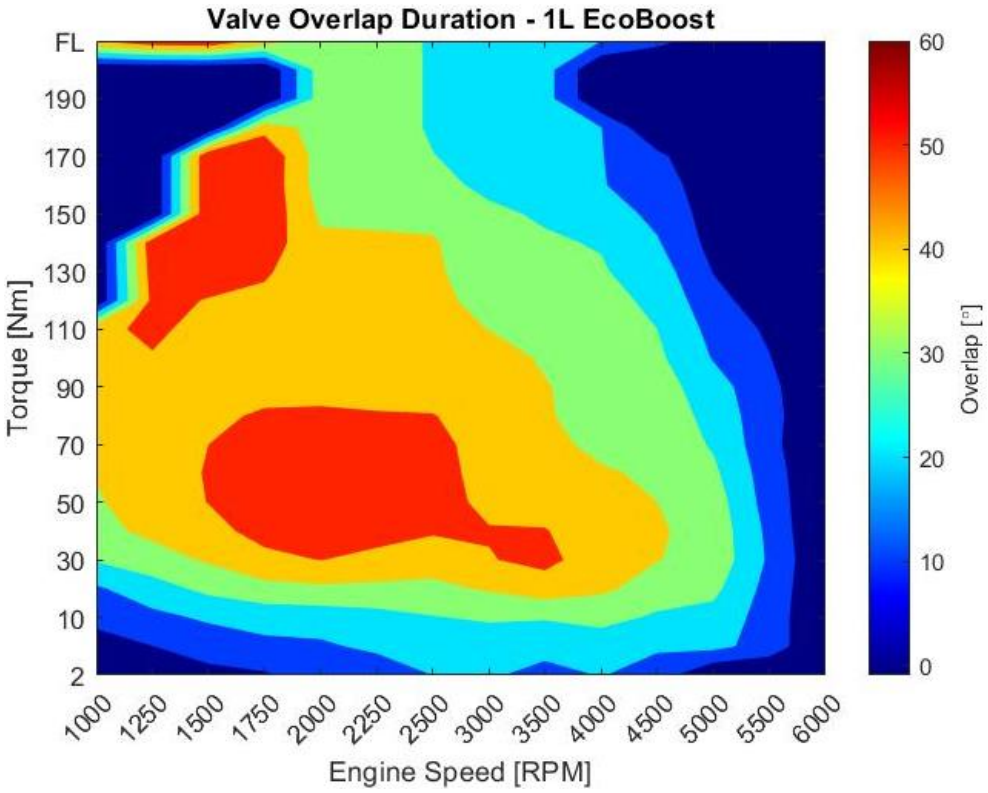

Figure 63 Valve overlap durations for the 1L EcoBoost engine.

As you can see the difference in valve overlap around the area of 70% load, lower engine speeds, between the two engines is vast and could be having an adverse effect on results.

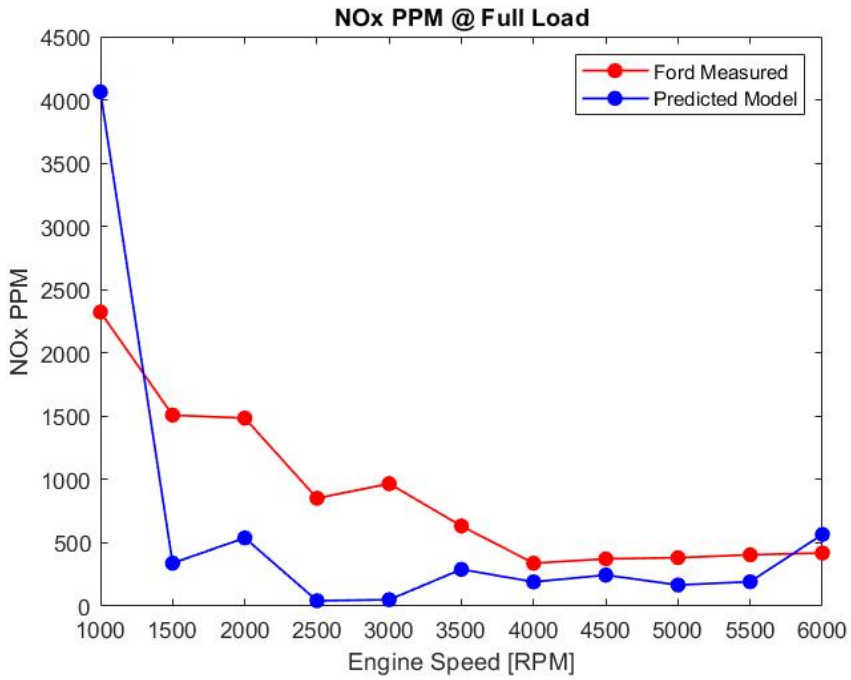

Figure 64 Predicted NOx PPM for the full load cases of the 1.5L EcoBoost Vs the measured results from Ford.

It's immediately clear that the results at full load are rather far out in both trend and respective value, although yes there is some correlation to trend for 2000 – 3000 RPM and then separately at 3500 – 4500 RPM, but elsewise the trend isn't followed, and results are relatively far out and yet they are actually the most accurate of all. Most of the issue here is believed to be back down to the fuel equivalency being used, more so than EGR this time round. Because, yes, the trapped internal EGR will be increasing as engine speed increases, shown in; the 1L EcoBoost data, the Ricardo model discussed later, and *figure 59* identifying the increase of EGR used in modelling. The change in lambda used to calculate fuel equivalency [*Eq. 3* to *Eq. 4*], control module data to that of the dynamometers sensor, provides better results at full load because it runs slightly less rich which increase the NOx PPM calculated. However, it does provide "worse" results for the other two load situations, all of which can be seen in the following.

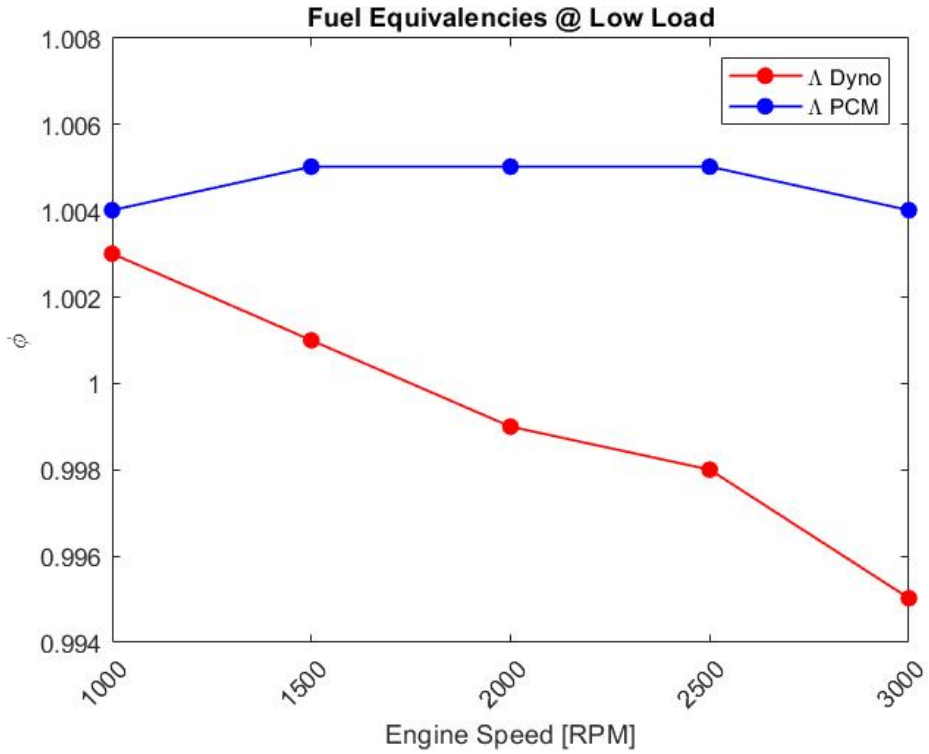

Figure 65 Difference between calculated fuel equivalency using either PCM, or Dyno Lambda, at low load.

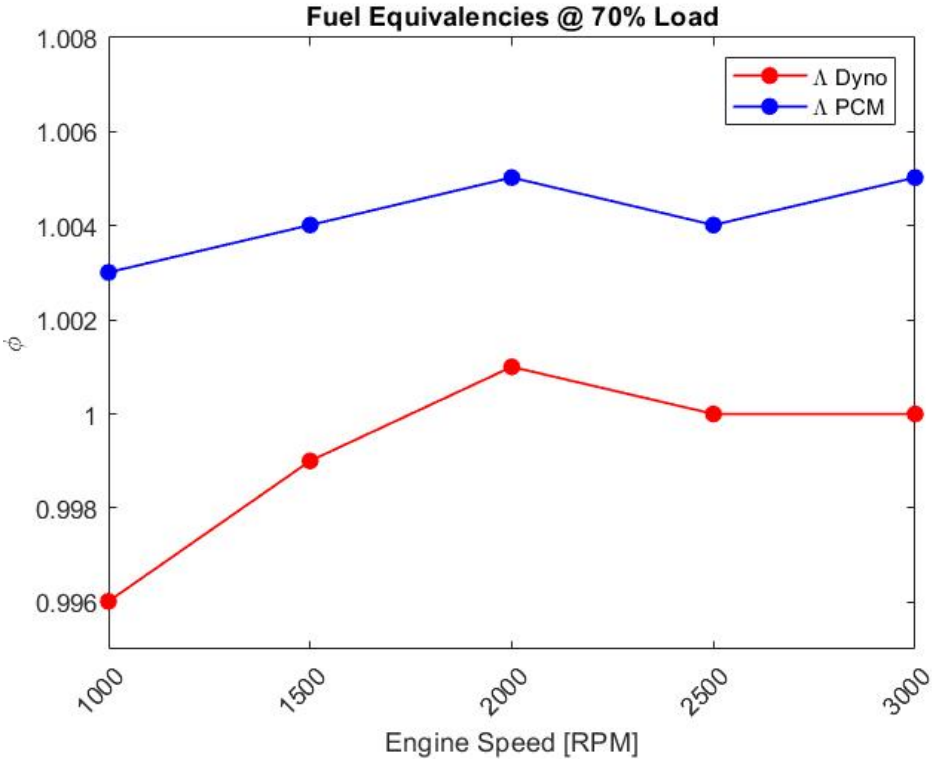

Figure 66 Difference between calculated fuel equivalency using either PCM, or Dyno Lambda, at mid load.

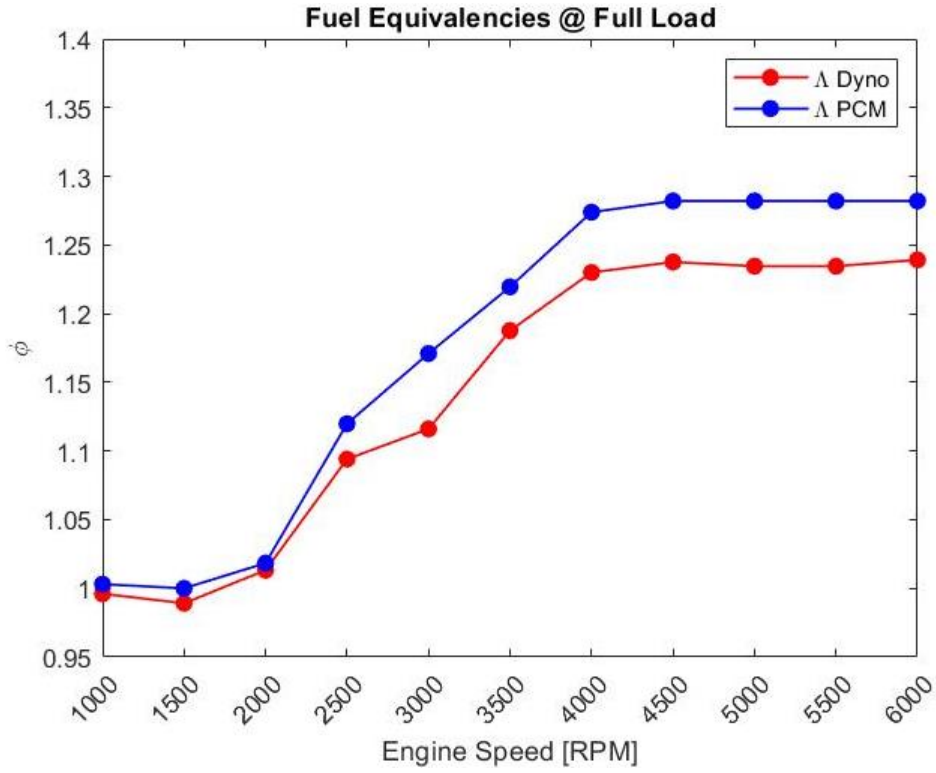

Figure 67 Difference between calculated fuel equivalency using either PCM, or Dyno Lambda, at full load.

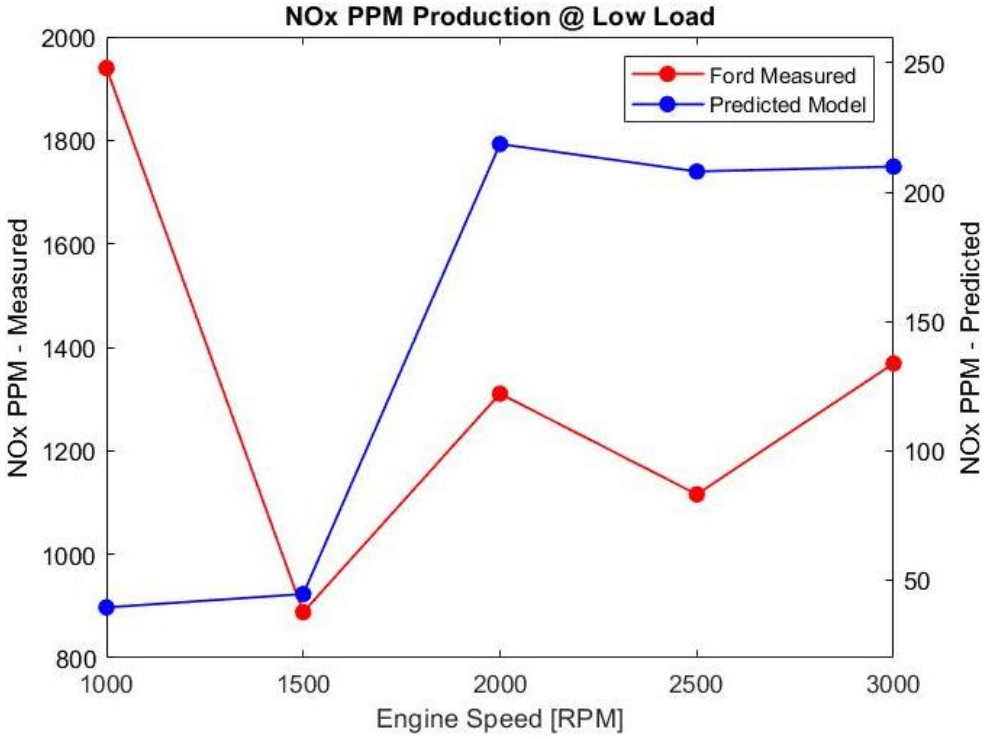

Figure 68 Secondary method of fuel equivalency results for NOx PPM at low load.

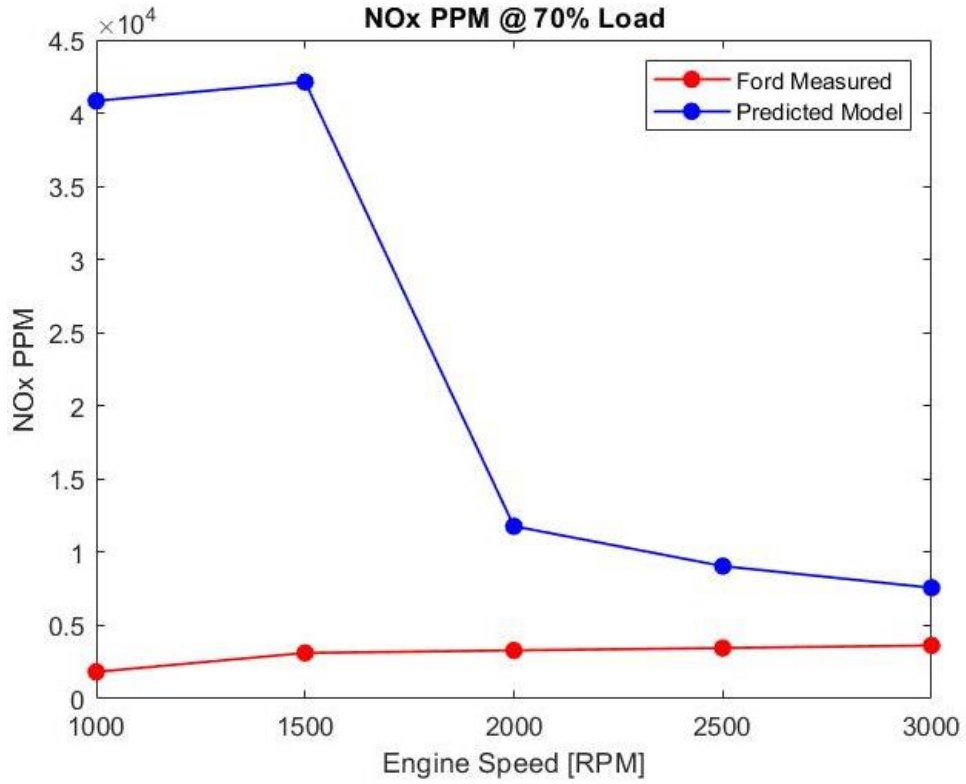

Figure 69 Secondary method of fuel equivalency results for NOx PPM at mid load.

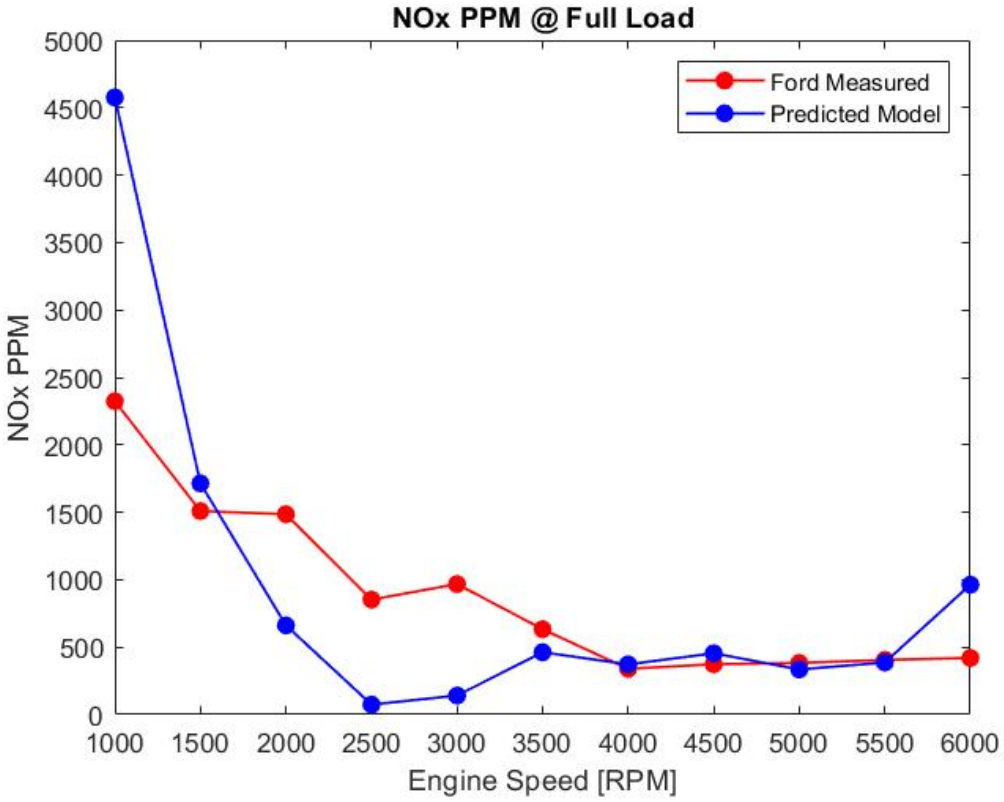

Figure 70 Secondary method of fuel equivalency results for NOx PPM at full load.

We can see that when using the alternative measured lambda the results are rather different, but more so by magnitude than trend and this is one of the most important parts of this entire investigation because it highlights the shear sensitivity of the methods used to calculate NOx in internal combustion engines. Although it can be seen the results at low load, 2000 – 3000 RPM, do change respective pattern in results and this is believed to be because of the dependence on the idea the system is in equilibrium and where the temperatures are relatively low in this case, fuel equivalency can influence the trend, as well as the magnitude. Whereas the higher load cases, that have higher combustion temperatures, and more of a chance of reaching equilibrium in the time available, fuel equivalency seems to effect the magnitude of results only really and not necessarily the trend. There is obviously a change in trend for the mid load, low speed cases (1000 & 1500RPM) and the results do show a large difference when compared to the initially modelled results, but we can see that the apparent combustion cases fall to be lean instead of rich. And as we already know that has a profound impact of NOx production because the worst-case scenario is $\varphi = 0.97$ which has been proven many times in the past, but crucially the difference is only 0.7% between the fuel equivalencies used and yet the prediction increases by order of around 3.8 for these two conditions, because it is now apparently lean instead of rich [0.996 instead of 1.003]. But we can see that for the other three engine speeds the change in results is only an increase of 7% because the apparent equivalency ratio remains on the rich side of stoichiometric, albeit only slightly, but that is enough and again just perfectly outlines how sensitive the model is to fuel equivalency for the magnitude of results.

And we can now see that the results for full load are more accurate regarding the magnitude of results, at the higher engine speeds mind, because this is where the chances of reaching equilibrium are increased because both pressure and temperature are higher than that of the lower speeds. And as mentioned, importantly you can see that the trend hasn't changed compared to previous results, only magnitude, because the EGR% recycled remains the same, as does the fuel and air mass.

NOx production is very difficult to model in ICE's and even more so when engine speed & load is low, which is arguably the most important area regarding introduction of on-board system modelling in the real-world because this is currently the main point of operation in homologation testing. It has been seen that the reliance on definite fuel equivalency in-cylinder is high with respect to accurately predicting the magnitude of NOx PPM, along with the total percentage of exhaust gas recirculated being the key to correct trend definition, and this is backed up in the next section for the 1L EcoBoost because the data is more specific and accurate regarding these two key components.

5. 1L EcoBoost NOx Modelling Results & Discussion.

The 1000cc Ford EcoBoost engine is a world-renowned feat of engineering and is a well-documented engine regarding its technology, reliability, efficiency, and adaptability. It is the predecessor and successor of the 1500cc 4-cylinder engine at least which shares a lot more commonalities with the again, world-renowned 1.6L EcoBoost which is known for being brilliant on road and in all variations of motorsport. Because of this, there is far more specifications and real-world results available for these engines compared to the 1.5L 4-cylinder, which in-turn makes modelling considerably easier for this engine.

Despite this fact mind, the data used to compare against is from a different engine and different time than that of the cylinder pressure data used to model, and this has caused its own difficulties regarding the validity of results, in particular the mass fraction burnt points and profiles. As for the NOx prediction model however, the results are much more realistic and accurate compared to the 1.5L because the data for; lambda, air and fuel mass, and total exhaust gas recycled is both known and more specific. (RON 95 – Stoichiometric 14.55:1)

5.1. Mass Fraction Burnt profiles.

The modelling process was of course the same between models, utilising the process known as the ‘Rassweiler-Withrow’ method, with individual bounds set to define the start and end of combustion. However, as stated, the data used to model is from a different engine and different time than that used to compare against which naturally means there is always going to be some form of discrepancies between results. And that comparable tabulated reference data will be referred to as ‘engine – 2’ from here on out.

Unfortunately neither the coefficient of variation, nor the standard deviation is known for the burn profile points of the 1L and therefore it is harder to characterize if the predicted burn, although different, is still within bounds of the seemingly very sporadic average points that Ford have defined. Another “difficulty” with the 1L is the definition of SOC to use as a starting point to then define the relatable curve for engine – 2 because the data given is that of either; ‘0002’, ‘0010’, ‘1090’, and MFB50, which relays to time from 0 – 2%, 0 – 10%, 10 – 90%, and of course 50% burnt.

Therefore because they’re brackets of data and not specific locations like the 1.5L data the initial definition of SOC causes discrepancies in comparable profiles, especially at the lower load and lower speed situations, which was also found to be an area of concern for the 1.5L because combustion is both slow and slightly unstable in this region, hence the typically large distribution of results. All modelled case results can be seen below.

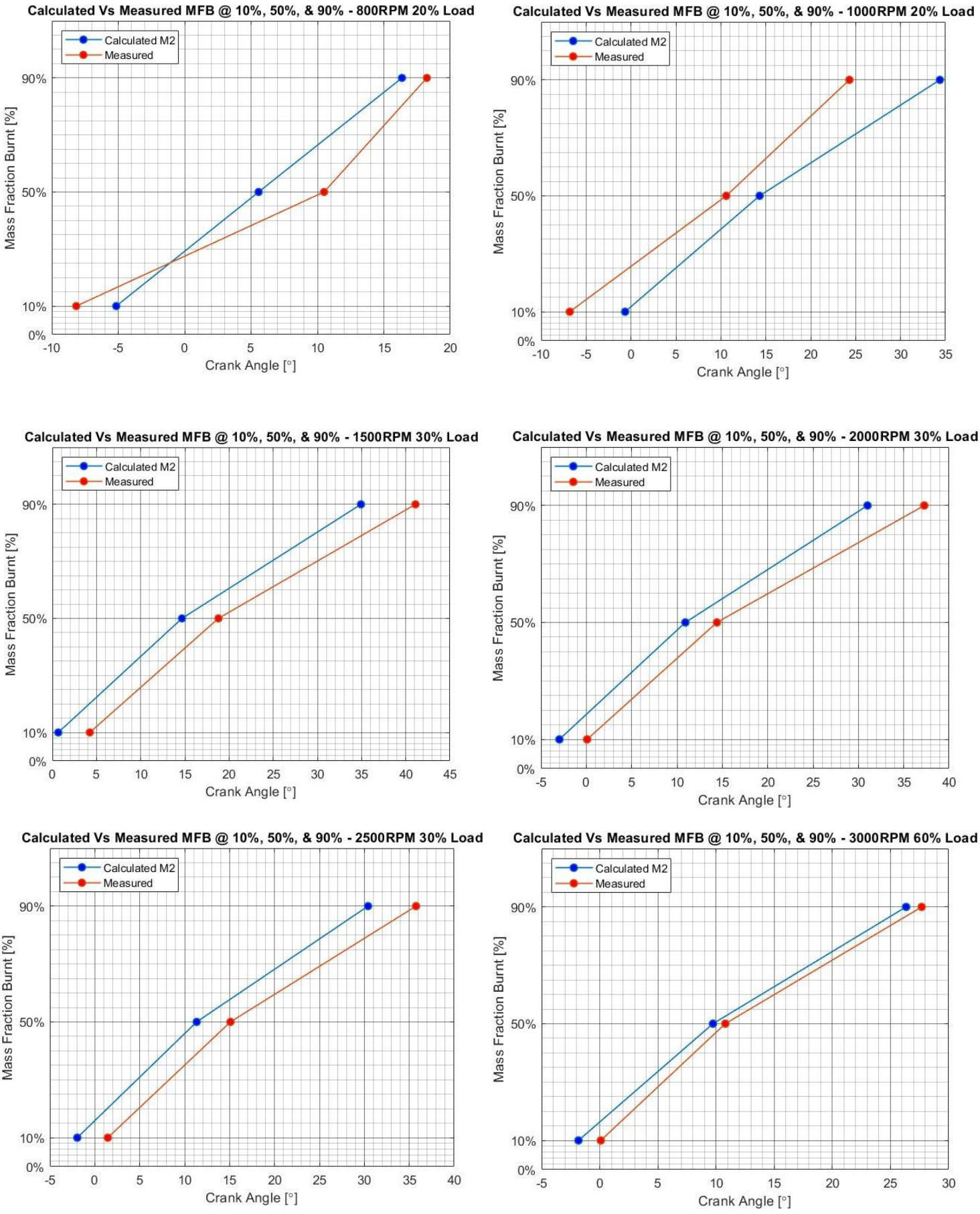

Figure 71 MFB profile points comparison for the lower load cases at various engine speeds on the 1L EcoBoost.

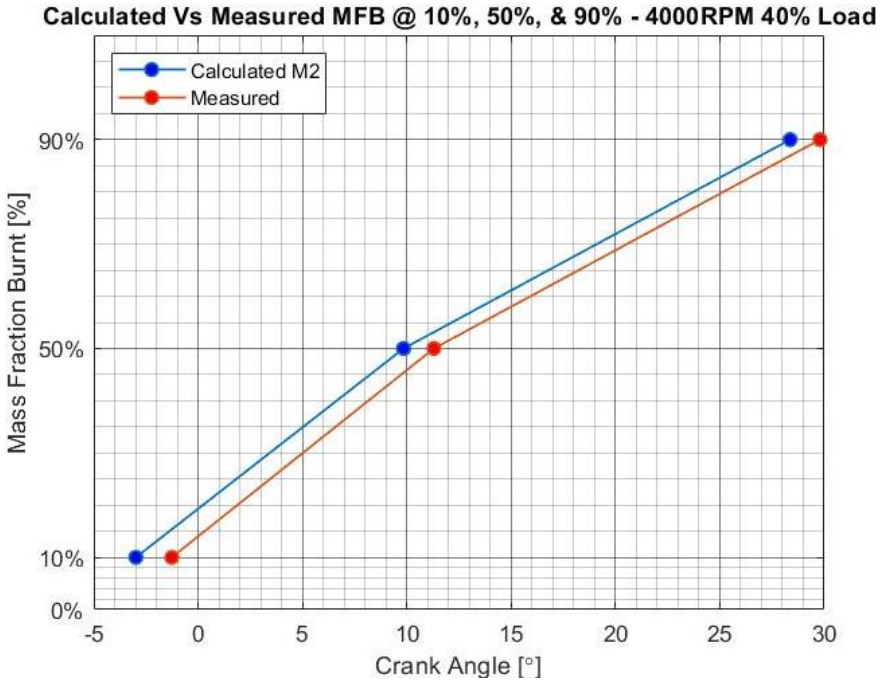

Figure 72 MFB points comparison at 4000 RPM, Low load. 1L EcoBoost.

We can clearly see there is definite issues regarding the modelling of the burn profiles for the very low cases of 800 & 1000 RPM where combustion is presumably very unstable and not necessarily complete. The result of which has caused not only relatively different profile generation, but more importantly the location with respect to crank angle that it occurs at. The discrepancies for location are admittedly not horrendously far from the comparable data, but they are further than those at all other sites and don't provide the correct rate of change from one stage to the next anywhere near as well as the other sites. This immediately has a detrimental effect on results for NOx PPM and this will be discussed shortly.

As for essentially all other cases studied, we can see that yes the profiles aren't in the exact locations, which is again believed to be partly due to the definition of SOC, joint with the fact that it is from a different engine, and then also that there is most likely going to be a large variation in results for these locations because of the instability of combustion, because there is: high exhaust gas percentage in the mixture, low injection pressure, no boost pressure, and a most likely it is running as a stratified mixture in the area of 30% load and below. But regarding the rate of change from one point to the next they follow very closely, which means as rate of production and time available to reach equilibrium during combustion is as similar as can be. The only real foreseeable issue to occur from the deviations shown is its effect on the volumes for the burnt and unburnt zones, as the piston moves through the cycle, and as we know volume is required to calculate NOx PPM.

As for the higher load cases, the results show stronger correlation and have been defined more accurately which suggests the there is no issue regarding the method used to define SOC, instead the most likely reason is that the data is of only one cycles run, whereas Ford will define these points using at least 500 cycles at the singular load and speed condition.

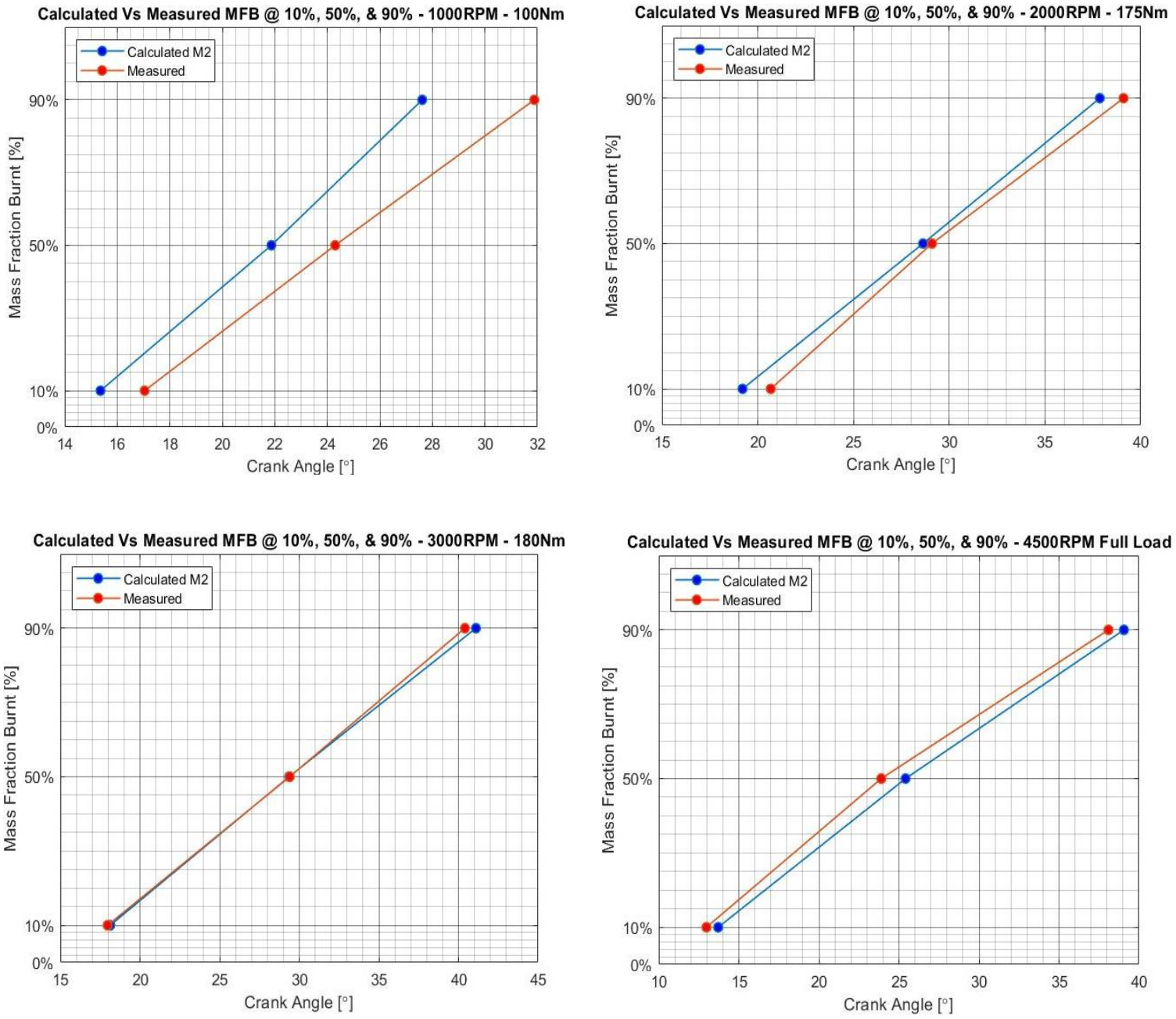

Figure 73 MFB profile points comparison for various engine speeds at high load for the 1L EcoBoost.

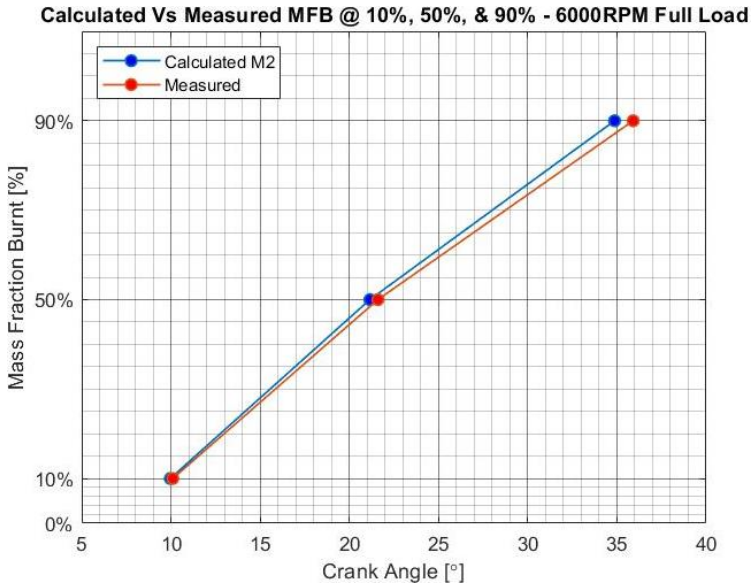

Figure 74 MFB points comparison at 6000 RPM, Full load. 1L EcoBoost.

It's clear that the points at higher load and speed match far better than the lower cases and again the only real issue is relayed back to the definition of SOC for the comparable data. It had to be taken as spark timing point because the data only provides a period from 0 – 10% burnt and because there isn't any other reference point to define this, and because of that there is most likely to be some form of delay, no matter how small, from the initial spark to actual combustion and especially so when the load and speed is low. This is because the mixture in cylinder will be in a very different state when there is low/no boost pressure and low injection pressure, the mixture will be in a stratified state with low turbulence, causing "patches" of rich and lean mixtures which destabilise combustion and delay the rate at which it occurs. And this fact is definitely evident in the data where some areas take as long as 100° to even reach 90% burnt.

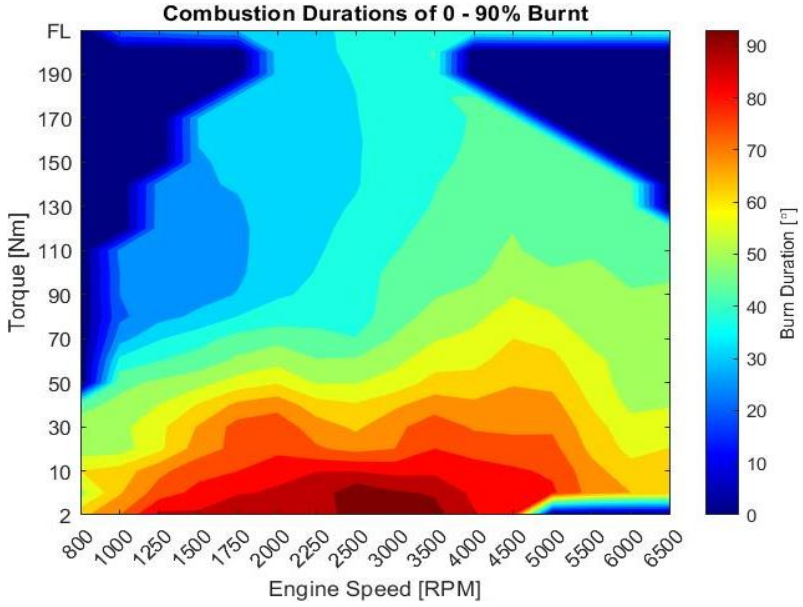

Figure 75 Combustion Durations [0 - 90%] using Ford's defined durations.

5.2. Unburned Temperatures.

The unburnt temperatures are another area that could be argued as cause for concern because there are two points that bridge 1000K and as discussed earlier, this is typically the area associated with knock. The reason for this is thought to be either that the data provided was of a run where Ford were testing the knock limit of the engine, or it is simply that for this specific engine the earliest possible ignition timing limit was slightly more tolerable in engine – 1 than engine – 2. To show this there is a figure showing what engine – 2 has defined as their final spark, and the knock limited earliest timing, then a comparable column to show the timings for engine – 1. (SPT – spark timing)

	Engine - 1 SPT CA° BTDC	Engine - 2 Final SPT CA° BTDC	Engine - 2 Earliest SPT CA° BTDC	Difference to final SPT	Difference to earliest SPT
800	35.03	26.08	35.02	8.95	0.01
1000	40.30	33.75	33.75	6.55	6.55
1500	30.37	29.43	29.42	0.94	0.95
2000	40.70	40.43	40.41	0.27	0.29
2500	36.63	36.51	36.52	0.12	0.11
3000	26.63	26.37	26.36	0.26	0.27
4000	34.50	37.92	37.95	-3.42	-3.45

Table 1 Spark timing comparison between that attached to engine - 1's data, and then what Ford state is the final and earliest before knock for engine - 2. All lower load cases.

	Engine - 1 SPT CA° BTDC	Engine - 2 Final SPT CA° BTDC	Engine - 2 Earliest SPT CA° BTDC	Difference to final SPT	Difference to earliest SPT
1000	-5.83	-5.41	-5.41	-0.42	-0.42
2000	-4.77	-4.06	-4.05	-0.71	-0.72
3000	1.10	0.51	0.74	0.59	0.36
4500	5.63	7.27	7.25	-1.64	-1.62
6000	9.57	9.89	9.96	-0.32	-0.39

Table 2 Spark timing comparison between that attached to engine - 1's data, and then what Ford state is the final and earliest before knock for engine - 2. All high/full load cases.

We can see that the change across the board at higher loads hasn't changed by a large degree for either engine, or away from the earliest limit available due to knock. However at the lower load cases, specifically the problematic areas of 800 and 1000 RPM, the timing is vastly different with respect to the finalised calibration timing that will be respective of the mass fraction burnt locations, hence the difference. But as mentioned, there is two areas that appear to be bridging the chance of knock at 2000 & 2500 RPM, but we can clearly see that the earliest before knock timing is very similar between the two engines and this gives a form of confidence that yes, it is close, but it shouldn't knock any more so than is desired.

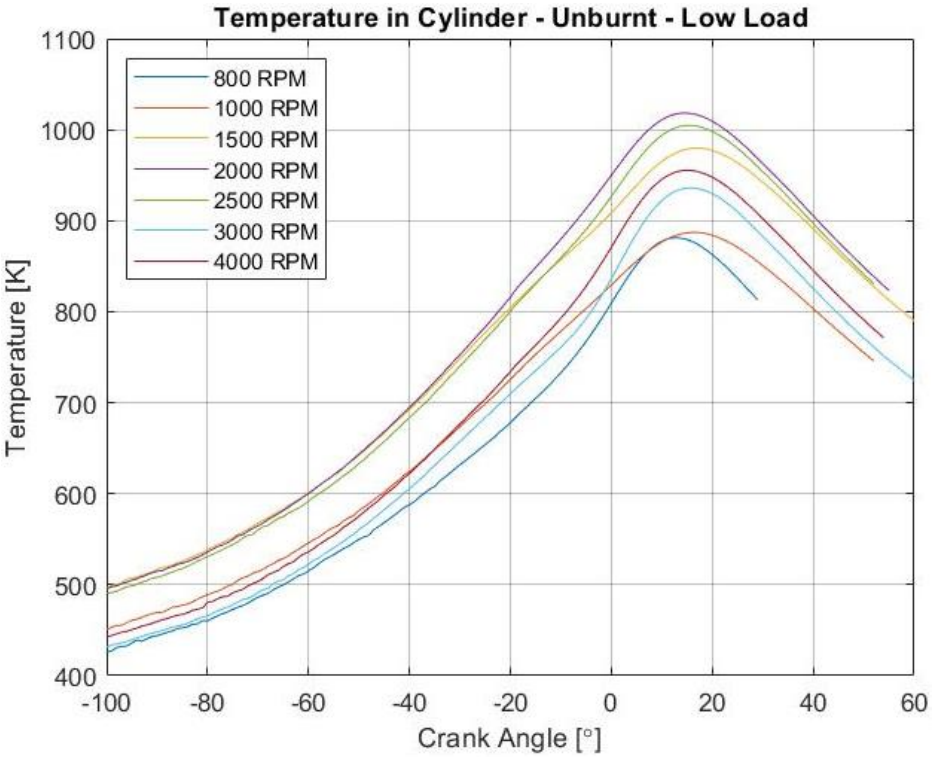

Figure 76 Unburned temperatures for the lower load cases of the 1L EcoBoost.

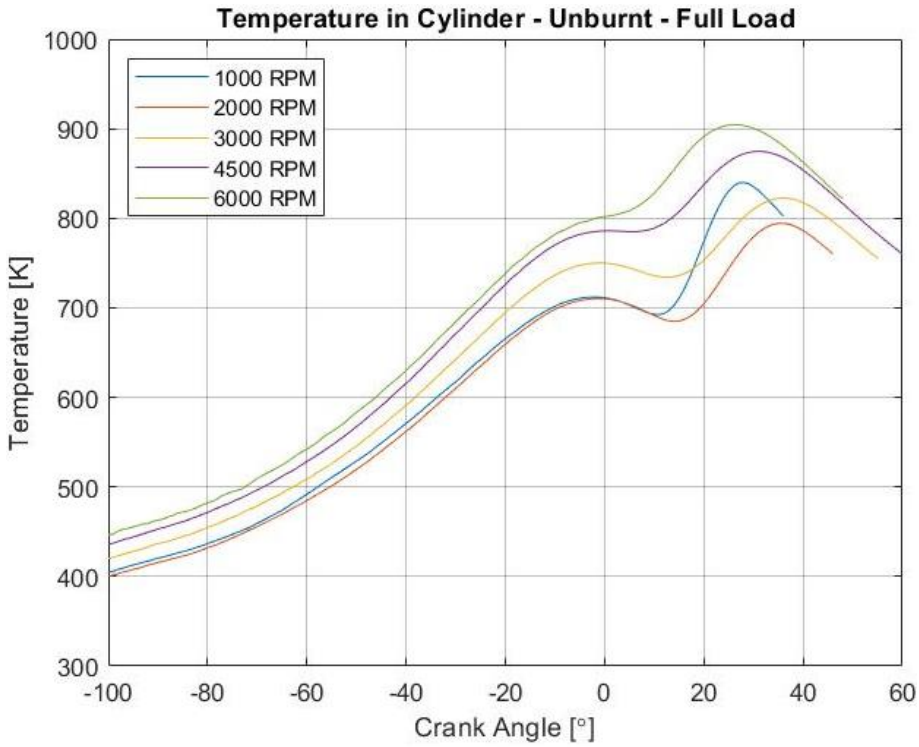

Figure 77 Unburned temperatures for the high load cases of the 1L EcoBoost.

The temperatures predicted follow the expected trend where the high EGR% at 800 and 1000 RPM bring temperatures down considerably, the next few speeds are higher and then the highest speeds drop again because of the issues with knock and needing to

control it by adding air mass because pressure doesn't increase. With each of these cases we can also see they peak around the same sort of relative crank angle position, and this links brilliantly with the respective points for MFB50 and how similar they are for each of these cases.

The higher load temperatures also follow the same trend seen in the 1.5L at full load where the temperatures slowly increase as speed is increased which correlates to the fact that there will be less time for heat transfer and again with 1000 RPM the load case is close to its limit but compared to the other speeds the effective load isn't as high and hence the peaking here compared to 2000 and 3000 RPM.

5.3. Burned Temperatures.

With the burned zone temperatures the modelling appears to show no obvious issues and the trends are following the expected patterns, other than perhaps the temperatures at 800 & 1000 RPM low load are slightly too low and this could suggest a reason why the NOx modelling is poor here. But considering the number of issues surrounding these cases there isn't any more that can be done from a modelling prospective besides full detailed kinetic models, and/or real-world testing of the engine to measure the data relative when running at the same condition's engine – 1 is to compare against.

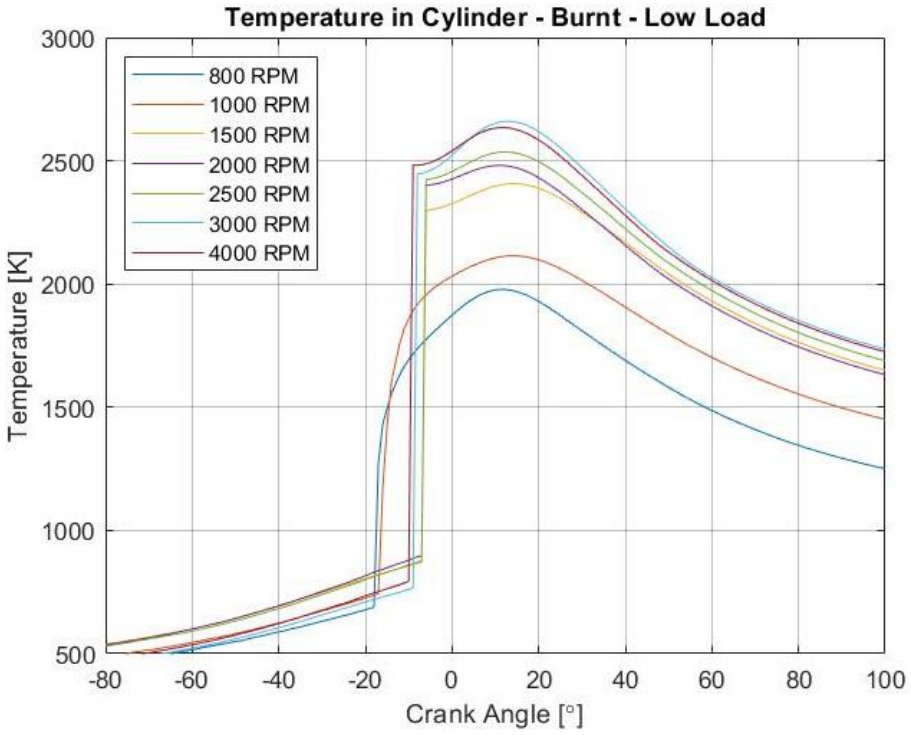

Figure 78 Burnt temperatures for the lower load cases of the 1L EcoBoost.

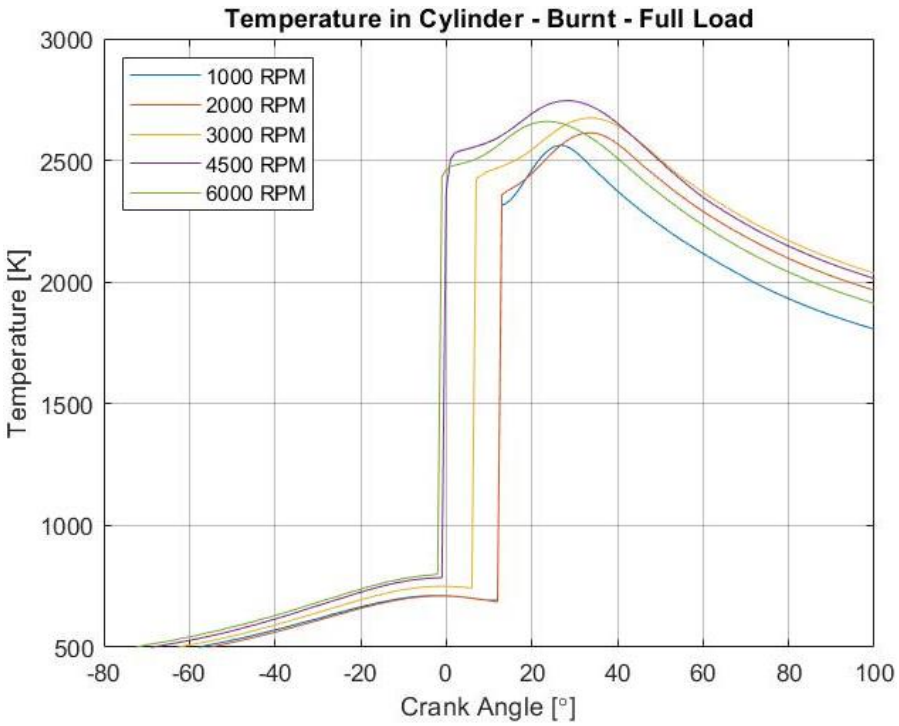

Figure 79 Burnt temperatures for the higher load cases of the 1L EcoBoost.

We can see that all profiles are running at higher speeds are within the target area of 2600K and that naturally drops as engine speed and load decreases because there is realistically more time for heat transfer to occur in cylinder, joint with much lower pressures and large percentages of exhaust gas recirculated.

5.4. NOx Modelling.

The modelling of NOx for the 1L EcoBoost is considerably more accurate than that of the 1.5L because of the availability of more accurately recorded data for the lambda at each point, along with the measured (or calculated, this is unknown) air-to-fuel ratio trapped in-cylinder. These together with the fact the EGR% of both internal and external is known for each case the results are profound and show that despite having to make assumptions, and at sometimes perhaps crude methods of calculation, it can still provide good results and those results give confidence that real-time predictive modelling could be a future option.

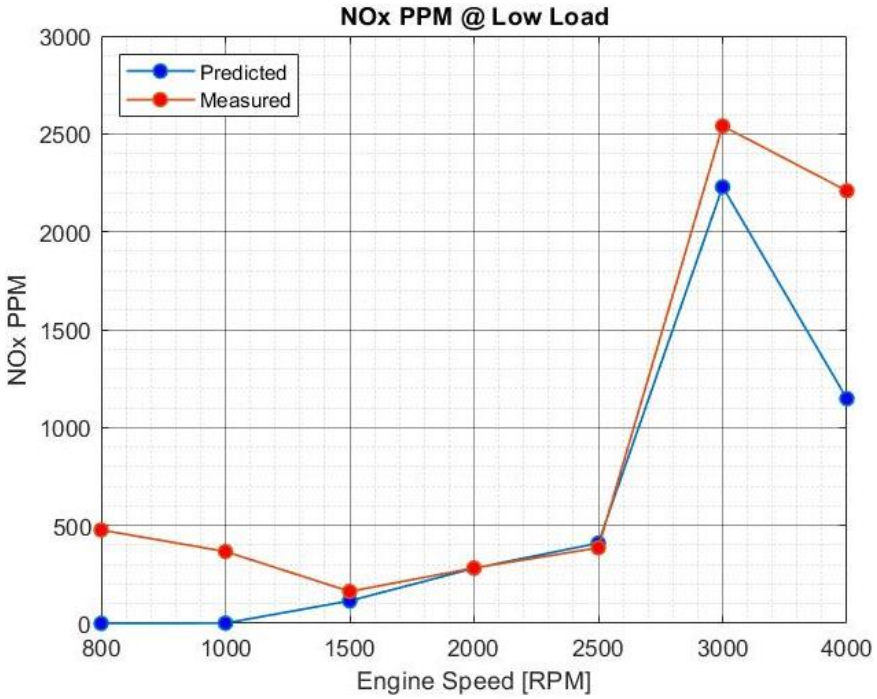

Figure 80 NOx production predicted Vs stated measured for the lower load cases of the 1L EcoBoost.

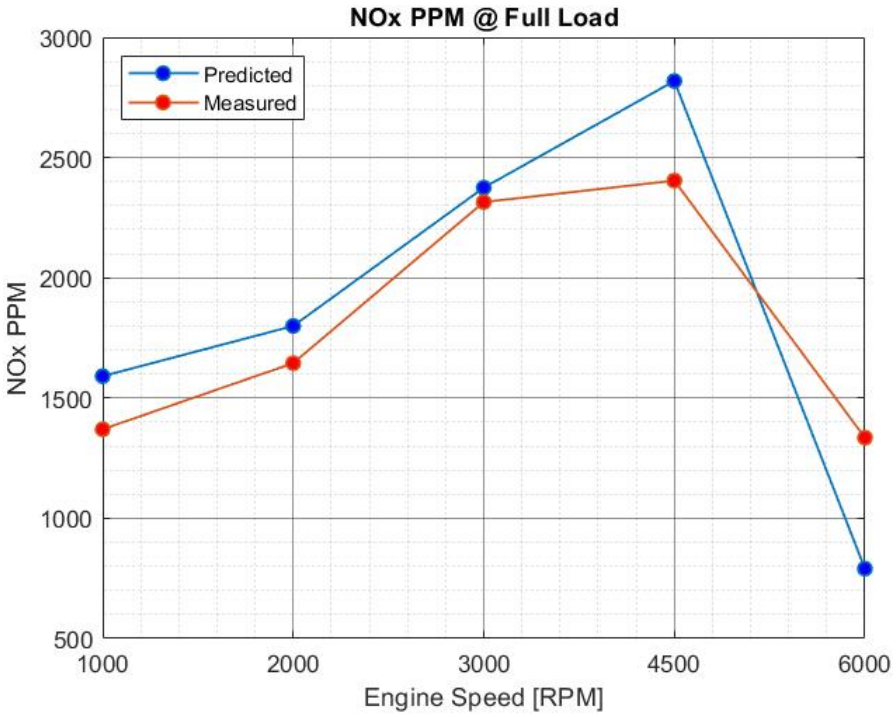

Figure 81 NOx production predicted Vs stated measured for the higher load cases of the 1L EcoBoost.

The results shown for the 1L are not only incredibly more accurate than the 1.5L, but they provide a good level of confidence regarding all the methodologies and assumptions that have been used in this investigation. However it should be said that they do lead to some controversy regarding the importance of volumes for the burnt zone knowing that there is a slightly higher discrepancy between the calculated and

predicted of the 1L than the 1.5L, along with what was presumably an issue, the apparent lack of time available to reach equilibrium. Because there is no change between the model cases and the results of the 1L provide light on the fact that despite it being an assumption, there doesn't appear to be a great issue in the results when assuming it at the conditions typical of a GTDI engine.

Considering the lower load case results it's clear that as thought, there is issues for the two lowest of 800 & 1000 RPM which has been shown to be problematic at all steps. The reasoning for this clear issue is thought to be due to the issue of another assumption that must be made for this type of modelling, that the situation is tended towards a homogenous mixture, not stratified. But it is believed that with these two situations because there is essentially no boost pressure, the waste gate is closed, fuel pressure and injection time is very low, the mixture in cylinder is tending noticeably more towards a stratified mixture.

This can be seen in the measured emissions data because the NOx production is relatively high considering the temperatures arguably very low temperatures, because there is rich zones burning that are near lean zones, and this increases the chance for NOx because oxygen defuses from the colder lean patches to the dramatically hotter rich burning zones. Joint with the known principal that stratified combustion in GDI engines leads to a strong chance of soot/unburnt hydrocarbons in the exhaust gases, and although soot isn't specifically measured the HC PPM is and the figure below shows the area for high production of, is that of these two problem cases.

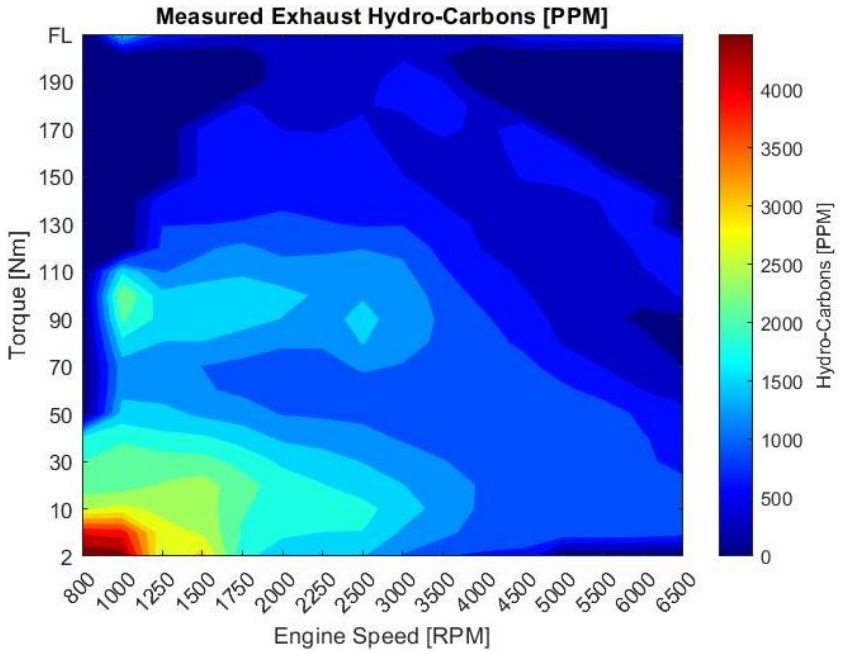

Figure 82 Measured unburnt hydrocarbons in terms of PPM for the 1L EcoBoost.

In summary however the ability to predict nitric-oxide production in GTDI engines has been shown as possible for this 1L EcoBoost using techniques that take less time, less computational power, and less money than using powerful chemical kinetics models. Although these are arguably more accurate than this traditional approach, not only has the trend been correctly predicted for almost every case, but occasionally the actual value to [with some allowance for the currently un-modellable reverse reactions] and this brings back to show that modelling of internal combustion engines can often prove very beneficial and cost effective.

However, this has only been made possible because of the considerably more accurate data, which undoubtedly requires more time and money to do obtain, for the in-cylinder characteristics and the importance of that accuracy cannot be understated regarding the accuracy of subsequent modelling, which is clear when you compare accuracy of the 1.5L NOx model to the 1L.

Final point to mention on this set of data for the 1L EcoBoost, engine – 1, there is an issue regarding the defined torque measured point and what the engine's torque is. The data say's it is at 40Nm of torque at 2000 RPM, but calculated show's it should be 31.34, which is clearly closer to the load of 30Nm than it is 40Nm and this was one reason why there was issues with case before the change to comparable data. Also, as for the apparently full load cases, not all of them are. 1000, 2000, & 3000 RPM are just below the points of full load which again would case issues when trying to compare against and find influencing data, so this is something to be aware of for future reference.

6. 1L EcoBoost Cyclic NOx Modelling Results & Discussion.

As for both a furthering of the modelling capabilities and validation, along with a justification upon the influence of the specific pressure data used to model from, it was thought best that an example of modelling across 500 individual cycles within each cylinder would be the perfect representation of the irregular pattern of prediction, because of the inherently chaotic nature of combustion. There was data available for the individual cycles that it is believed Ford use to average across for their tabulated data sets (500 cycles), at 6000RPM under the full load condition. The data does include burn point locations for 2, 5, 10, 50, and 90%, along with PMEP, GMEP, NMEP, and then also the related crank angle for the start and end of fuel injection.

This section of the model is the only one in which you could argue computational efficiency could be improved if you were to encounter an issue, or at least something to assess if more were to be done like it, i.e. the 500 individual cylinder cycles. Because it takes on average 35 minutes to complete all calculations of the 1500 different pressure traces, using a HP ZBook 15V G5 Mobile Workstation, compared to the average of 4 minutes for the 1.5L's 21 cycles and 2 minutes for the 1L's 12 cycles.

Regardless of the time taken, the results do highlight yet another issue when trying to develop real-time modelling in terms of the erratic pattern of production calculated from one cycle to the next, which at 6000RPM is only 20ms, and how this would have a profound effect on the efficiency of trying to change calibration characteristics in time to have a positive effect before the situation has changed drastically.

The main reason for any issue regarding accuracy of results, bar the already mentioned assumptions and limitations, is the fact that the AFR in-cylinder along with the specific EGR at every measured case isn't known and therefore must be assumed as "constant" with respect to the value used in modelling. Obviously, this isn't reality because it's not only for every cycle that these will be different, but also each cylinder and that is obvious considering the differences in pressures for each cylinder with cylinder 1 prevailing as the consistently higher-pressure cylinder compared to the other two. Therefore we can already predict that results will be of an order out regarding accuracy, but either way it is a useful study to demonstrate the potential change in production of NOx on a cyclic basis and not just generally averaged.

6.1. Mass Fraction Burnt profiles.

As mentioned, the data provided consisted of a few additional respective characteristics for each cylinder across their cycles, one of which is the various mass fraction burnt percentages and these were used to compare the modelled results against. Doing this obviously helps not only identify if there is corrections needed, but also the effectiveness of the fundamental methodology and resulting “code” designed to calculate the burn profiles when assessing large sets of data. The accuracy of each cylinder’s respective crank angle position for the points of 10, 50 and 90% burnt can be seen collectively in the following table, and then individually in the subsequent figures.

		Average [%]	Minimum Accuracy [%]	Maximum Accuracy [%]
1	Cylinder 1 - 10%	100.88	97.171	102.99
2	Cylinder 2 - 10%	101.44	99.537	104.85
3	Cylinder 3 - 10%	100.59	98.29	102.52
4	Cylinder 1 - 50%	99.785	96.971	101.7
5	Cylinder 2 - 50%	100.15	97.821	103.38
6	Cylinder 3 - 50%	99.364	95.701	100.98
7	Cylinder 1 - 90%	99.827	92.545	109.1
8	Cylinder 2 - 90%	101.31	93.29	145.91
9	Cylinder 3 - 90%	98.932	88.77	105.84

Table 3 Table of accuracy for the average, minimum and maximum accuracy percentages across the 500 cycles, for each cylinder, and each point of 10, 50 and 90% burnt modelled.

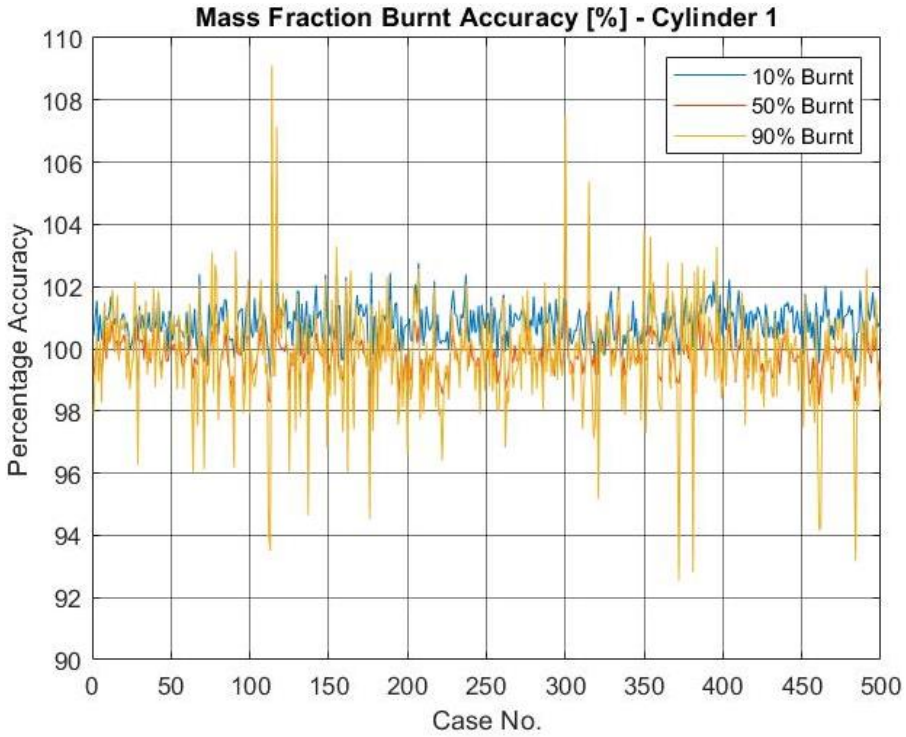

Figure 83 Accuracy of the individual burn locations for 10, 50 and 90% modelled Vs stated in cylinder 1.

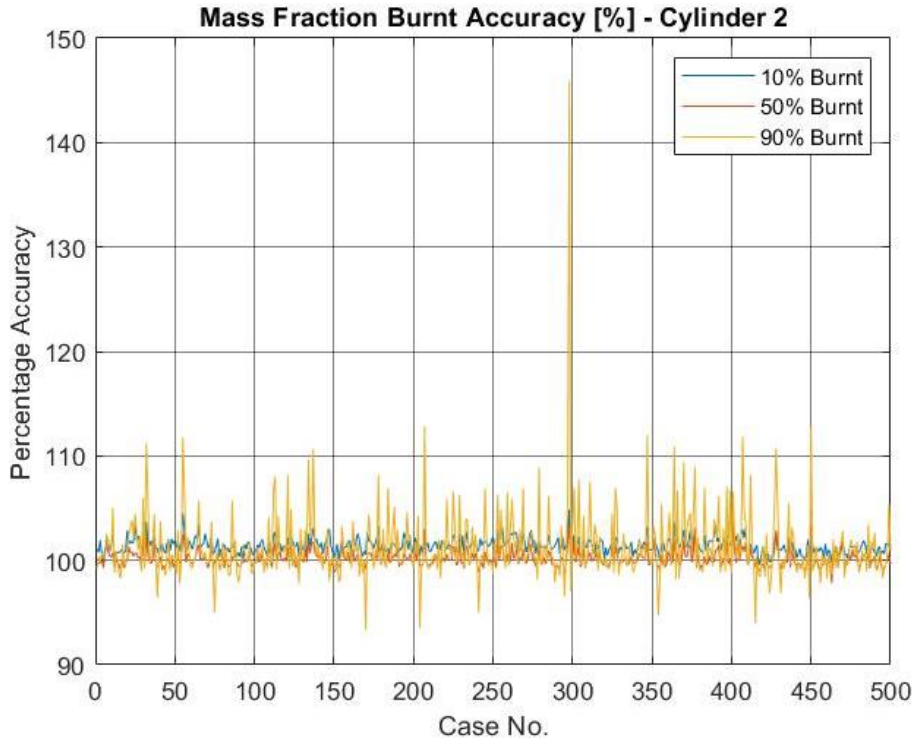

Figure 84 Accuracy of the individual burn locations for 10, 50 and 90% modelled Vs stated in cylinder 2.

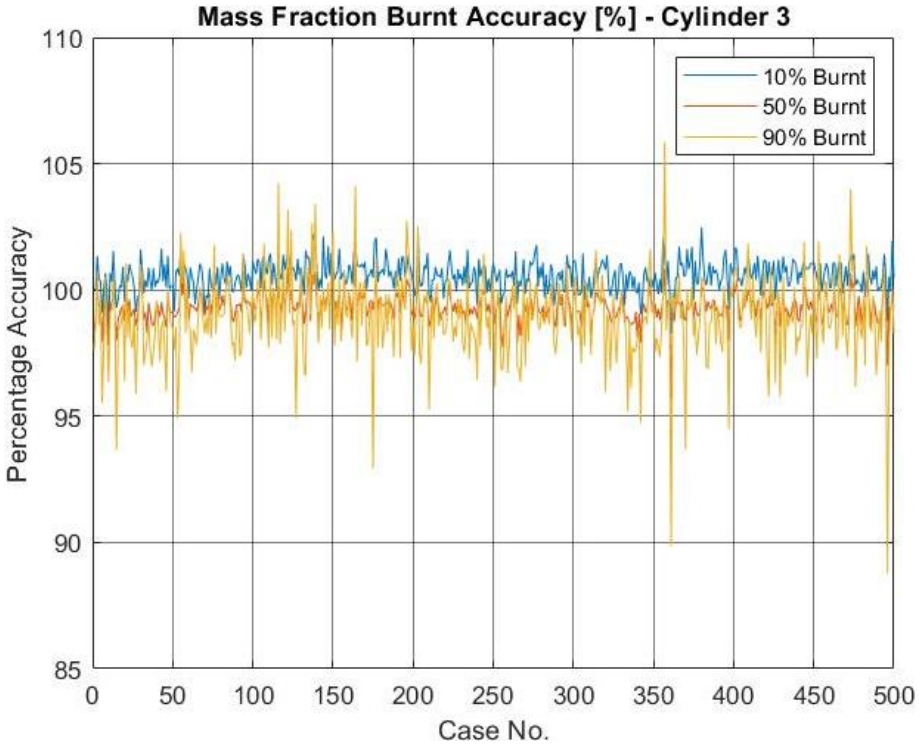

Figure 85 Accuracy of the individual burn locations for 10, 50 and 90% modelled Vs stated in cylinder 3.

It is clear from these results that there is no issue in either the modelling, nor the influential data used to reach this point because the average accuracy across the board is 101.47% and that is well within an acceptable limit considering the assumptions made.

6.2. Unburned Temperatures.

The unburned temperatures are relatively stable considering the engine is spinning 6000RPM and at full load, and the minimum and maximum peaks for each cylinder are all within the correct range, relatively to each other. Although again there is point's that reach above the threshold of 1000K, albeit not by much, and there is the genuine possibility that the engine was experiencing knock. This would explain the sine wave effect when taking the average of the peak cylinder pressures because they will retard ignition and slowly advance again, causing the peaks and troughs of the curve seen below.

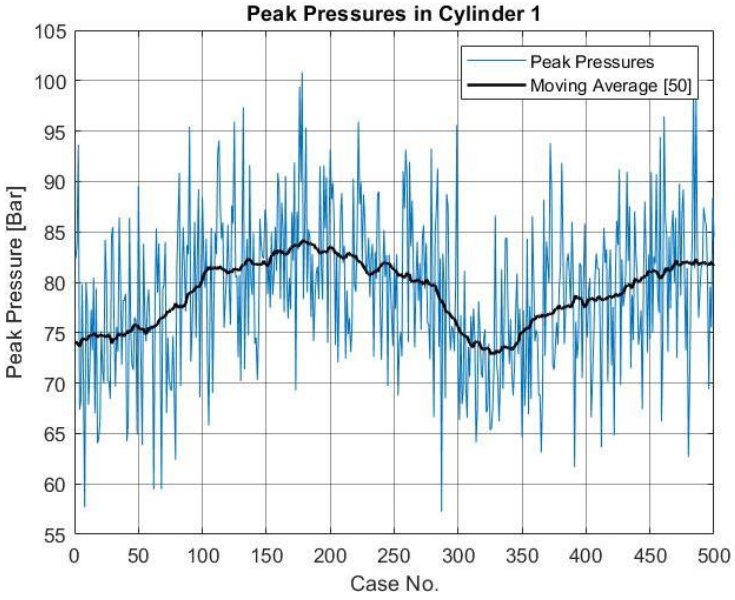

Figure 86 Peak cylinder pressures for cylinder 1 with the moving average (50) demonstrating the sine wave effect of timing changes.

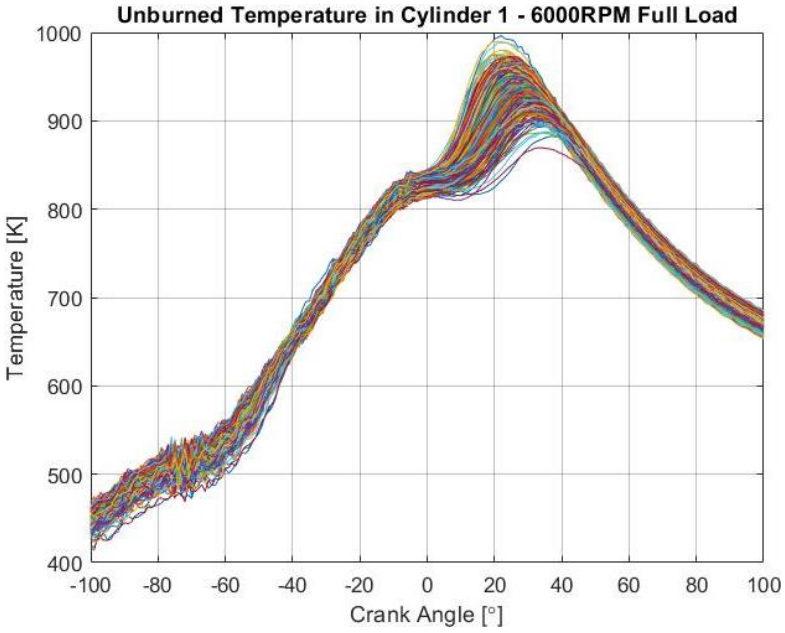

Figure 87 Unburned temperatures for cylinder 1 – 500 Cycles.

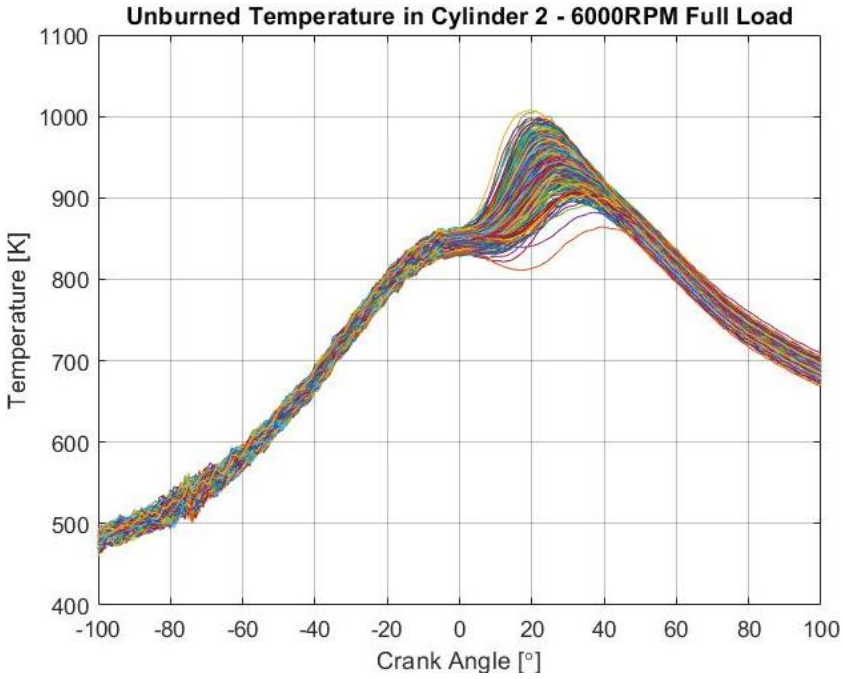

Figure 88 Unburned temperatures in cylinder 2 – 500 Cycles.

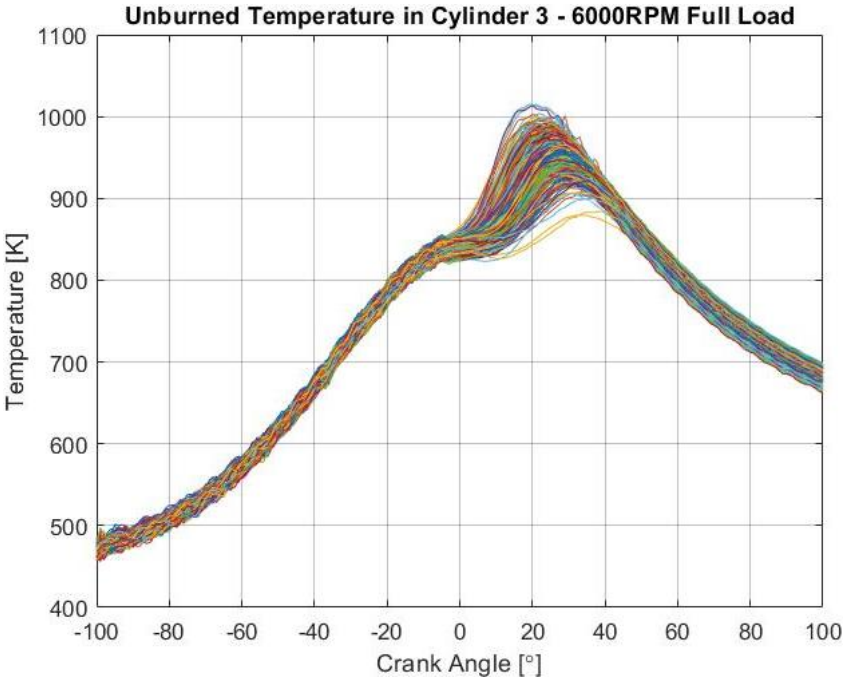

Figure 89 Unburned temperatures in cylinder 3 – 500 Cycles.

All the unburned zone temperatures modelled are within bounds and follow the expected trend regarding the positions of the peaks and the related peak pressure positions. The most interesting area highlighted here however, is the early section in cylinder 1 (-100° to -40°) and how chaotic it is in comparison to the same area for cylinder 2 and 3. Although this is not currently specifically understood, it does pose interesting as a future study and could lead to an explanation for why cylinder 1's pressure are consistently higher than the other two.

6.3. Burned Temperatures.

The burned zone temperatures again are following the expected trend of being in the vicinity of 2600K with the average peak temperatures being; 2617.4K for cylinder 1, 2562.5K for cylinder 2, and 2643.7K for cylinder 3.

The most interesting part however is occurring in cylinder 2, with the spread of peaks being around an extra 20 degrees of crank angle compared to both cylinder 1 and 3 which are spread over around 20 degrees alone and not 40. The reason for this is again not specifically known, however it could be due to physically limitations regarding heat transfer in-cylinder and having the two outer cylinders more able to efficiently control their temperature because they have an outer wall that isn't in direct "contact" with a combustion chamber. With that situation the knock occurrence in cylinder 2 could be more substantial than that of the other two and this would require a later ignition at the very least to stop/control this, meaning it burns both later and potentially for longer because of heat loss during combustion because the flame will be travelling across a larger area as the piston moves down. Again these are only hypothesis and would require further investigations to understand this, but that in-turn would require more cycle specific data that is currently not available.

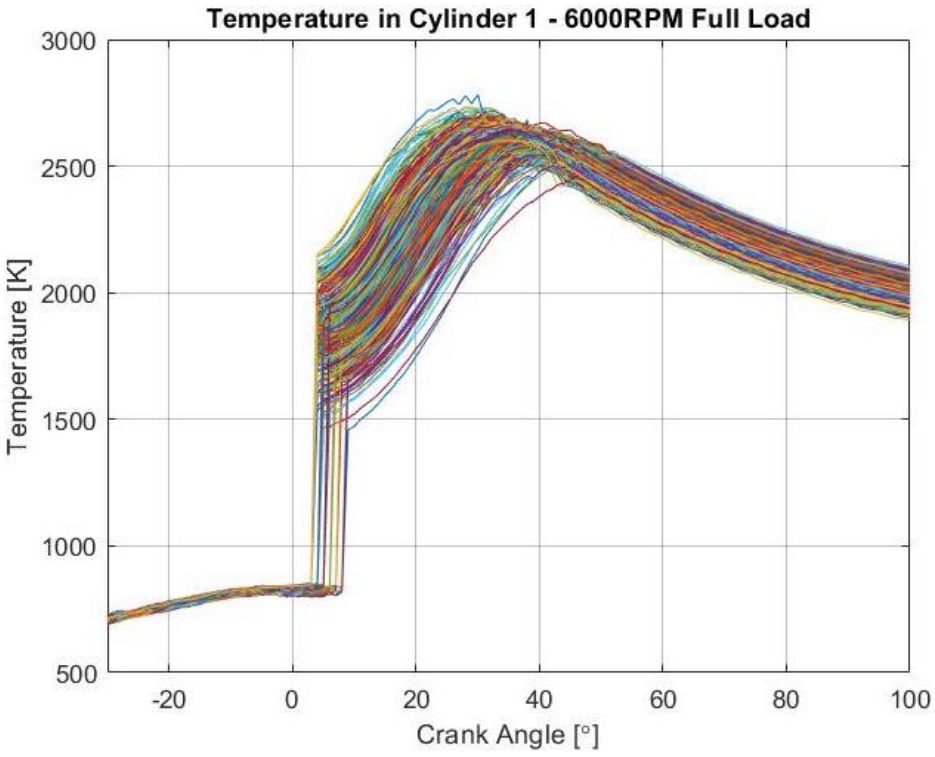

Figure 90 Burned zone temperatures in cylinder 1 - 500 cycles.

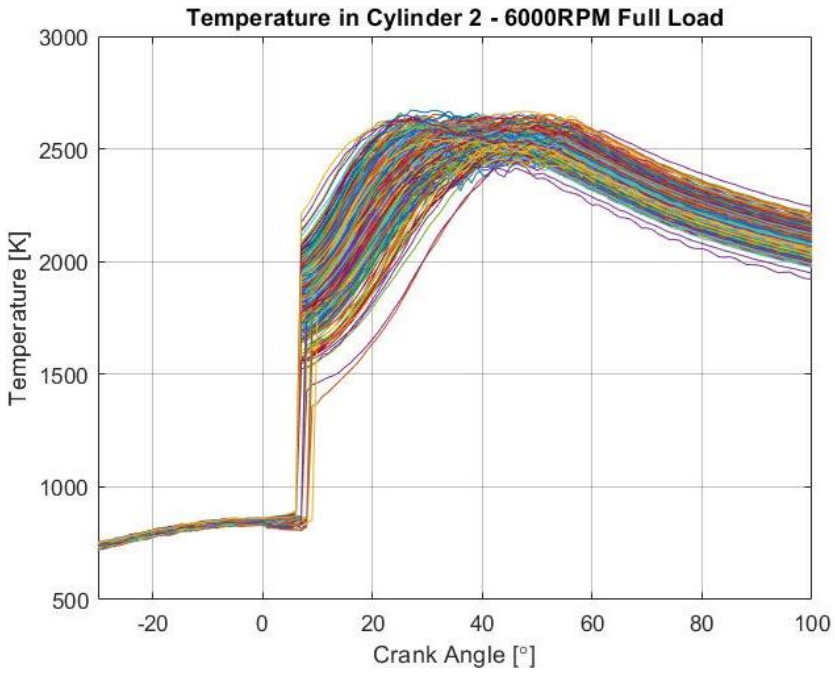

Figure 91 Burned zone temperatures in cylinder 2 - 500 cycles.

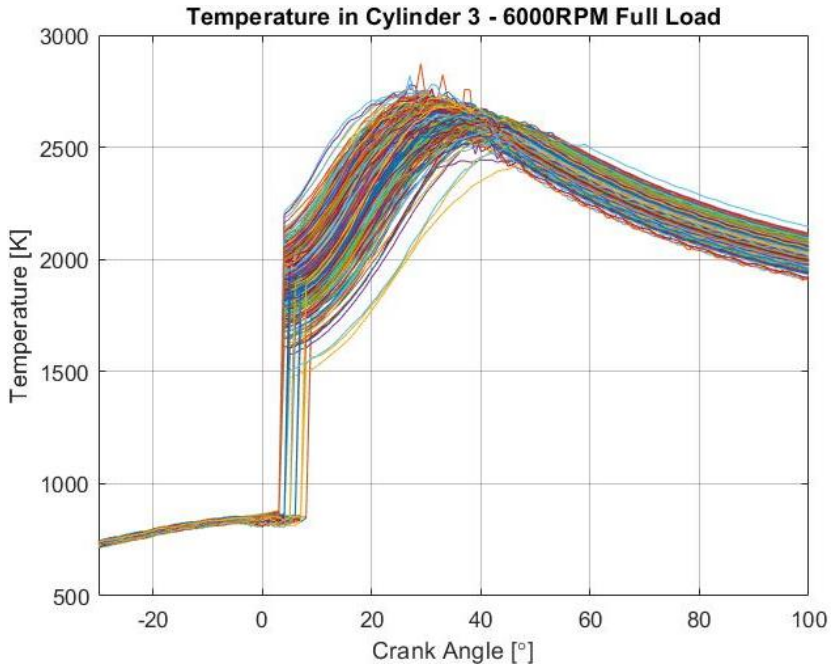

Figure 92 Burned zone temperatures in cylinder 3 - 500 cycles.

The results do raise some other interesting questions as mentioned, but these were not particularly pertinent to this study and would require full analysis to answer. However, we can see that there is no real abnormalities in these profiles across the full 500 cycles, other than in cylinder 3 there is one case that resulted in a rather jagged and unrealistic profile that caused the peak to increase unnecessarily. Due to time constraints and other various factors this cycle had to be left and wasn't assessed any further because the influence of the results of this one cycle, is arguably negligible when averaging together with the other 499 cycles.

6.4. NOx Modelling.

The NOx model for this study was done considering four situations, i.e. the individual cylinders and their contribution, and then the sum of each cylinder for their individual cycles. The reason for this was that it enables visualisation of production from each cylinder and how that could then effect the subsequent result of predicted PPM compared to the stated value from Ford which is of course averaged over 'x' number of cycles, presumably at some point in the exhaust system, which again is being assumed to be pre-catalytic converter. The results from this study provide a brilliant representation of the sensitivity to this methodology again, because there is a multitude of variation of the influencing factors but targeted around what it arguably very similar conditions, i.e. the apparent same load and engine speed, all within the same cylinder, generating vastly different results from one cycle to the next.

The results from the individual cylinders are obviously "distant" from the stated result from Ford because not only is it a single cylinder's contribution to the result, but there is also the possibility that there is residual gases that the sensor is measuring which of course again effects the accuracy. Not only are these conditions influential, but we must also consider the fact that not all cycle specific data is known and considering the variations in the original data, the is most definitely going to be cyclic variation of the required data. None the less, the results for the four 'cases' mentioned are below, each with the cyclic specific, the overall averaged and then the stated Ford NOx PPM.

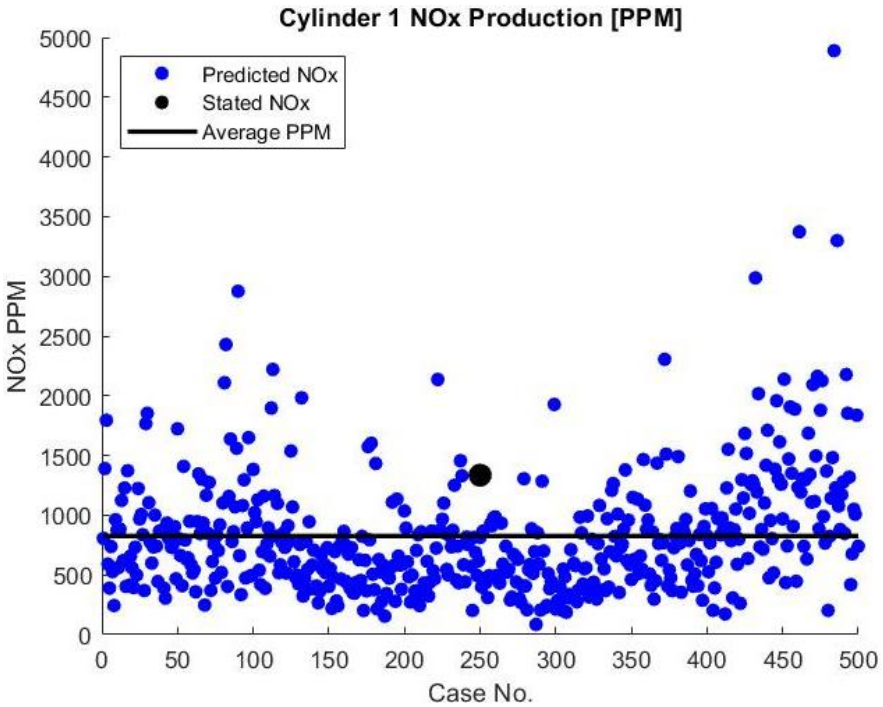

Figure 93 Predicted NOx PPM for cylinder 1 of the 500 cycles study.

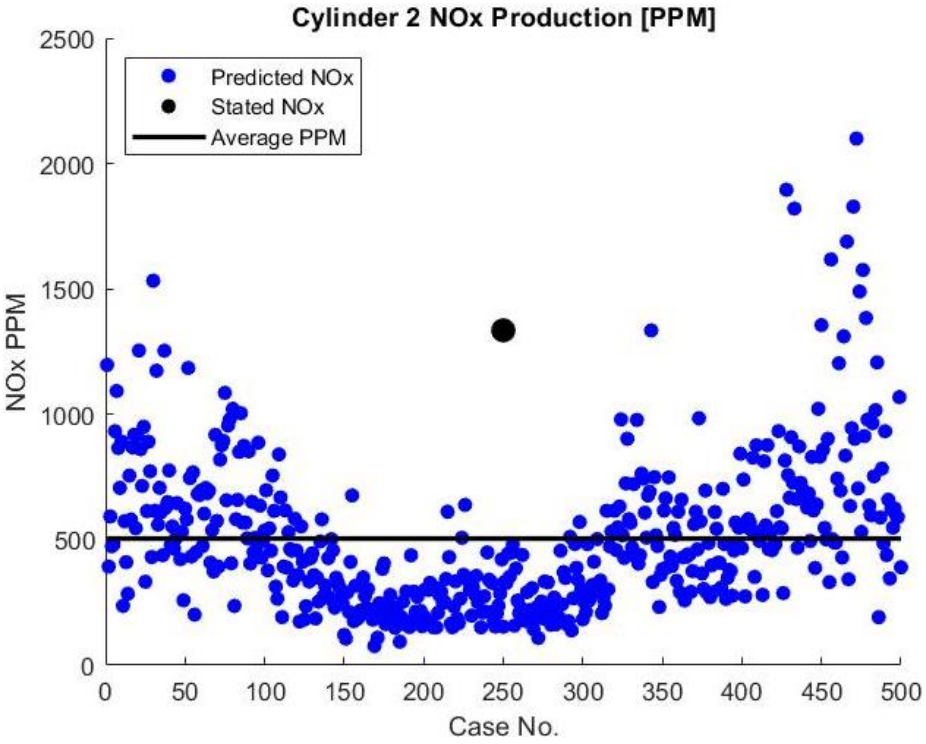

Figure 94 Predicted NOx PPM for cylinder 2 of the 500 cycles study.

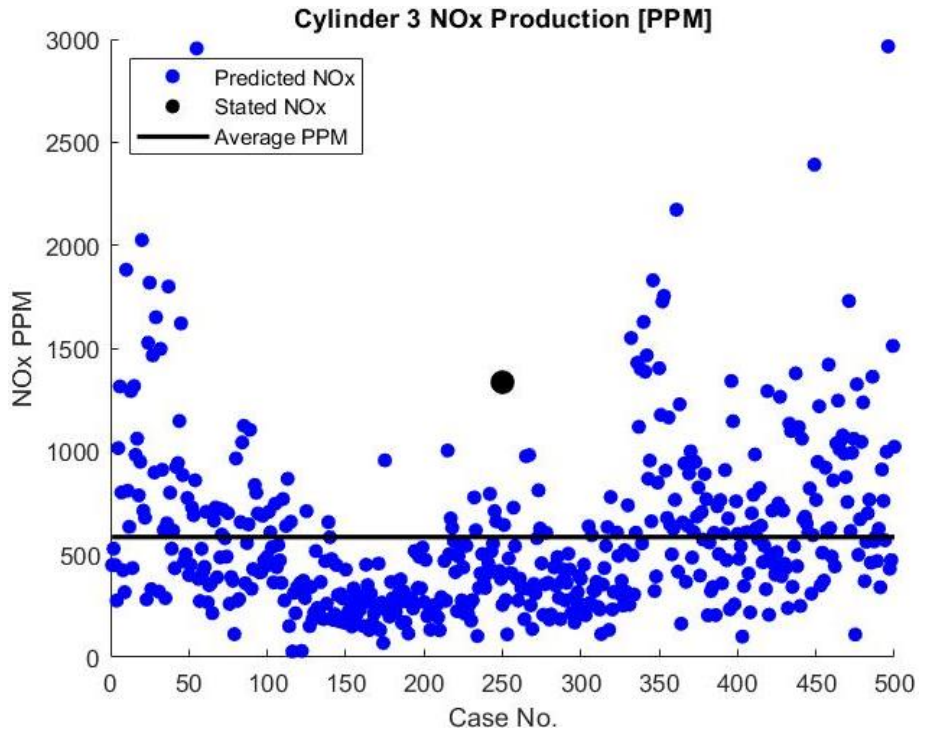

Figure 95 Predicted NOx PPM for cylinder 3 of the 500 cycles study.

The results for the individual cylinder contributions are interesting because we already know the distinct reliance on temperature to both production and modelling said production of NOx in a combustion engine. However, even though the temperatures average roughly the same, the maximum and minimum peaks are very similar, the

results are clearly quite different from each other cylinder wise. With that being said, there is definite correlation between the original pressure data and the cylinders experiencing the highest, i.e. cylinder 1, resulting in the highest production of NOx at each cycle. The temperature profiles with respect to their combustion duration, for example cylinder 2 is seen to be producing the least amount of NOx of the three, which relates to the already mentioned longer burn durations modelled for this cylinder's combustion. And then finally with cylinder 3, it is essentially in the middle of cylinder 1 and 2 regarding all aspects, i.e. maximum pressures, temperatures and burn durations which corresponds to why it predicts more than cylinder 2 and less than cylinder 1.

However we can see that on average cylinder 2 & 3 have been calculated as producing roughly the same PPM across the full 500 cycles, with theirs averages being; 504.96 and 583.56 PPM respectively. But cylinder 1 currently sits at 825.45 PPM, but this could be due to the rather randomly excessive predictions for some cycles, as well as the physical properties of the cylinder which relays well with the modelling predicting cylinder 1 to be the worst case.

As mentioned, the stated value from Ford will be an average number across a certain number of cycles that relates to the production from all three cylinders involved, hence an additional figure for the sum of NOx PPM per cycle was generated and is believed to be the more realistic representation of the models' accuracy.

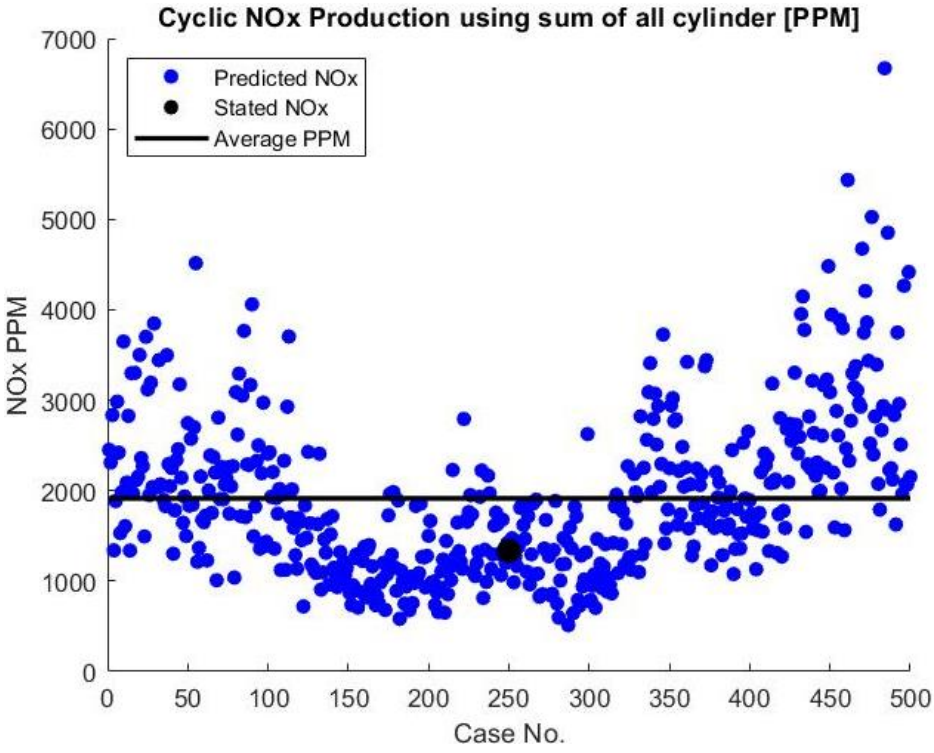

Figure 96 NOx PPM results throughout each cycle using the sum of the individual cycles, including the average across and the stated Ford measured NOx PPM.

The results from the summed predictions show that the model is overpredicting production once again, however this is necessarily a distinctive pattern of inaccuracy because the modelling methodology used throughout, does not allow for the possibility of reverse reactions, of which are almost always guaranteed. So it could be argued that a resulting average over the measured value is more accurate than if it was under predicting because future work could involve the addition of a reverse reaction model alongside the forward reactions to account for potential reductions in the total production. Although it should also be noted that reverse reactions occur less often at higher temperatures than the lower of situations like the other cases studied, this is still one potential area that would improve results.

Again it should also be remembered that the definite cyclic data is unknown, there is a multitude of assumptions throughout, and then on top of these Ford could be averaging over a different number of cycles which would change results completely. Leading to the conclusion that the model is adequate considering all factors and it clearly demonstrates not only the sensitivity of NOx modelling, but the magnitude of variation in production across a period which in the case is only 10 seconds for a combustion cycle that should in theory remain relatively consistent throughout.

7. Ricardo WAVE Modelling – 1.5L EcoBoost.

As with measured data there is always parts that are missing, and in the case of 1500cc EcoBoost, the key parts are the trapped internal exhaust gases (as well as the external), and then the different actual trapped ‘mass of air /mass of fuel’, compared to the apparent measured/PCM calculated. Of course by now these have been shown as fundamental influences of the ability to predict NOx and it was therefore thought because resource was unavailable the best solution to find an appropriate value for these elements would be a model made within Ricardo WAVE.

Ricardo WAVE was chosen because of its renowned ability to predict airflow through an internal combustion engine system on a 1-D platform. However, it should be noted now that there is a vast number of areas in the model that are highly dependent on the other and because there was/is limitations regarding the sizing, shape, and material of some system components, plus “unknown” definitions of how data was collected or specifically relates to a system, many ‘errors’ were encountered.

Therefore this will be a discussion of both how to build a model of a modern G-TDI engine, plus what the author believes to be the reasoning behind discrepancies, what the most sensitive elements are, and potential methods to solve these if provided with more information on all aspects.

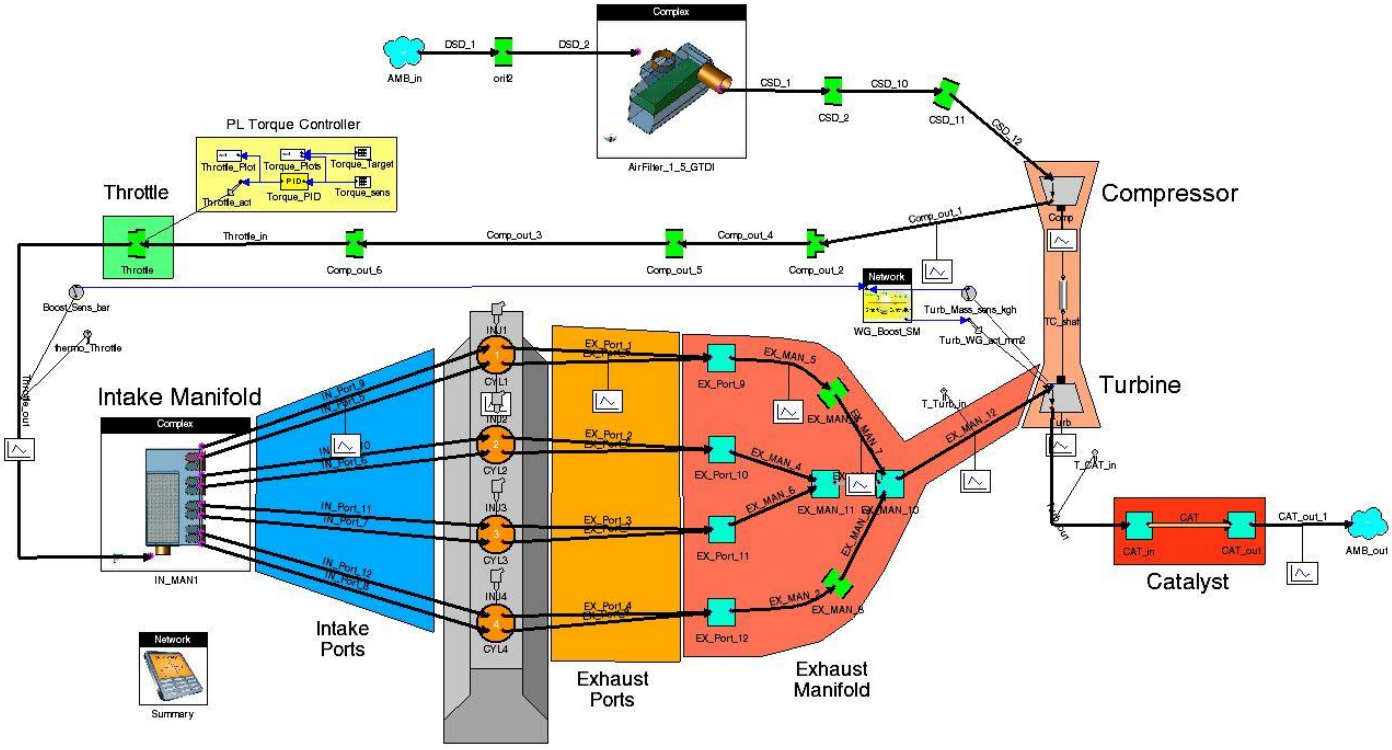

Figure 97 Ricardo WAVE model generated to represent the Ford 1500cc EcoBoost GTDI Engine.

7.1. Known Areas of Concern and Errors.

As mentioned, there is a variation of important data missing from Ford and components that weren't available to be measured, namely the full inlet and exhaust systems. Then we also must consider the fact that the exhaust manifold is integrated in the cylinder head on the 1.5L EcoBoost to help Ford control temperatures more efficiently, and this brought about extreme difficulty when trying to both measure and construct the manifold representative within WAVE. Because of this multitude of unknowns, below is a list starting from the inlet system through to the end of the exhaust of key data that was missing and would require further study to therefore enhance prediction capability of the model.

Inlet System.

Beginning right from the start of the engine's system, the complete system of piping and airbox right up to the inlet manifold itself wasn't available. The lengths and overall dimensions of the piping network pre-compressor didn't appear to have too much on an impact of the model because the pressure could be controlled by the modification of 'hole' size in the air filter that is modelled. However, it was somewhat obvious that there was issues regarding dimensions of openings and lengths because through the system, pre & post compressor, wall, and gas temperatures were excessively high initially until modification of the heat transfer coefficients used. Ricardo recommends that this coefficient doesn't exceed 10 when modelling, and it most cases where dimensions, pressure and apparent temperatures were known, this multiplier remained in the bracket of 1 – 3. Whereas most of the inlet system required a multiplier of 10 to generate the correct temperature profiles throughout the engine speeds, all at full load, and this is clearly identifying an issue regarding the sizing specifications because there isn't enough surface area/the correct thermal conductivity of materials used to dissipate the heat increase due to the compressor.

The dependence on correct mass air flow, calculated from stated volumetric flow data, dependent on pressure ratio is ultimately the downfall of the model produced and is the key focus for future work. The results are suggesting that the volume flow/air speed through the inlet system aren't high enough and decrease unrealistically as engine speed increases and given the known effectiveness of Bernoulli's equation that relates area to speed, it's thought that to remove all doubts regarding the inlet system and its effect on the control of the compressor's calculated flow rate, the dimensions of the inlet system are fundamental to achieving higher accuracy.

Inlet Manifold.

The inlet manifold itself was available for measurement and therefore reconstruction within CAD software. The intention here was to use Ricardo's 3D modeller to generate the most accurately constrained version of the rather complex inlet manifold, by loading in the SolidWorks made model and for it to "automatically" define the relevant entrance and exits. However, because the manifold is rather complex, and includes the charge-air cooler in it, the capabilities of Ricardo's additional software is thought to be too far behind that of proper CAD software's. Naturally because of this issue the more accurate model couldn't be used, and it then required the re-generation of the manifold in the rather crude and simple modelling software so that it could at least be representative of Ford's manifold. There was an unresolvable issue of sort's using the Ricardo generated manifold that is still unknown as to the specifics of it, and/or its effect on the model because across the board, pressures and temperatures where seen to be a very close match to Ford's measured MAP and charge temperature. This therefore suggests that either training/discussion with Ricardo themselves is required in the future to remove this potential error. Or the construction of an even more simplified model using ducts and orifices in the build platform itself should be used instead of the 3D modeller.

Valve Lift Profiles.

The valve lift profiles had to be calculated because only cam lift was measured by the author because of the availability of resource, time, and personal. The measured cam lift profiles resulted in potentially "wrong" results because it showed an asymmetric lift profile and it is believed, from researching Ford's use of this type of camshaft, this isn't the case, and the resulting valve lift profile should symmetrical both sides of peak lift. Because of this the generation of the valve lift profile was matched to be symmetric in MATLAB by rearranging the measured cam lift profile to show equal lift either side of their peaks.

Therefore it is recommended that again, for any future modelling, correct measurement of the direct valve lift profile should be measured instead of calculating from cam lift because it eliminates any potentially encountered error here and is an actual possibility. The reason it is recommend is because of the extreme impact on accuracy of results that was seen during the countless number of runs completed, when a slightly different valve timing and lift profile was used, making it one of Ricardo's most sensitive components.

Port Flow Coefficients.

Again considering the limitations of time and resource, new runs using the universities Flow Bench was not an option. However, during a previous investigation that the author was part of required the measurement of the flow coefficients for the inlet and exhaust ports of the cylinder head in question. Although discrepancies were seen between the peak lift's calculated between the two times, the flow coefficients were thought to be relevant and accurate. Because the model used was developed from an original Ricardo tutorial, this meant there was a comparison available with respect to flow coefficients of mid-sized GTDI engines because the tutorial models a VW 1.4L GTDI engine that has very similar characteristics to that of Ford's 1.5L. Comparing the data sets did raise questions on the validity of and accuracy of said flow coefficients because there was seemingly a large variation between them, despite being very similar engines. Because of this and the notable impact on results when using different flow coefficients, it is suggested that the flow coefficients of the 1.5L cylinder head are measured again to ensure accuracy.

Another note on the flow coefficients is also the effective area sizes of the valves themselves used when collecting the data, because again the change in results when modifying Ricardo's reference valve diameter is large enough to cause unwanted discrepancies in results.

Valve timing.

The importance of correct valve timing cannot be overstated when modelling in Ricardo WAVE.

The data provided by Ford shows the points which are presumed to be the opening of the inlet valve and the closing of exhaust valve's respective of crank angle, with 0 CA being the beginning of a new cycle and then positive values of VVT being past TDC and negative before TDC. Unfortunately the points at the inlet valve closes in unknown, as is the opening of the exhaust valve and this brought about another substantial level of dependency on the correct calculation/measurement of the valve lift profiles. Because it was again very evident in results predicted that the influence of the duration and overlap duration of the valves plays are monumental role in how the air flows through the system, along with the trapped inlet and exhaust gases in-cylinder which was arguably the whole point of this study. Therefore it can be said that there is no issue regarding the defined overlap durations because Ford provide the VVT definitions, but the definition of the other not stated locations is paramount to correctly measuring the valve lift profile.

Fuel Mass.

Ford state the fuel mass in terms of kg/h in all of their data and this can be easily modified to find the mass injected in cylinder, presumably at every event, as explained in the previous work. But the important factor in WAVE is the injector method used, i.e. active automatic adjustment to match a required fuel equivalency, or to simply inject a certain amount of mass regardless. The latter method was initially used because it was presumed the model's results wouldn't be as far from the real results as they were, specifically the MAF, and because of this it was effectively always over fuelling resulting in poor combustion/not complete, along with unjust results of in-cylinder AFR. Hence it was decided that although the model wasn't working correctly regarding MAF the injection type was changed to use an active automatic adjust of fuel mass injected to result in a target AFR pre-defined in the constants table. The idea being that if all other aspects could be corrected, this would autocorrect and the subsequent results later in the system wouldn't be restricted by incorrect combustion and at which point the injection type could be changed back to definite fuel consumption allowing us to find the correct missing values.

Combustion Control.

The method used to control the combustion profile had to be reduced to the commonly used Wiebe function, of which you have the two exponents, 'a' & 'm', that define the shape of the curve for the mass fraction burnt through the cylinder. However, Ricardo only allow you to input the value of exponent 'a', and then the duration of combustion from 10 – 90% with the additionally defined location of 50% burnt. There is an alternative method of Wiebe profile construction, but the exact inputs required to achieve the required burn profile aren't known by the author, nor could they be exclusively found/defined in the help files provided by Ricardo, hence the "SI Wiebe profile" type had to be used.

Another unfortunate factor of Ricardo's approach to MFB profiles is that you can input the specific profile to burn from, however this can only be done for a singular case, i.e. you would have to run the study at an engine speed, extract the appropriate results, change the profile for a new speed and run again. This method is clearly time consuming and to frank a bit ridiculous considering the other capabilities of the software, but with that said there does appear to be some form of scope to change the method in which Ricardo will assign its constants allowing the definition of the multiple profiles and for it to select the correct one depending on another defined variable, i.e. engine speed. How this is done could not be determined using the help files and within

the time frame available, suggesting again that either contact with Ricardo themselves to explain or training courses would be required to enable this feature.

There is a method of calculation that allows the user to find the at least ‘ballpark’ values of the exponents used for the Wiebe function, and this was followed by author to try and reduce the margin of error encountered regarding the results predicted for combustion temperatures in the model, which would then effect the results of the admittedly crude emissions production models. But these models can be correlated upon validation of the other aspects which would then allow for modifications of the calibration of the engine to be changed and assessed with respect to reducing, or increasing the emissions produced.

Pre-Turbine exhaust conditions.

Because the 1.5L engine has an integrated exhaust manifold into the cylinder head itself, allowing for further control and reduction of exhaust gas temperatures, the modelling of this is rather difficult with respect to all aspects. For example the specific dimensions through the port and manifold itself are very difficult to find and accurately model after, unless moulds are made, removed carefully and then either measured in person or scanned into a space file to be rendered in a CAD software. Because of this the dimensions used in the model could most definitely be enhanced and made to be more realistic of the real system so this is certainly an area of concern, but it is not seen as a heavily influencing aspect. Elsewise we have the wall temperatures of these sections that are being water cooled in the real world and the exact temperatures of the “sections” and the actual temperature around the manifold is unknown, although the ECT (presumed as engine coolant temperature) is stated in the tabulated data and it provides some idea of the coolant temperature at least. Then again with pressures and the location of the sensory devices Ford used to measure from, because the change in pressure from the port to the entry of the turbine is significant at times which again means correlation is not necessarily correct with respect to location.

Furthermore, although not necessarily a pre-turbine issue, but certainly post is the EBP (exhaust back pressure) and how that effect’s the flow and temperatures post-turbine. Because these will influence the modelled operation of the turbine and could cause incorrect speeds, or pressure ratios again, which links back to the compressor and essentially runs and a big loop of consistent issues which void results.

Wastegate.

In this model, the situations considered were only that of full load because it is strongly believed that the addition of external EGR isn't going to de occurring here, along with the fact it is a more stable condition of combustion, and then is also "easier" to model using the available components and calibration requirements in Ricardo WAVE.

The method used to control the simulation at full load for a GTDI engine in WAVE is to use the wastegate and allow it to fluctuate accordingly through each calculation step in a run to control the speed and pressure ratio across the turbine. This method is a considerable amount easier than using the throttle butterfly to control the system, as is the case when modelling the lower load conditions, but WAVE includes a module named "Smart Wastegate". This module is a prefabricated drop-in component that Ricardo have developed to allow easy installation and control of the wastegate during cycles, because it only requires a few components inputs, i.e. live sensor data, three defined constants of the; initial area, minimum area, and maximum. This can then be used in its defined functions to correctly operate the actuator of the wastegate to control its effective open area, ensuing the "correct" amount of air is allowed to bypass the turbine.

The wastegate has seemed to be the most important component of the model and the fact the maximum area is unknown has essentially capped the entire study. Because Ford do state the percentage of wastegate they run across the engine, but with no reference to the maximum it can't be used and unfortunately the author was not allowed access to strip and measure the turbocharger that was on-site at the university.

The dependence on the wastegate area is paramount to correctly predicting the speed of the turbine, which admittedly can be defined as constant, but with that it doesn't mean the pressure ratio across the turbine is correct. That then leads into incorrect definition of its operating point, making the compressor work incorrectly, causing poor combustion results, which of course then feeds back in the turbine resulting ultimately in a situation that is impossible to solve.

Compressor & Turbine.

The compressor data used in the model is from the excel spreadsheet titled "Ford 1.5 PPAP_Compr_overlap_2_with_intake" because although obvious, it is the data from BorgWarner that includes the pressure data when fitted with the engine's inlet system, when it is believed the other data set is just simply the compressor itself with no attachments of sorts. In that data there is two sets to choose from, however the data

under the tab of SAE2 is the correct map to be used with the single set of turbine data. We can see this when comparing the part numbers associated with the data, for example on the turbine there is two similar numbers of; 123005T1 & 123008T1, which is the closet match the number on SAE2 of the compressor map of 123006V1.

Along with another associated number on the compressor maps of '046K77AF23B82AN' which is SAE2 and '046K77AF21B68AR' which is SAE1. The significance of which is then seen on the turbine maps where both sets of data refer to the number associated with SAE2 and not SAE1. It is believed that the data for SAE1 is possibly of a smaller compressor size/housing that was initially tested and thought not to be appropriate. Or that it simply relates to different measurement times because on the data there is a figure that refers to SAE1 as VP and SAE2 as PPAP, and these acronyms are believed to stand for volume production and production part approval process respectively. And with this it suggests that the PPAP data would be more appropriate because all other data used to model would have been pre-production and still in the development stages.

Regarding the modelling itself, WAVE allows for some degree of variation in terms of the units of data input. For example the compressor requires; Speed, Mass Flow, Pressure Ratio, and Efficiency, with the speed being input as either corrected or non-dimensional (data is corrected), and then the mass flow units as either; corrected, non-dimensional, or as volume flow instead (data is corrected).

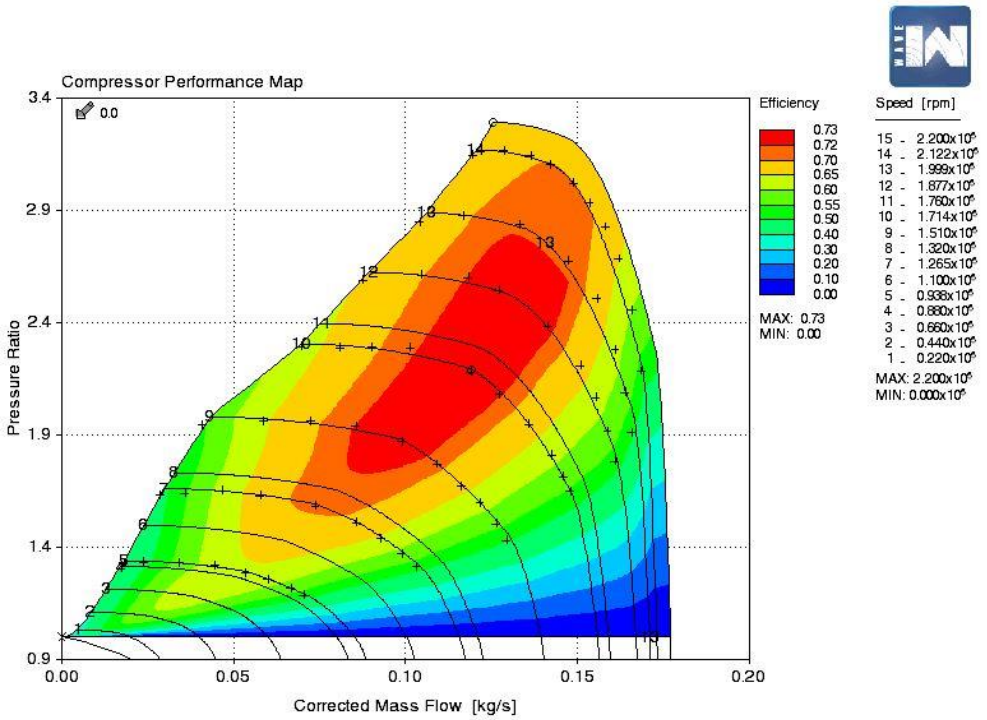

Figure 98 Compressor map generated by Ricardo WAVE using the measured data from BorgWarner.

The only real consideration here, and potential for error, is that WAVE requires inputs for; Temperature, pressure, specific heat ratio, and the gas constant, these are then used by wave to account for the 'correction' of the inputted data. And the issue is the values used by BorgWarner to correct against are not known and although presumably they are similar, or even the same, there is no guarantee. This is at least one potential reason why mass flow in the model is not correct, despite showing that the; pressure ratio, shaft speed, and temperatures around are very similar to the measured from Ford.

As for the turbine map, the inputs are the same and have the same variability regarding the units of, however the mass flow of the turbine is specified as non-dimensional. The issue here is again that the reference values used for defining the non-dimensional units of, $\frac{Kg}{s} \cdot \frac{K^2}{kPa}$, are even more important and yet remain unknown. It is presumed that there is commonality in industry and that BorgWarner will modify their results based on the typical values that Ricardo predefines when inputting this data, because the data is already in order and has the correct titles above it in the original spreadsheets. So perhaps this isn't an issue, but without speaking to either Ford or BorgWarner about it, it will remain as an unknown.

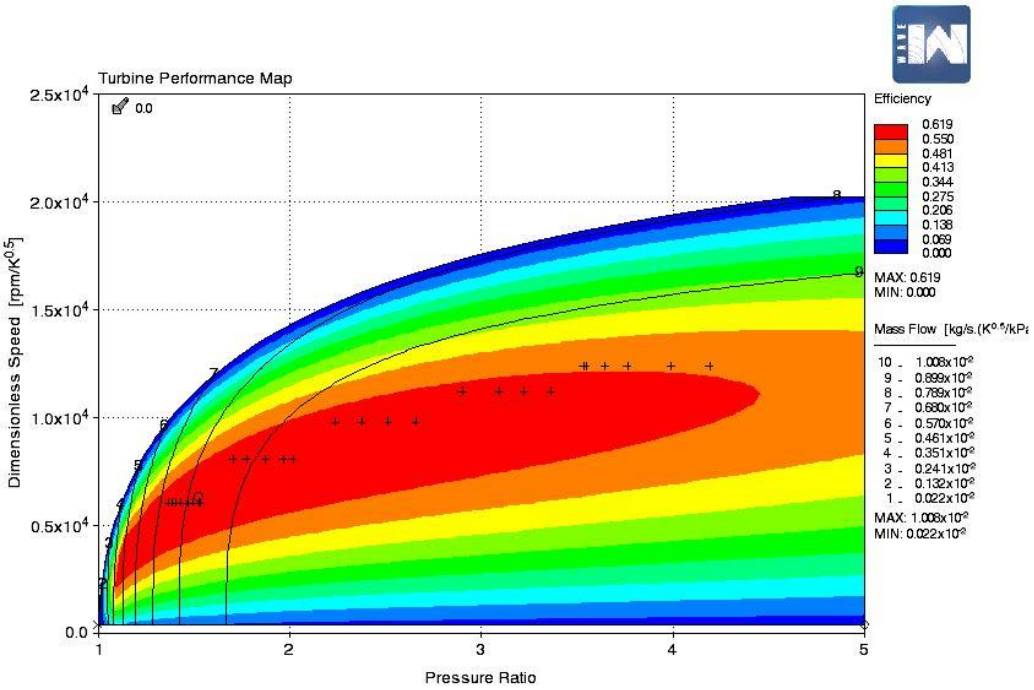

Figure 99 Turbine map generated in Ricardo WAVE using the measured data from BorgWarner.

Final note of these maps is again where the pressure ratio is in reference to across the systems, i.e. their actual physical location and then also the pressure type, either static or total, which does influence the results but is unfortunately unknown and assumed static.

7.2. Model Generation & Constants.

The model itself was generated initially using a Ricardo WAVE tutorial file that was a complete and validated simulation of a very similar VW 1.4L GTDI engine with very similar; power and fuel consumption, apparent emissions output, and technological development. The full model can be seen in figure 97 and the adjustments were made to the; inlet manifold model, the port sizes, valve lift and timing, exhaust manifold shape and junctions, then obviously the compressor and turbine maps. Elsewise any additions in the form of sensors and actuators were left because they were prominent to the engine and its control system. The only part that left in the model that relates to the tutorial is the air-box itself because the one for the 1.5L was not available, nor could any of the dimensions be found from research because the 4-cylinder version of the 1.5L EcoBoost wasn't around for long enough for data on parts to become readily available.

As mentioned, the model consists of a "smart" wastegate module that is included in WAVE and it runs like an internal network system, as if in Simulink, and is in constant "communication" with the sensor inputs of the boost pressure and mass flow into the turbine, which then through a series of functions that have limits define, will control the actuator to adjust the area of the wastegate allowing a certain mass to bypass. The controlled is constantly adjusting through the calculation steps till then point it establishes the correct area that results in the target boost pressure and/or speed.

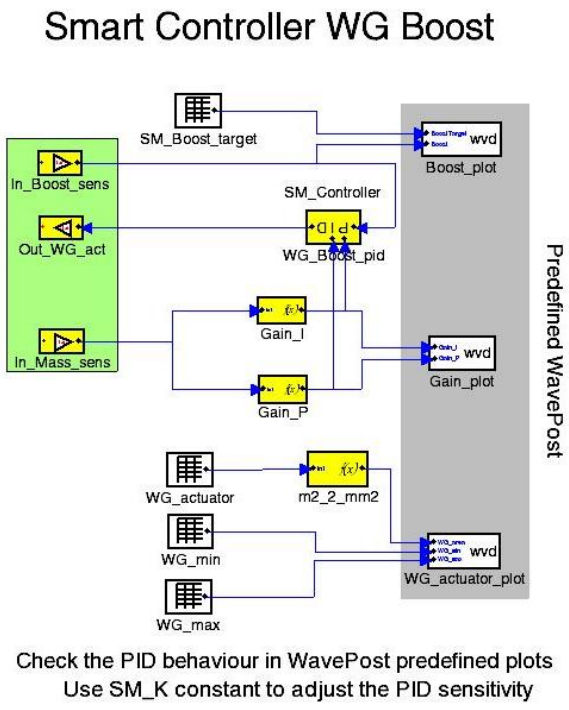

Figure 100 Smart Controller system layout for the wastegate boost controller.

The downside to this controller method is that it settles the boost to the target defined regardless of the shaft speed and mass flows, i.e. it will force the compressor into a potentially incorrect area of operation if that produces the “correct” boost pressure, and then because of that it changes the point on the map that the pressure ratio corresponds to, meaning mass flow is down. And that is fundamentally where the current model is failing, the mass air flow is very far from the measured result.

Because of the various data and measurements that are missing that have already been mentioned, it was thought that to maintain some form of realism and accuracy that the inlet manifold should be modelled using wave’s 3D add-in. Specifically because Ford have placed their charge-air cooler (CAC – Intercooler) within the manifold itself which enables them to run it as a water-cooled system and do not have to rely on air-to-air cooling like engines of old. WAVE does offer the ability to model charge coolers using their ducts and changing the type that it is, and this alone does offer a different level of accuracy in the sense you can change the “coolant” temperature (wall temperature) for each speed case. Whereas in the 3D modeller you can only define one condition and you are unable to have this vary depending on the case being studied.

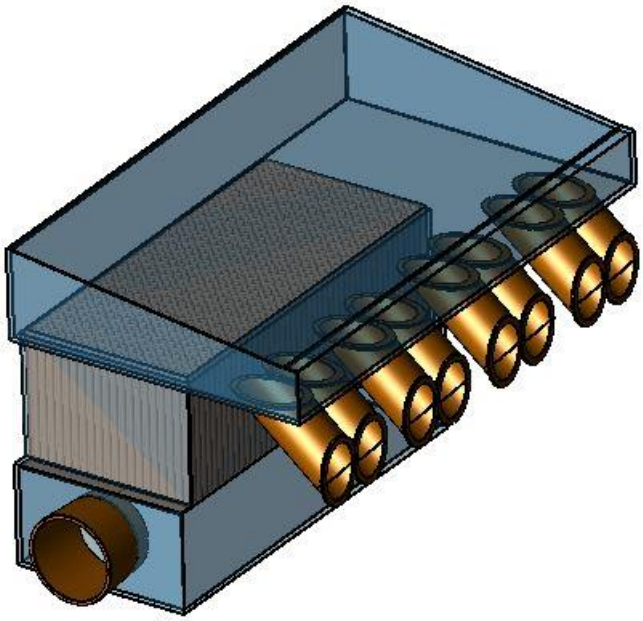

Figure 101 Intake manifold modelled in Ricardo WaveBuild 3D containing the CAC and as accurate as possible volumes either side.

This is obviously an inconvenience, but the reality is that with the other temperature modifiers throughout the rest of the system that is modelled within WAVE you can easily control the temperatures to be correct either side of the CAC and therefore reduces, or perhaps even mitigates this potential error.

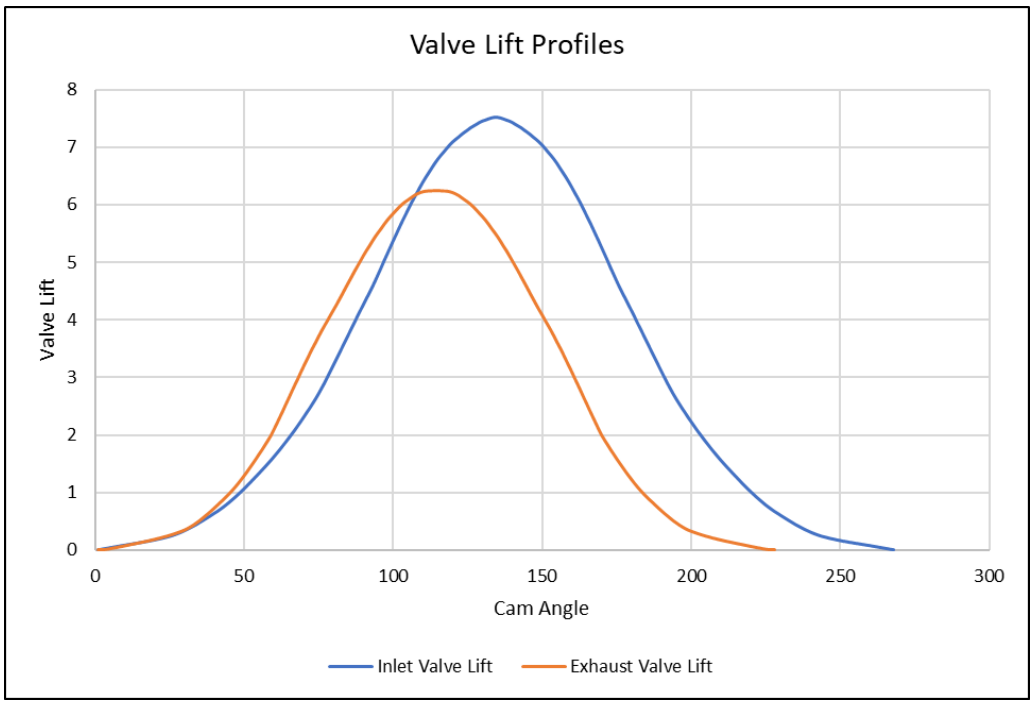

Figure 102 Valve Lift profiles calculated and used in the Ricardo model.

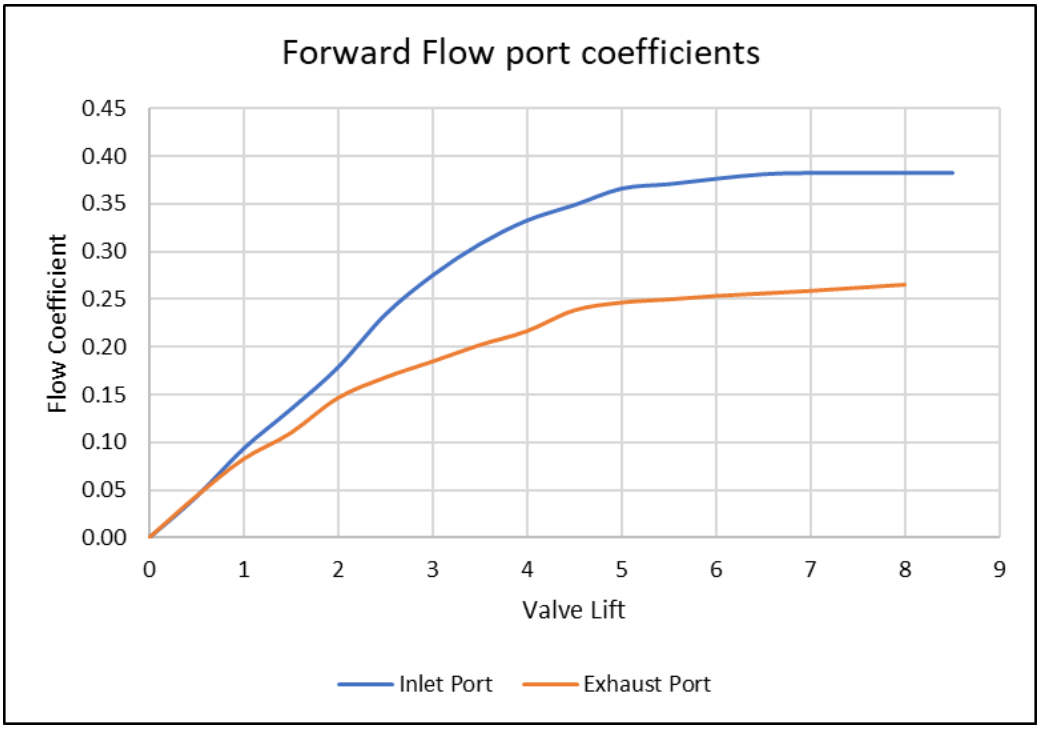

Figure 103 Port flow coefficients measured by (Englebrecht & Chapman, 2019).

Within the model it is also important to note that the forward flow coefficient was assumed to be the same as the reverse flow and this is most likely not true, however it is typical to make this assumption. Along with the fact the reverse coefficients weren't measured so they couldn't be added.

The constants used in the model were defined to help specify initial guess conditions, target values, and then controls for actuators and such in the model. The full table with the relative constant names can be seen in appendix C, but the most important will be shown here and are related to the measured data from Ford and some of the predicted results from the initial combustion model.

		6000	5500	5000	4500	4000	3500	3000	2500	2000	1500	1000
Pre - Comp P	Bar	0.9268	0.9344	0.9437	0.9615	0.9710	0.9871	0.9941	1.0033	1.0110	1.0164	1.0264
Pre - Comp T	K	293.82	293.98	296.46	299.37	300.76	297.56	293.55	294.60	295.50	297.23	297.65
Post - Comp P	Bar	1.807	1.860	1.895	1.808	1.836	1.757	1.696	1.747	1.797	1.838	1.123
Post - Comp T	K	377.6	377.8	379.6	373.6	374.9	363.4	353.6	360.0	368.3	383.5	310.6
Pre - Turb P	Bar	2.8934	2.7830	2.7406	2.4373	2.4341	2.1230	1.9276	1.9845	1.8403	1.8367	1.1600
Pre - Turb T	K	1163.46	1154.05	1154.14	1125.63	1124.28	1130.94	1141.04	1125.72	1095.39	1032.70	784.73
Post - Turb P	Bar	1.359	1.336	1.299	1.242	1.212	1.176	1.169	1.143	1.107	1.070	1.033
Post - Turb T	K	1067.1	1065.2	1056.1	1031.4	1026.8	1030.9	1065.8	1046.2	1024.4	949.5	723.6

Table 4 Compressor and Turbine pre & post pressures and temperatures initial condition constants defined by measured data.

		6000	5500	5000	4500	4000	3500	3000	2500	2000	1500	1000
Ambient P	Bar	1.0183	1.0192	1.019	1.0198	1.0206	1.0238	1.024	1.0259	1.0264	1.0261	1.0273
Ambient T	K	308.83	308.83	309.76	305.52	305.73	303.12	300.57	300.40	299.90	301.27	300.00
MAP	Bar	1.767	1.825	1.864	1.777	1.805	1.724	1.663	1.714	1.770	1.811	1.093
MAF	Kg/h	483	467	440	386	357	308	282	243	198	152	46.522
Fuel Flow	Kg/h	40.911	39.48	37.173	32.694	30.02	25.052	21.522	18.232	13.754	10.301	3.166
TW_CAC	K	322.9	322.4	322.8	313.1	313.2	311.7	310.4	310.5	310.8	311.4	308.0
TW_CAT	K	771.9	768.1	757.3	733.0	730.9	748.1	860.5	875.5	903.8	819.5	517.8
inj_dur	°CA	192.3	184.7	173.7	153.4	141.3	118.4	101.6	86.6	65.8	49.9	17.3
Inj_P	bar	146.6	146.4	146.6	146.2	144.1	145.5	143.8	145.3	144.4	143.3	127.9
inj_Temp	K	285.4	285.6	286.7	288.0	288.1	285.9	284.3	284.4	284.5	284.9	284.0
SOC	°CA	-12	-10	-9	-9	-7	-6	-6	-3	-1	5	-4
SOI	°CA	393.479	394.197	395.15	403.632	411.497	416.194	425.716	429.345	441	459.047	461.187
EBP	bar	1.347	1.331	1.299	1.236	1.212	1.160	1.186	1.162	1.133	1.099	1.064
Phi		1.282	1.282	1.282	1.282	1.274	1.220	1.171	1.120	1.018	1.000	1.003
WG Area	mm^2	405.78	406.64	407.51	395.39	406.64	395.39	390.20	415.29	434.33	463.13	535.25
IVP	°CA	329.9	330.0	329.9	329.9	319.9	317.3	315.0	315.0	315.0	315.0	315.0
EVP	°CA	130.5	130.3	130.2	129.9	136.1	141.4	155.9	156.0	156.0	156.0	146.0

Table 5 Various measured and predicted constants used to control targets and pinpoint initial guesses.

		6000	5500	5000	4500	4000	3500	3000	2500	2000	1500	1000
Wiebe A		0.757	0.720	0.689	0.765	0.677	0.821	2.231	2.203	2.623	2.490	2.148
MFB 1090	°CA	23.16	22.24	21.16	20.68	20.64	19.63	18.57	17.99	18.01	16.48	15.10
MFB 50	°CA	8.92	10.42	12.94	12.08	14.80	15.42	15.13	17.68	21.29	24.15	12.60

Table 6 Component constants that are required to control the MFB profiles in the Ricardo Wiebe model.

Final note on the construction of the model regarding the emissions production “modelled” by WAVE, there is essentially a temperature dependent multiplier than can be used to correlate back to measured data upon validation of the model. Because the model was not operating correctly this became negligible and any model enhancements regarding adjustment of timing to see the effect of something like the miller cycle is currently unavailable.

7.3. Final Model Results & Discussion.

The finalised model is the product of a countless number of runs and independent sensitivity studies to reach the final point, that yes isn't accurate in the sense of mass air flow, but regarding all other aspects of temperatures, pressures, and general operating conditions are as similar to Ford's measured data as can be. The completed model is running under the balanced speed turbo shaft and utilises the smart wastegate as a control for boost pressure, and although this can/or does lead to issues regarding the software's ability to select the correct operating point in the compressor map, it is the best available considering the specific waste gate area is unknown.

It can clearly be seen that as the engine speed increases the error percentage incurred does so to, primarily because the boost pressure increases linearly with, and the difficulties explained regarding the compressor are causing higher error percentages as MAF is meant to increase. Regardless of the inaccuracies explained, one of the key targets for this model has been meet, i.e. the potential for an increased trapped percentage of exhaust gas (internal EGR) as the engine speed increases, as shown in the 1L data. This trend has been found and confirms the hypothesis stated, however the results are excessive because the mass flow of air that is meant to enter the cylinder isn't correct, which of course means the percentage of exhaust gases trapped is unrealistically increased because there is less fresh air than there should be.

Also, unfortunately the target result for the difference between the supposed AFR compared to that of the trapped is not currently available, because the injection type is running as an active type based on the target fuel equivalency. Meaning that regardless of the air trapped in-cylinder, the injector will only model a specific amount of fuel to match the target and not simply inject the defined mass that is representative of Ford's measured mass flow. The reason for this is because the model is still being developed and given the models reliance across the board, i.e. each bit relies on the previous component and previous calculation for the next. In the future however if the MAF could be matched and the issues resolved the injector type can be changed back to input the specified mass of fuel, instead of matching the target fuel equivalency, and this will then signify the trapped AFR that could be compared to the supposed stated.

The results can be seen in the graphs below showing the comparison of the measured and modelled values of various characteristics throughout the system and the relative engine speed.

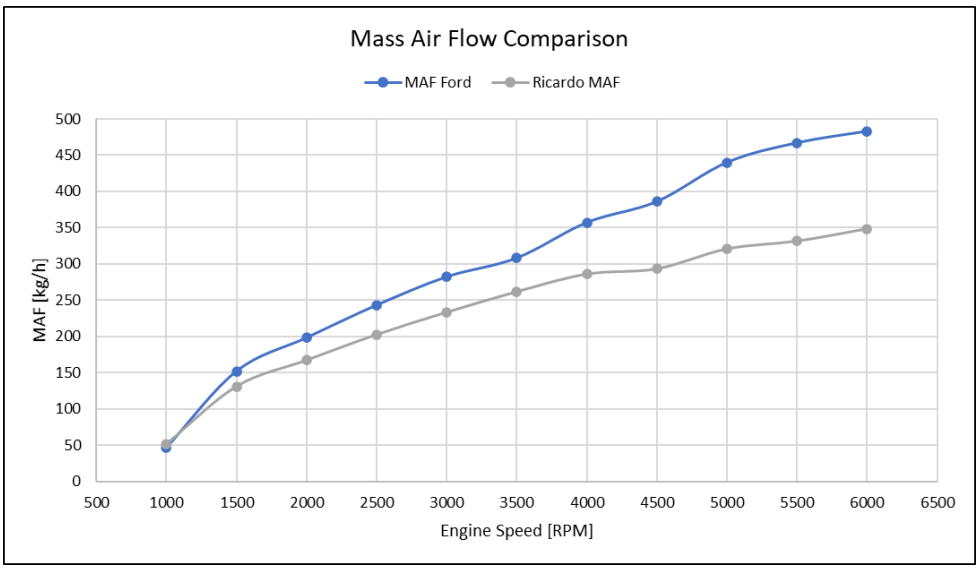

Figure 104 MAF comparison from Ford and the final Ricardo model.

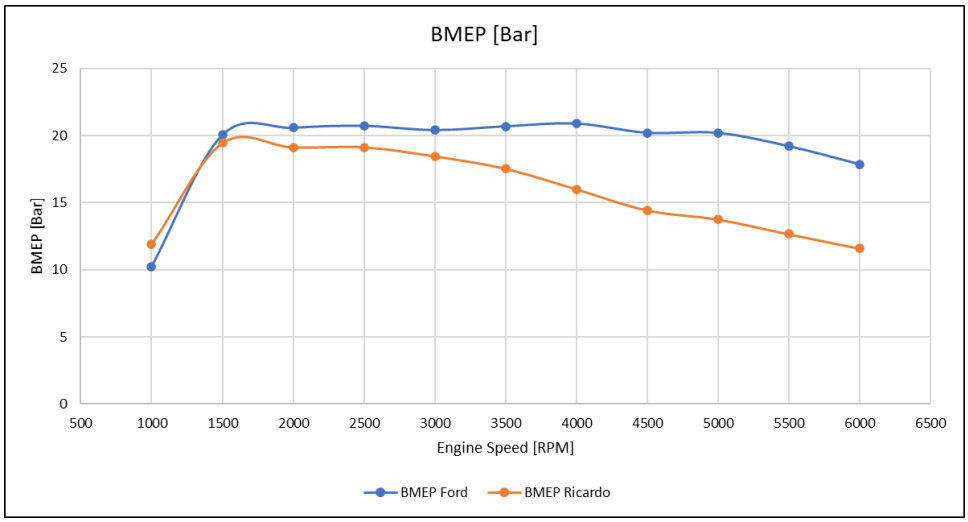

Figure 105 Comparison of BMEP from Ford and the final Ricardo model.

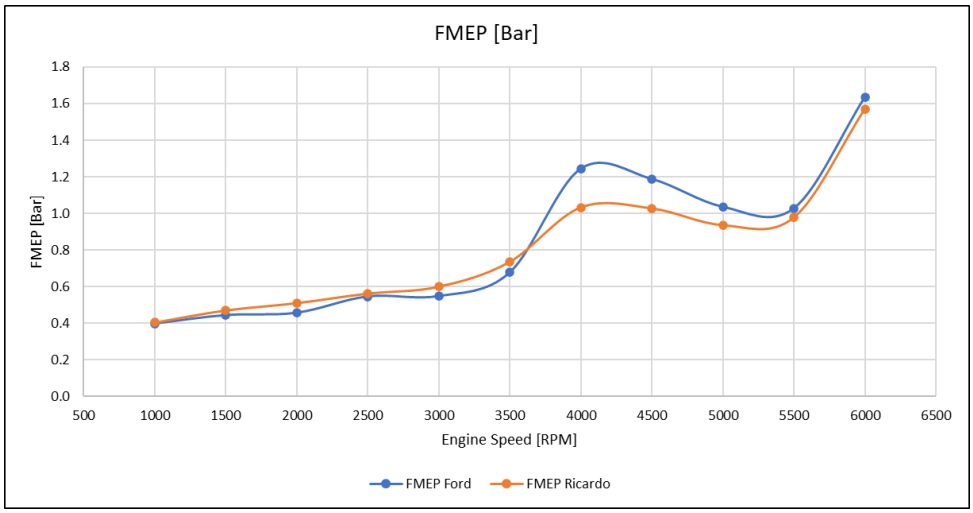

Figure 106 Comparison of FMEP from Ford and the final Ricardo model.

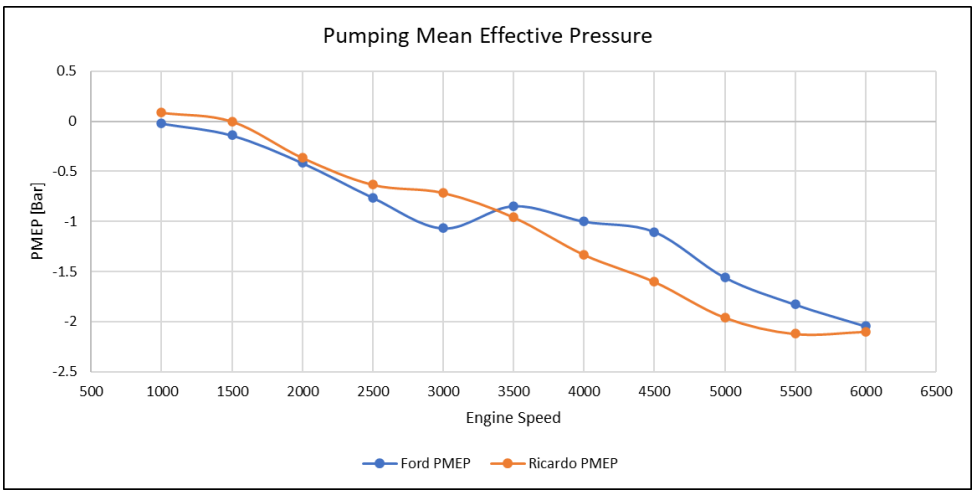

Figure 107 Comparison of PMEP from Ford and the final Ricardo model.

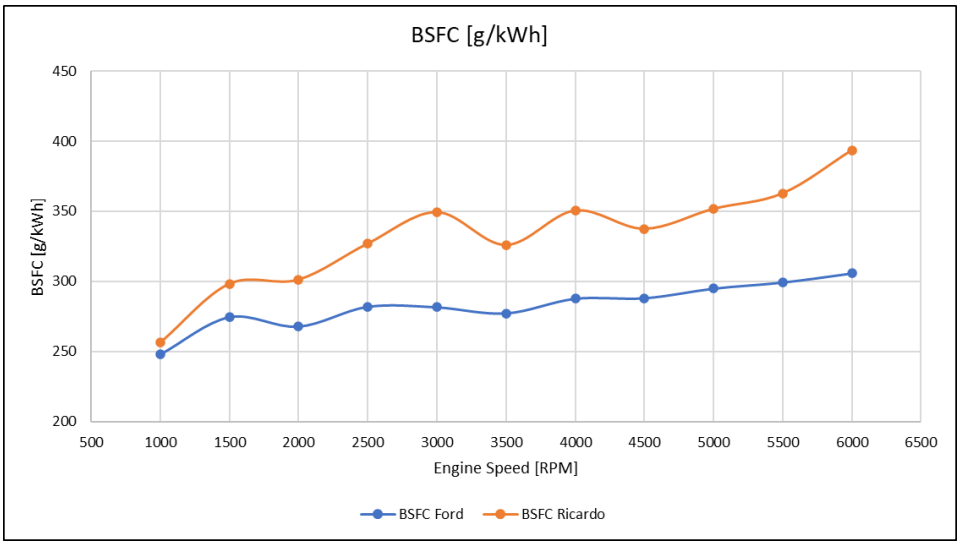

Figure 108 Brake specific fuel consumption comparison of Ford's measured and the Ricardo models predicition.

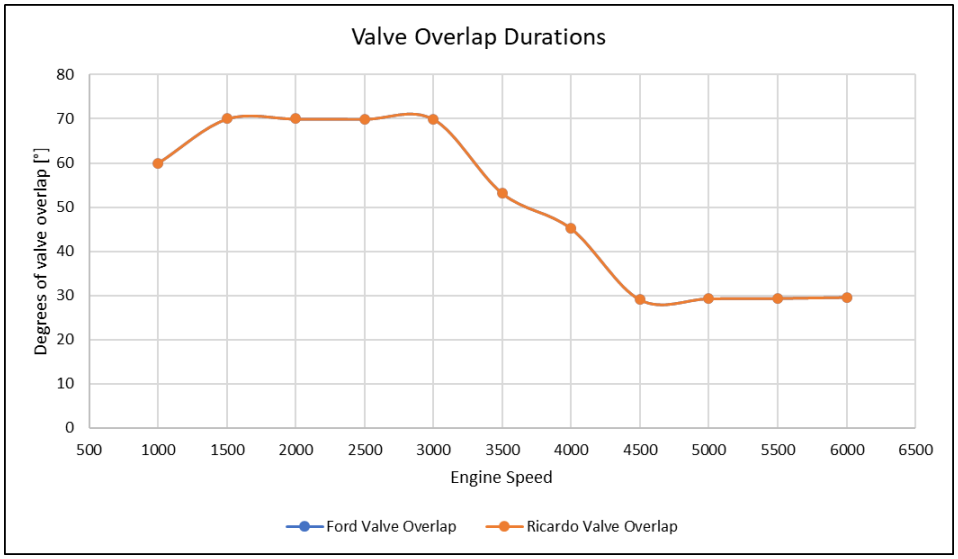

Figure 109 Evidence that the Ricardo model is correctly controlling the degrees of valve overlap.

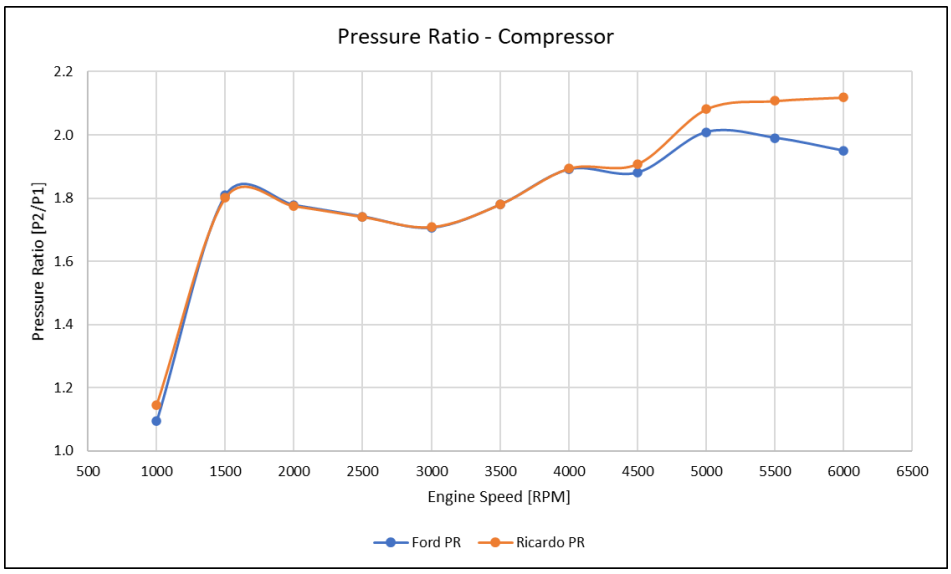

Figure 110 Pressure ratio comparison for the compressor between Ford's measured pressures either side of the compressor and Ricardo's calculated pressure ratio.

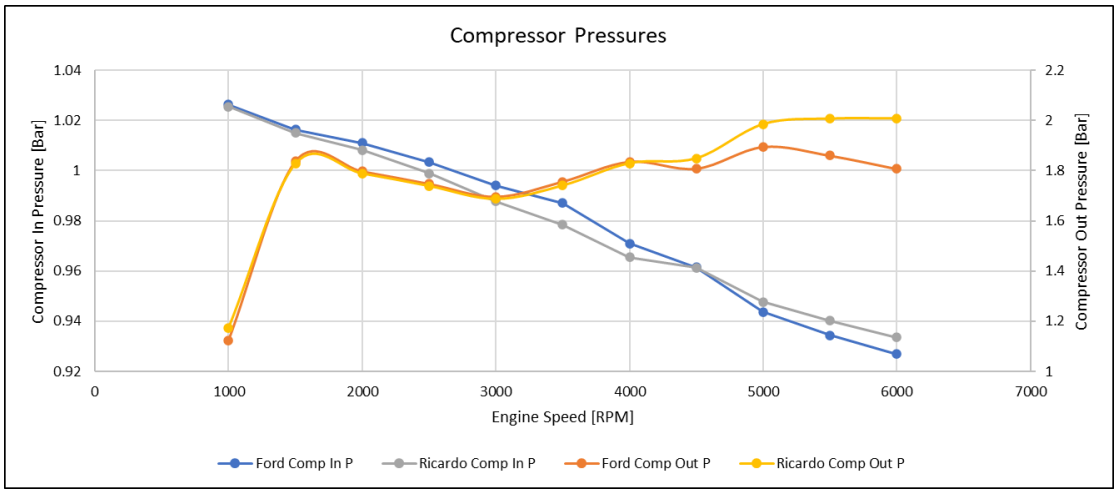

Figure 111 Comparison of the modelled and measured pressures at both the inlet and exit of the compressor.

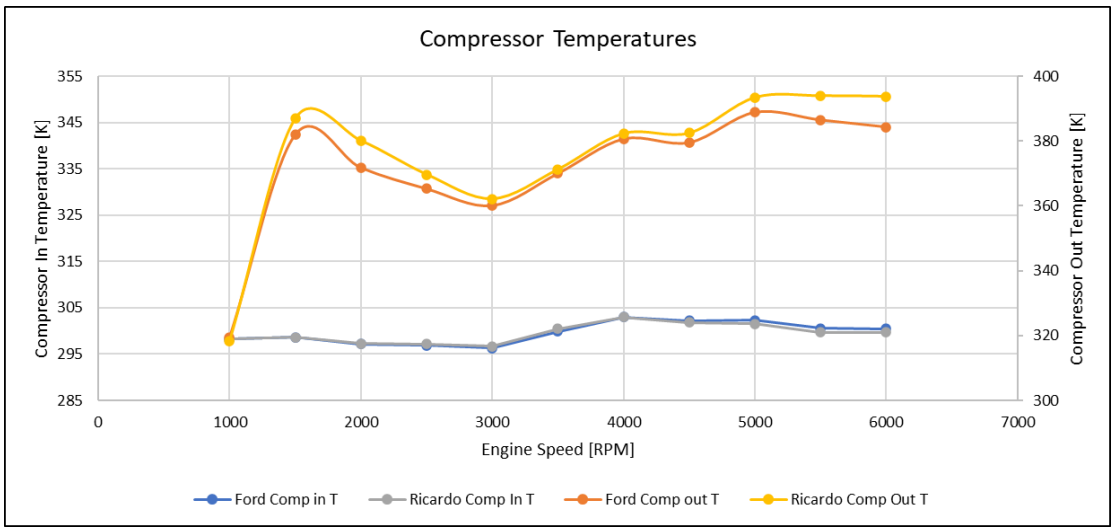

Figure 112 Comparison of the modelled and measured temperatures at both the inlet and exit of the compressor.

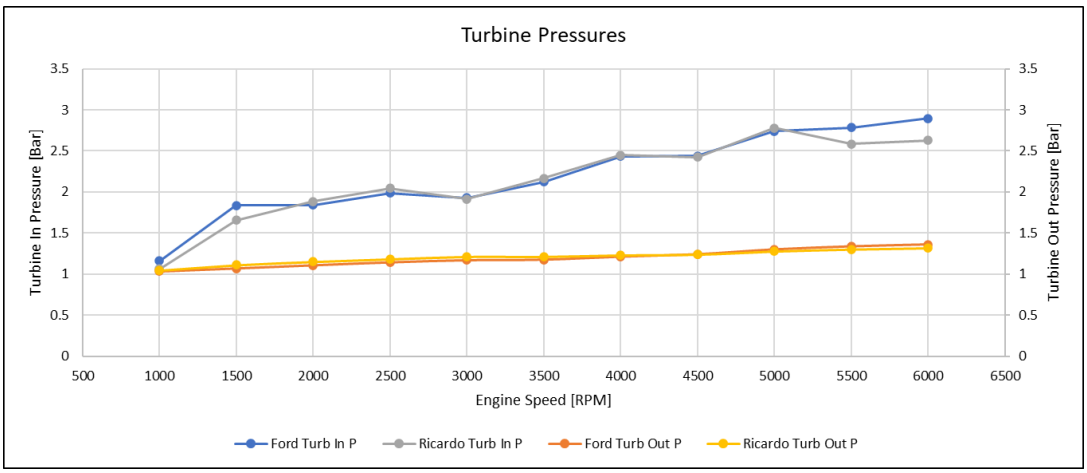

Figure 113 Comparison of the modelled and measured pressures at both the inlet and exit of the turbine.

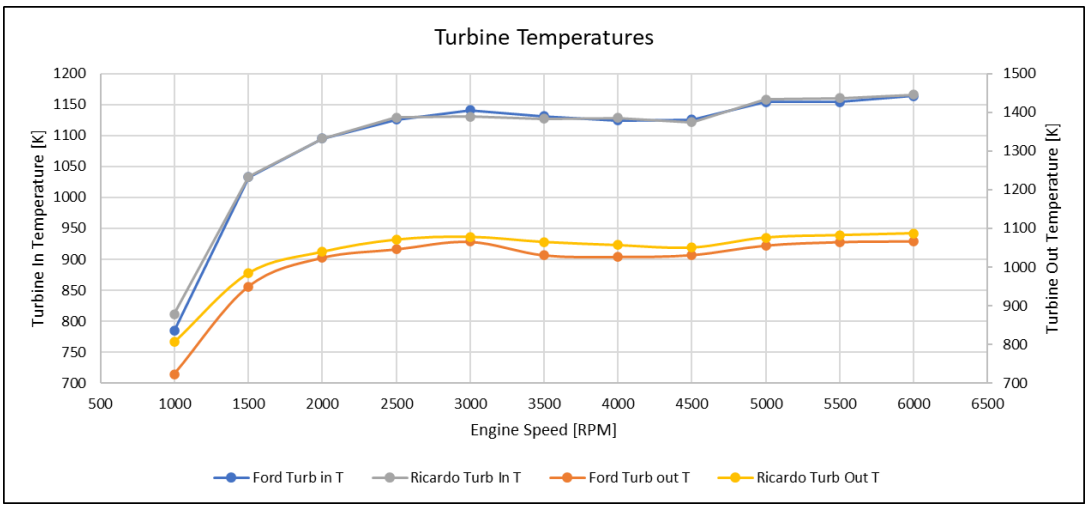

Figure 114 Comparison of the modelled and measured temperatures at both the inlet and exit of the turbine.

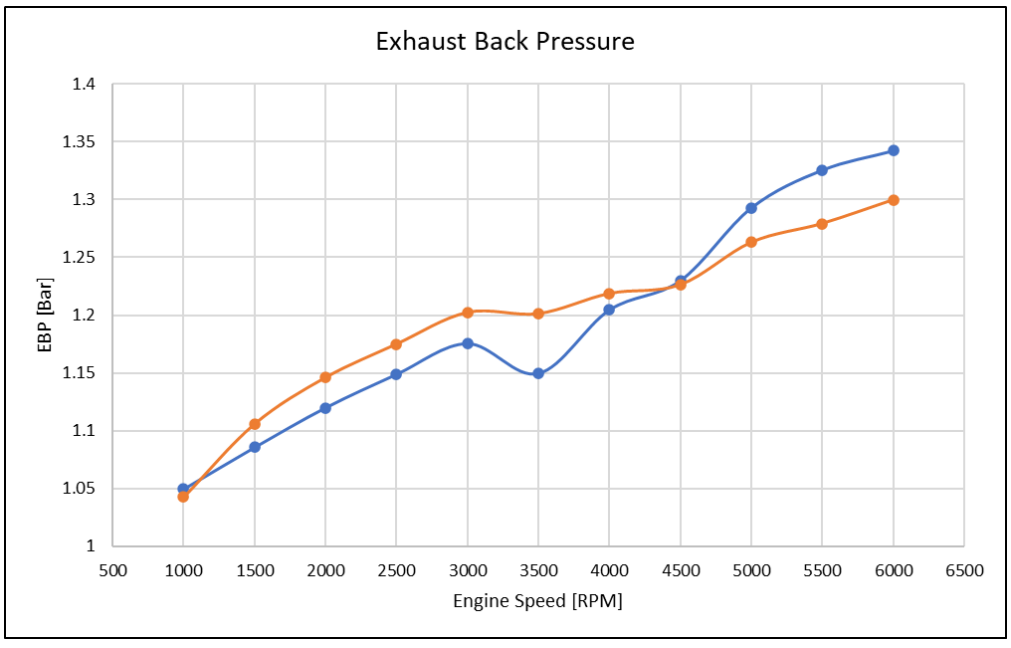

Figure 115 Exhaust back pressure comparison, assuming the location is somewhere post-catalyst.

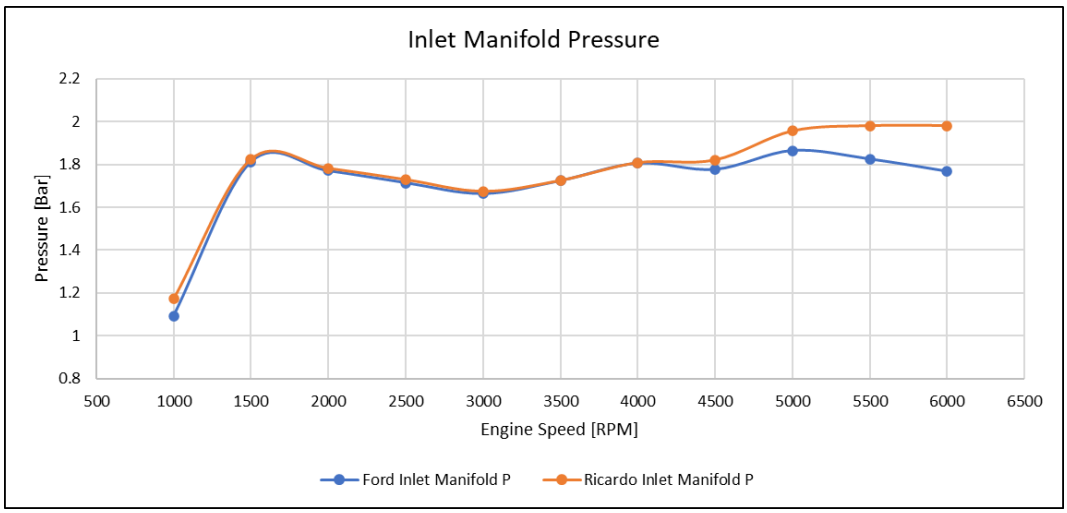

Figure 116 Manifold absolute pressure comparison.

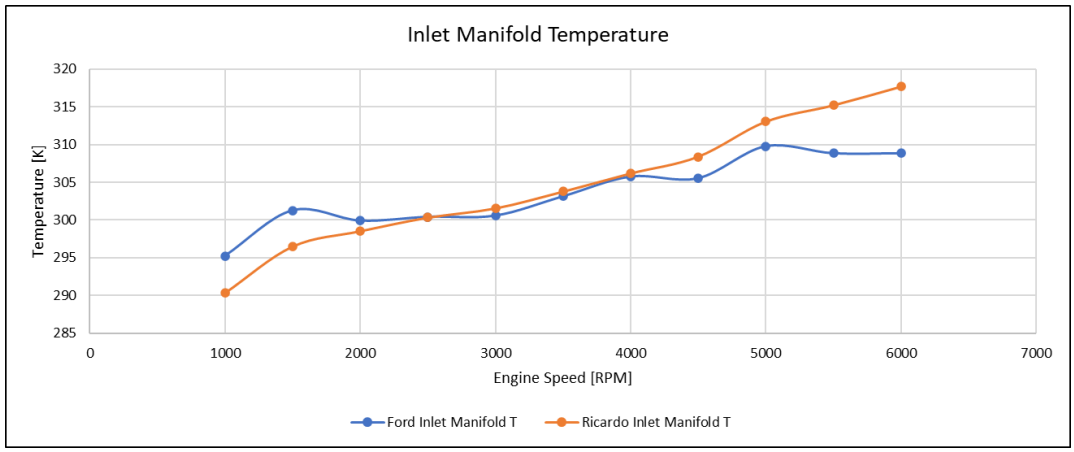

Figure 117 Inlet Manifold temperature comparison. [Highlighting the fact that the wall temperature multiplier and initial temperature can't be changed with speed].

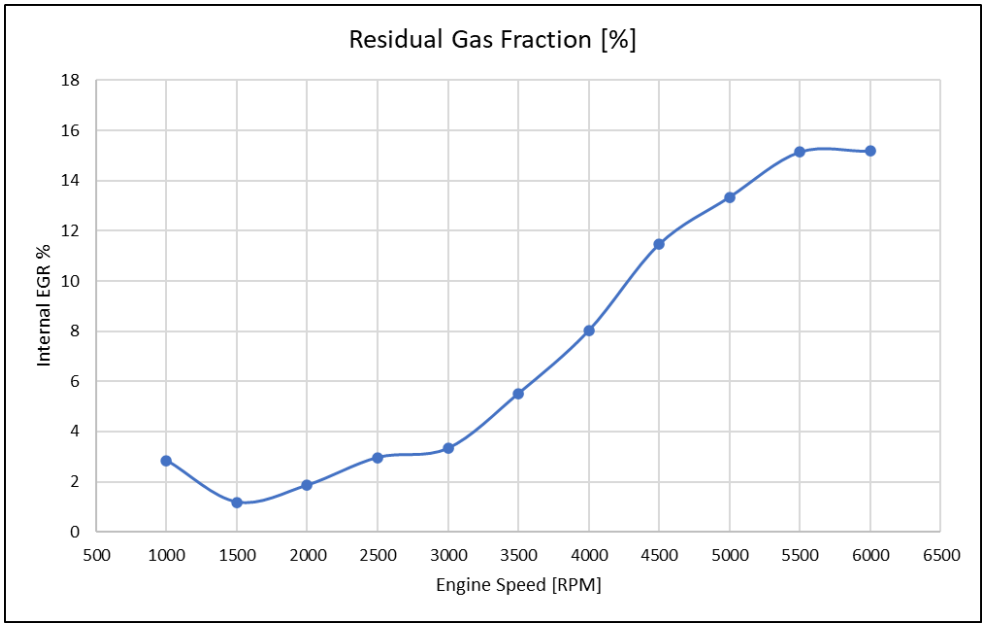

Figure 118 Apparent trapped exhaust gas percentage through engine speed as predicted by Ricardo WAVE.

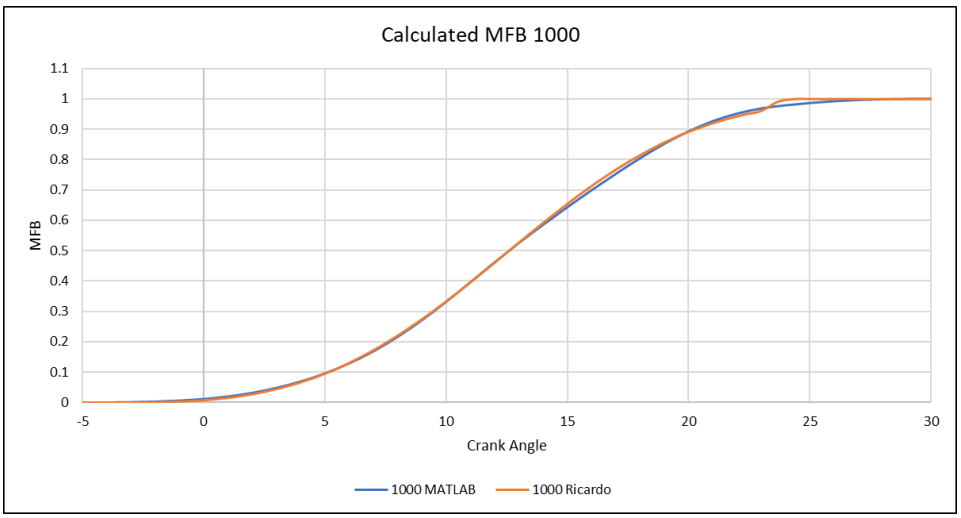

Figure 119 Predicted MFB profile comparison from Ricardo WAVE using the Wiebe function and the validated MFB modelled in MATLAB. 1000RPM and the best result of the model.

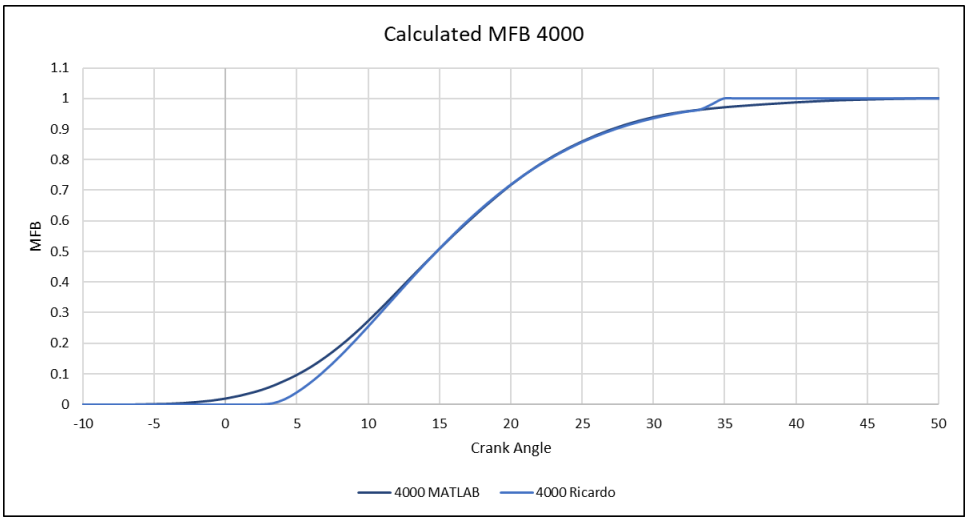

Figure 120 Predicted MFB profile comparison from Ricardo WAVE using the Wiebe function and the validated MFB modelled in MATLAB. 4000RPM and the worst result of the model.

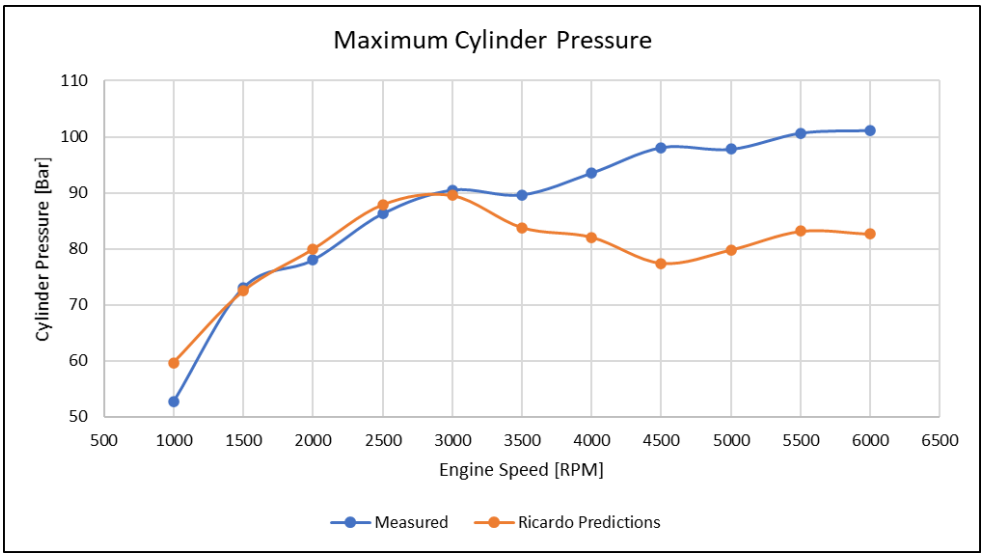

Figure 121 Maximum cylinder pressure comparison between the Ricardo model and Ford's measured data.

8. Conclusion.

Conclusions to be drawn from this investigation and the results that have been found are that two-zone combustion modelling is an adequate method to predict combustion and the characteristics associated with a measured pressure trace. Although we can see that there are limitations to it, in the sense that the predictions are typically “idealistic”, and because there is various assumptions required the mathematical solutions are currently unable to predict the rather chaotic profiles of the burning mixture exactly. Regardless of this though, the methodology used throughout the investigation to find the representative crank angles that percentages of the mass fraction burnt occur at, has been proven to produce acceptable results concerning their dependents. Along with showing strong correlation to the OEM’s stated values, and remain within the boundaries of Ford’s own investigations, which brings a level of validity to this investigation, because if a manufacturer as significant as Ford Motor Company are producing the same results as this study, we can trust the answers found.

The results of the dissociation models for each of the studies done have been able to bring a brilliant representation to how sensitive and difficult it can be to predict the production of NOx during a combustion event. For example the 1.5L was shown to be an extremely difficult engine to model throughout nearly all load and speed condition’s, with only the highest of them being able to produce results that could be regarded as worthy. Because there is no external EGR, temperatures remain high enough to suggest equilibrium throughout, and the mixture is most likely close to homogenous because of length of injection time, and all these factors added together making the chance of predicting NOx more probable because we are eliminating, or at least reducing, the dependence on assumptions and reducing sensitivities. In summary of this specific study, the model is as accurate as it can currently be without the addition of definite values for the exhaust gas percentage recirculated, in-cylinder AFR, and more accurately measured lambda.

The investigations involving the 1L EcoBoost however has provided us with vastly more accurate results all-round, bar perhaps the MFB profiles. But with no comparable data regarding the deviation in results from Ford’s measurement studies these can unfortunately neither be confirmed as in, or out of bounds leaving only one area of uncertainty. Elsewise however, the influence of the more accurate data on results of NOx production predictions is profound, leaving us with the conclusion that this investigation has been a success and would only demand further work as an opportunity to increase that accuracy and eliminate any scepticism. This accuracy is also supported by the results of the cyclic investigation because it highlights just how hectic and sporadic combustion can be in a period of only 10ms, during a situation that is supposedly remaining consistent throughout, i.e. 6000 RPM, full load. And

with the results shown we can see that the probability of predicting the average NOx production across a set of cycles is high, which also brings about the question on just how many cycle's Ford have averaged their data over for the comparable tabulated set, which is currently assumed as 500, but could be only 300. That difference change's the accuracy of results drastically and is perhaps the only further question that is left to be answered.

As for the results as a whole for the NOx dissociation modelling it has been shown that when using accurate data to inform the model itself, the predictions are well within the bounds acceptable for suggesting that further correlative studies are done to investigate the application of live modelling. However, we can see just how sensitive the models are to essentially all data used to inform; air and fuel mass, exhaust gas in-cylinder, and the exact fuel equivalency of said mixture. And with that being said, the requirement of additional sensory devices which could easily be very costly, is paramount to enabling models too predict sensibly and reliably, suggesting that this is a subject area that may need further development to enhance adaptability within industry applications.

As for the Ricardo WAVE model it became apparent rather quickly that results from the simulation were going to remain with large margin of error. However, the study was able to demonstrate that there will be a difference in the stated AFR to what is trapped in-cylinder, along with showing that as engine speed increases so does the percentage of trapped exhaust gases, meaning that internal EGR will increase with speed just like the 1L EcoBoost shows. These conclusions answer the questions proposed from the initial investigation and therefore warrant further development of the model to achieve the level of correlation required so results could then be fed back into the mathematical model of NOx prediction. The development of the model and inclusion of specific data has unfortunately reached its limit considering the time and resources available, but the areas of highest concern and those that are believed to be able to fix the current issues are; the measured waste gate area, turbocharger internal dimensions, port moulding for accurate dimensions in model, and specifics from the manufacture on measurement locations for various sensors.

Collectively this investigation has shown the difficulties & the sensitivities when modelling modern GTDI engines using mathematical relationships and computer software's. The results found have manged to both answer questions, and perhaps raise more in terms of the applications of such models in the real world, because it has been shown that a for a majority of conditions the production of nitric oxides can be predicted within an acceptable level of accuracy.

9. Further Work.

Further work recommendations regarding the two-zone modelling and NOx production predictions would be to include the possibility of reverse reactions rates within the modelling to help increase accuracy and fully develop the model. Alongside this it is recommended that additional zone modelling be investigated to gain a better understanding of temperatures across more points within the cylinder, specifically to hopefully help with the predictions at lower load and lower speeds because it is currently thought that these are stratified conditions. Because of that the predictions are vastly inaccurate for one, and that is if anything more than a negligible value is being predicted at all.

Regarding the further development again of the modelling accuracy, it is recommended that real-world testing is carried out to confirm data that is currently missing from Ford's tabulated data, along with potentially validating some of the predictions, especially for the 1.5L engine. The 1L models' results are currently showing strong correlation and accuracy, hence further measurements and validation is not necessarily needed for this engine.

Elsewise it is recommended that moulds be made and "3D – scanned" into a point cloud that can manipulated in a CAD software to establish vastly more accurate measurements and scaling of the 1.5L's inlet port, but specifically the integrated exhaust manifold. These CAD models could also then be taken further and used to develop models within a CFD combustion package, such as ANSYS Forte, to simulate emissions production more accurately with the help of chemical kinetic analysis.

Again, concerning the Ricardo WAVE model, it is highly recommended that the valve lift profile is measured directly, the flow coefficients of the cylinder head are re-assessed and validated against those currently being used, and also the waste gate and turbocharger in general be stripped and correctly measured. All this additional information is believed to be the key to advancing the current model and will help to eliminate questions that currently have no definite answer.

If this work was to be done the turbocharger could be made as a fixed shaft speed model so the positioning on the map would be definite and the boost control could then be more finely tuned by adjusting respective values around it, because to wastegate area would be known and this is thought of as the fundamental issue in the current model. With these issues solved, it also allows the investigation of the trapped AFR and internal EGR at each speed under full load and this can then be used to influence the 1.5L combustion model to again see if the results can be made as accurate as the 1L. Obviously the high external EGR% areas (low load) are still unknown, and this is why physical testing with a stock ECU would be required.

10. References.

ACEA, 2018. *ACEA Report: Vehicles in use - Europe 2018,* Brussels: European Automobile Manufacturers Association.

ACEA, 2019. *Fuel types of new passenger cars.* [Online] Available at: https://www.acea.be/statistics/tag/category/share-of-diesel-in-new-passenger-cars
[Accessed 15 March 2021].

AMWEL Enterprises, 2008. *A Brief History of CFD.* [Online] Available at: http://www.amwel.com/history.html
[Accessed 21 March 2021].

Ashdown, K., 2018. *Mazda Once Made A 2.25L V6 And It's Spectacularly Complex.* [Online] Available at: https://www.carthrottle.com/post/mazda-once-made-a-225l-v6-and-its-spectacularly-complex/
[Accessed 19 March 2021].

ATKINSON, J., 1886. *GAS ENGINE.* England, Patent No. 336,505.

Baratta, M., Chiriches, S., Goel, P. & Misul, D., 2020. CFD modelling of natural gas combustion in IC engines under different EGR dilution and H2-doping conditions. *Transportation Engineering,* Volume 2.

Blair, G. P., 1998. Combustion in Four Stroke Engines. In: *Design and Simulation of Four-Stroke Engines.* Warrendale: Society of Automotive Engineers , pp. 512 - 513.

Chen, B., Zhang, L., Han, J. & Zhang, Q., 2019. A combination of electric supercharger and Miller Cycle in a gasoline engine to improve thermal efficiency without performance degradation.. *Case Studies in Thermal Engineering,* Volume 14.

Chesterton, A., 2018. *How many cars are there in the world?.* [Online] Available at: https://www.carsguide.com.au/car-advice/how-many-cars-are-there-in-the-world-70629
[Accessed 15 March 2021].

Clifford, J., 2015. *Why does Toyota use Atkinson cycle engines?.* [Online] Available at: https://mag.toyota.co.uk/toyota-use-atkinson-cycle-engines/#:~:text=As%20the%20name%20suggests%2C%20these,piston%20stroke%20inside%20the%20cylinder.
[Accessed 18 March 2021].

Cromer, O. C. & Proctor, C. L., 1999. *Gasoline engine.* [Online] Available at: https://www.britannica.com/technology/gasoline-engine [Accessed 15 March 2021].

Daniels, C. F., 1998. *The Comparison of Mass Fraction Burned Obtained from the Cylinder Pressure Signal and Spark Plug Ion Signal,* Detroit: SAE International.

Decan, G. et al., 2018. Evaluation of wall heat flux calculation methods for CFD simulations of an internal combustion engine under both motored and HCCI operation. *Applied Energy,* Volume 232, pp. 451-461.

EEA, 2019. *Greenhouse gas emissions by aggregated sector.* [Online] Available at: https://www.eea.europa.eu/data-and-maps/daviz/ghg-emissions-by-aggregated-sector-5#tab-dashboard-02
[Accessed 15 March 2021].

EEA, 2020. *Average CO2 emissions from newly registered motor vehicles in Europe.* [Online] Available at: https://www.eea.europa.eu/data-and-maps/indicators/average-co2-emissions-from-motor-vehicles/assessment-2
[Accessed 15 March 2021].

EEA, 2020. *Greenhouse gas emissions from transport in the EU.* [Online] Available at: https://www.eea.europa.eu/data-and-maps/daviz/greenhouse-gas-emissions-from-transport#tab-chart_1
[Accessed 15 March 2021].

Englebrecht, C. P. & Chapman, A., 2019. *Ford 1.5L EcoBoost engine port flow coefficients.* Swansea: UWTSD.

European Automobile Manufacturers Association, 2018. *Vehicles in Use.* [Online] Available at: https://www.acea.be/statistics/tag/category/vehicles-in-use

Gahruei, M. H., Jeshvaghani, H. S., Vahidi, S. & Chen, L., 2013. Mathematical modeling and comparison of air standard Dual and Dual-Atkinson cycles with friction, heat transfer and variable specific-heats of the working fluid. *Applied Mathematical Modelling,* 37(12-13), pp. 7319 - 7329.

Gamma Technologies LLC, 2021. *Combustion and Emissions.* [Online] Available at: https://www.gtisoft.com/gt-suite-applications/propulsion-systems/combustion-and-emissions/
[Accessed 15 March 2021].

Gao, J. et al., 2021. Investigation into the Relationship between Super-Knock and Misfires in an SI GDI Engine. *Energies,* 14(2099).

Glassman, I. & Yetter, R. A., 2008. FREE ENERGY AND THE EQUILIBRIUM CONSTANTS. In: *Combustion Fourth Edition.* London: Elsevier Inc., pp. 9 - 16.

Gonca, G. et al., 2015. Theoretical and experimental investigation of the Miller cycle diesel engine in terms of performance and emission parameters. *Applied Energy,* Volume 138, pp. 11-20.

GOV.UK, 2020. *Government takes historic step towards net-zero with end of sale of new petrol and diesel cars by 2030.* [Online] Available at: https://www.gov.uk/government/news/government-takes-historic-step-towards-net-zero-with-end-of-sale-of-new-petrol-and-diesel-cars-by-2030
[Accessed 15 March 2021].

Guzzella, L. & Onder, C. H., 2010. *Introduction to Modeling and Control of Internal Combustion Engine Systems.* 2nd ed. Verlag Berlin Heidelberg: Springer.

Hershey, A. E. & Paton, R. F., 1933. *FLAME TEMPERATURES IN AN INTERNAL COMBUSTION ENGINE MEASURED BY SPECTRAL LINE REVERSAL,* Champaign: UNIVERSITY OF ILLINOIS ENGINEERING EXPERIMENT STATION.

Heywood, J. B., 1988. ENGINE TYPES AND THEIR OPERATION. In: A. Duffy & J. M. Moms, eds. *INTERNAL COMBUSTION ENGINE FUNDAMENTAL.* s.l.:McGraw-Hill Education, pp. 2 - 5.

Heywood, J. B., 2018. CHEMICALLY REACTING GAS MIXTURES. In: *Internal Combustion Engine Fundamentals.* s.l.:McGraw Hill Education, pp. 160-170.

Heywood, J. B., 2018. Combustion in Spark-Ignition Engines. In: *Internal Combustion Engine Fundamentals - Second Edition.* New York : McGraw Hill Education, pp. 495 - 630.

Heywood, J. B., 2018. Properties of Working Fluids. In: *Internal Combustion Engine Fundamentals - Second Edition.* New York: McGraw-Hill Education, pp. 164-220.

Heywood, J. B., 2018. TABLES OF PROPERTIES AND COMPOSITION. In: *Internal Combustion Engine Fundamentals.* New York: McGraw Hill Education, pp. 189-191.

Hou, S.-S., 2007. Comparison of performances of air standard Atkinson and Otto cycles with heat transfer considerations. *Energy Conversion and Management,* 48(5), p. 1683–1690.

Jääskeläinen, H., 2019. *Miller Cycle Engines.* [Online] Available at: https://dieselnet.com/tech/engine_miller-cycle.php#:~:text=The%20Miller%20cycle%20is%20an,emissions%20at%20high%20engine%20load.
[Accessed 18 March 2021].

Kasseris, E. P., 2011. *Knock Limits in Spark Ignited Direct Injected Engines Using Gasoline/Ethanol Blends,* Cambridge: MASSACHUSETTS INSTITUTE OF TECHNOLOGY.

Khosravi, M., Ruhland, H., Lorenz, T. & Weber, C., 2017. *Investigation into Occurrence of Megaknock and AutoIgnition in GTDI Engines,* s.l.: SAE International.

Klein, M. & Eriksson, L., 2004. A Specific Heat Ratio Model for Single-Zone Heat Release Models. *JOURNAL OF ENGINES,* 113(3), pp. 956-971.

Knop, V., Benkenida, A., Jay, S. & Colin, O., 2008. Modelling of combustion and nitrogen oxideformation in hydrogen-fuelled internalcombustion engines within a 3D CFD code. *international journal of hydrogen energy ,* Volume 33, pp. 5083-5097.

Kosmadakis, G., Rakopoulos, D. & Rakopoulos, C., 2015. Investigation of nitric oxide emission mechanismsin a SI engine fueled with methane/hydrogenblends using a research CFD code. *International Journal of Hydrogen Energy,* 40(43), pp. 15088-15104.

Li, C., Wang, Y., Jia, B. & Roskilly, A. P., 2019. Application of Miller cycle with turbocharger and ethanol to reduce NOx and particulates emissions from diesel engine – A numerical approach with model validations. *Applied Thermal Engineering,* Volume 150, pp. 904-911.

Li, T., Gao, Y., Wang, J. & Chen, Z., 2014. The Miller cycle effects on improvement of fuel economy in a highly boosted, high compression ratio, direct-injection gasoline engine: EIVC vs. LIVC. *Energy Conversion and Management,* Volume 79, pp. 59-65.

Li, Y. et al., 2021. Multi-objective energy management for Atkinson cycle engine and series hybrid electric vehicle based on evolutionary NSGA-II algorithm using digital twins. *Energy Conversion and Management,* Volume 230.

MAZDA, 2007. Mazda Develops New Naturally-Aspirated MZR 1.3L Miller-cycle Engine. *MAZDA NEWSROOM*, 31 May.

McAllister, S., Chen, J.-Y. & Fernandez-Pello, A. C., 2011. Properties of Mixtures. In: F. F. Ling, ed. *Fundamentals of Combustion Processes.* New York: Springer, pp. 15-43.

Merker, G. P., Schwarz, C., Stiesch, G. & Otto, F., 2006. *Simulation of combustion.* 1st ed. Berlin: Springer-Verlag Berlin Heidelberg.

Mikalsen, R., Wang, Y. & Roskilly, A., 2009. A comparison of Miller and Otto cycle natural gas engines for small scale CHP applications. *Applied Energy,* 86(6), pp. 922-927.

MILLER, R., 1957. *SUPERCHARGED ENGINE.* United States of America, Patent No. 2,817,322.

Müller, H., 2021. *Hildegard Müller: 2021 will decide industry's future in Germany and Europe.* Berlin: VDA.

Parry, T., 2019. *Vehicle Licensing Statistics: 2019 Quarter 3 (Jul - Sep),* London: Department For Transport.

Proctor, C. L., 2003. Internal Combustion Engines. In: R. A. Meyers, ed. *Encyclopedia of Physical Science and Technology (Third Edition).* Miami: Academic Press, pp. 33 - 44.

RAC, 2020. *Euro 1 to Euro 6 guide – find out your vehicle's emissions standard.* [Online] Available at: https://www.rac.co.uk/drive/advice/emissions/euro-emissions-standards/

Rassweiler, G. M. & Withrow, L., 1938. Motion Pictures of Engine Flames Correlated with Pressure Cards. *SAE Transactions,* Volume 33, pp. 185-204.

Sack, H., 2019. *Nikolaus Otto and the Four Stroke Engine.* [Online] Available at: http://scihi.org/nikolaus-otto-four-stroke-engine/ [Accessed 15 March 2021].

Sandman, A., 2003. Un inventor navarro: Jerónimo de Ayanz y Beaumont, 1553-1613. *Technology and Culture,* 44(2), pp. 379-381.

Tiseo, I., 2019. *Carbon dioxide emissions in the European Union 1965-2019.* [Online] Available at: https://www.statista.com/statistics/450017/co2-emissions-europe-eurasia/ [Accessed 15 March 2021].

Wang, Y. et al., 2007. An analytic study of applying Miller cycle to reduce NOxemission from petrol engine. *Applied Thermal Engineering,* 27(11-12), pp. 1779-1789.

Xiang, L., Song, E. & Ding, Y., 2018. A Two-Zone Combustion Model for Knocking Prediction of Marine Natural Gas SI Engines. *Energies,* 11(3), p. 561.

Yang, Z. et al., 2020. Investigation of high load operation of spark-ignited over-expanded Atkinson cycle engine. *Applied Energy,* Volume 262.

Zhao, J., 2017. Research and application of over-expansion cycle (Atkinson and Miller) engines – A review. *Applied Energy,* 185(Part 1), pp. 300 - 319.

11. Appendices.

Appendix A.

The following tables are the specifications for measured emissions produced by petrol passenger vehicle as the years have progressed and the regulations eventually got more stringent. The pattern of 5 years between can be seen, although with the final euro 6 emissions target starting in 2015, this was subject to a condition of vehicle release date.

The newest iteration of emissions targets are going to be put into action in the year 2021 because of the current legislation preventing it to come in earlier. These new targets are vastly more stringent than previous, joint with vastly more impacting fines and punishments for non-conformity, leading to the projected €30 Billion fines heading for the 8 major OEMs of the world.

Euro 6 Emissions		
CO	**1**	g/km
THC	**0.1**	g/km
NMHC	**0.068**	g/km
NOx	**0.06**	g/km
PM (direct injection only)	**0.005**	g/km
PN (direct injection only)	**6.0x10 ^11**	Per Km

Table 7 Euro 6 Target Emissions Standards (RAC, 2020).

Euro 5 Emissions		
CO	**1**	g/km
THC	**0.1**	g/km
NMHC	**0.068**	g/km
NOx	**0.06**	g/km
PM (direct injection only)	**0.005**	g/km

Table 8 Euro 5 Target Emissions Standards (RAC, 2020).

Euro 4 Emissions		
CO	**1**	g/km
THC	**0.1**	g/km
NOx	**0.08**	g/km

Table 10 Euro 4 Target Emissions Standards (RAC, 2020).

Euro 3 Emissions		
CO	**2.3**	g/km
THC	**0.2**	g/km
NOx	**0.15**	g/km

Table 9 Euro 3 Target Emissions Standards (RAC, 2020).

Euro 2 Emissions		
CO	**2.2**	g/km
HC + NOx	**0.5**	g/km

Table 11 Euro 2 Target Emissions Standards (RAC, 2020).

Euro 1 Emissions		
CO	**2.72**	g/km
HC + NOx	**0.97**	g/km

Table 12 Euro 1 Target Emissions Standards (RAC, 2020).

Appendix B.

Heywood coefficients for approximation of the specific heat capacity at constant pressure of certain fuels and chemical species.

		T Range, K	a_{j1}	a_{j2}	a_{j3}	a_{j4}	a_{j5}	a_{j6}	a_{j7}
1	CO_2 H	'1000-5000'	4.4608	0.0030982	-1.2393e-06	2.2741e-10	-1.5526e-14	-48961	-0.98636
2	CO_2 L	'300-1000'	2.4008	0.0087351	-6.6071e-06	2.0022e-09	6.3274e-16	-48378	9.6951
3	H_2O H	'1000-5000'	2.7168	0.0029451	-8.0224e-07	1.0227e-10	-4.8472e-15	-29906	3.227
4	H_2O L	'300-1000'	4.0701	-0.0011084	4.1521e-06	-2.9637e-09	8.0702e-13	-30280	-0.3227
5	CO H	'1000-5000'	2.9841	0.0014891	-5.79e-07	1.0365e-10	-6.9354e-15	-14245	6.3479
6	CO L	'300-1000'	3.7101	-0.0016191	3.6924e-06	-2.032e-09	2.3953e-13	-14356	2.9555
7	H_2 H	'1000-5000'	3.1002	0.00051119	5.2644e-08	-3.491e-11	3.6945e-15	-877.38	-1.9629
8	H_2 L	'300-1000'	3.0574	0.0026765	-5.8099e-06	5.521e-09	-1.8123e-12	-988.9	-2.2997
9	O_2 H	'1000-5000'	3.622	0.00073618	-1.9652e-07	3.6202e-11	-2.8946e-15	-1202	3.6151
10	O_2 L	'300-1000'	3.6256	-0.0018782	7.0555e-06	-6.7635e-09	2.1556e-12	-1047.5	4.3053
11	N_2 H	'1000-5000'	2.8963	0.0015155	-5.7235e-07	9.9807e-11	-6.5224e-15	-905.86	6.1615
12	N_2 L	'300-1000'	3.6748	-0.0012082	2.324e-06	-6.3218e-10	-2.2577e-13	-1061.2	2.358
13	OH	'1000-5000'	2.9106	0.00095932	-1.9442e-07	1.3757e-11	1.4225e-16	3935.4	5.4423
14	NO	'1000-5000'	3.189	0.0013382	-5.2899e-07	9.5919e-11	-6.4848e-15	9828.3	6.7458
15	O	'1000-5000'	2.5421	-2.7551e-05	-3.1028e-09	4.5511e-12	-4.3681e-16	29231	4.9203
16	H	'1000-5000'	2.5	0	0	0	0	25472	-0.46012

Where the secondary letter in the species name, ‘L’ & ‘H’, are relation to the higher and lower temperature ranges.

As for the fuels, they are in the following table.

		Formula	Molecular Weight	$(A/F)_s$	$(F/A)_s$	Af_1	Af_2	Af_3	Af_4	Af_5	Af_6	Af_8
1	Methane	'CH_4'	16.04	17.23	0.058	-0.29149	26.327	-10.61	1.5656	0.16573	-18.331	4.3
2	Propane	'C_3H_8'	44.1	15.67	0.0638	-1.4867	74.339	-39.065	8.0534	0.01219	-27.313	8.852
3	Hexane	'C_6H_{14}'	86.18	15.24	0.0656	-20.777	210.48	-164.13	52.832	0.56635	-39.836	15.611
4	Iso-Octane	'C_8H_{18}'	114.2	15.14	0.0661	-0.55313	181.62	-97.787	20.402	-0.03095	-60.751	20.232
5	Methanol	'CH_3OH'	32.04	6.47	0.1546	-2.7059	44.168	-27.501	7.2193	0.20299	-48.288	5.3375
6	Ethonal	'C_2H_5OH'	46.07	9	0.1111	6.99	39.741	-11.926	0	0	-60.214	7.6135
7	Gasoline N	'$C_{8.26}H_{15.5}$'	114.8	14.64	0.0683	-24.078	256.63	-201.68	64.75	0.5808	-27.562	17.792
8	Gasoline O	'$C_{7.76}$ $H_{13.1}$'	106.4	14.37	0.0696	-22.501	227.99	-177.26	56.048	0.4845	-17.578	16.235
9	Diesel	'$C_{10.8}H_{18.7}$'	148.6	14.4	0.0694	-9.1063	246.97	-143.74	32.329	0.0518	-50.128	2.514

Appendix C.

		Run	Run	Run	Run	Run	Run	Run	Run	Run	Run	Run
Speed	RPM	6000	5500	5000	4500	4000	3500	3000	2500	2000	1500	1000
ncyc		50	50	50	50	50	50	50	50	50	50	50
SM_K		1.3	1.3	1.3	1.3	1.3	1.3	1.3	1.7	1.5	1.5	1.5
ACF	Bar	0.5	0.22	0.23	0.25	0.28	0.2	0.16	0.16	0.16	0.16	0.16
Aft_Turb_P	Bar	1.35911	1.33604	1.29935	1.24213	1.21199	1.17588	1.16876	1.14325	1.10741	1.06973	1.03296
Aft_Turb_T	K	1067.104	1065.151	1056.133	1031.41	1026.764	1030.917	1065.834	1046.151	1024.355	949.499	723.633
Aft_Turb_Tw	K	600	600	600	600	600	600	600	600	600	600	600
BCF		0.005	0.003	0.003	0.004	0.004	0.003	0.003	0.003	0.003	0.003	0.003
BDUR		40	40	40	40	40	40	40	40	40	40	40
By_OA	mm^2	63	45	20	10	0	0	0	0	0	0	0
C_Den	1/in^2	100	500	500	500	500	500	500	500	500	500	500
C_WT	mm	0.254	1.5	1.5	1.5	1.5	1.5	1.5	1.5	1.5	1.5	1.5
CCF	Pa*min/m	270	230	230	250	270	210	150	150	150	150	150
Comp_eff		1	1	1	1	1	1	1	1	1	1	1
Comp_In_P	bar	0.92684	0.93444	0.94366	0.96148	0.97097	0.9871	0.99411	1.00334	1.01097	1.01636	1.02638
Comp_In_T	K	293.82	293.979	296.456	299.365	300.761	297.56	293.546	294.599	295.495	297.231	297.652
Comp_ME		1	1	1	1	1	1	1	1	1	1	1
Comp_Out_P	bar	1.80673	1.8599	1.89514	1.8082	1.83586	1.75653	1.69607	1.74737	1.79705	1.83803	1.1233
Comp_Out_T	K	377.607	377.822	379.565	373.581	374.863	363.362	353.632	360.042	368.261	383.5	310.557
Comp_REA	mm	5	30	30	30	30	30	30	30	30	30	30
CompDM		1	1	1	1	1	1	1	1	1	1	1
CRPM	rpm	167382.4	165814.4	163313.1	153005.3	150713.5	140355.6	133046.2	134330.9	136565.3	139815.3	52329.85
D_exh	mm	40	40	40	40	40	40	40	40	40	40	40
dxe	mm	100	100	100	100	100	100	100	100	100	100	100
dxi	mm	50	50	50	50	50	50	50	50	50	50	50
EBP	bar	1.34726	1.33146	1.2986	1.23643	1.21192	1.1602	1.18628	1.16156	1.13312	1.0985	1.06353
EV_DM		1.1	1	1	1	1	1	1	1	1	1	1
EV_LM		1.1	1	1	1	1	1	1	1	1	1	1
EVP		130.487	130.314	130.212	129.884	136.065	141.408	155.911	155.982	155.998	156.003	145.999
EWH_T		1.6	1.25	1.3	1.4	1.55	1.55	2.2	2.4	3	3.2	5
Exh_P	bar	3.774666	3.60647	3.46349	3.116704	3.183773	2.99266	3.314162	3.114057	2.882047	2.634246	2.4
FAR		0.088113	0.088113	0.088113	0.088113	0.087552	0.083815	0.080478	0.076964	0.069988	0.068729	0.068935
FUEL	kg/hr	40.911	39.48	37.173	32.694	30.02	25.052	21.522	18.232	13.754	10.301	3.166
gaind_Torque_PID		0	0	0	0	0	0	0	0	0	0	0
htc_exhPort		1	1.5	1.5	1.8	1.8	2.2	1.05	1.2	2.2	2.8	2.1
HTC_Head		10000	9000	8000	7000	6000	5000	4000	3000	2000	1500	1000
htc_intPort		5	5	5	6	7.5	6	6	5.7	9	9	10
HTC_Liner		3500	3050	2800	2500	2500	2500	2500	1500	1200	1000	800
HTC_Piston		1400	1400	1400	1400	1400	1400	1400	1400	1300	1100	900
HTVC		0.9	0.9	0.9	0.9	0.9	0.9	1	1	1	1	1
HTVO		0.9	0.95	1	1.05	1.1	1.2	1.2	1.2	1.3	1.4	1.6
IAT	K	308.828	308.828	309.755	305.523	305.732	303.121	300.568	300.404	299.904	301.265	300
In_Port_Height	mm	32.3	32.3	32.3	32.3	32.3	32.3	32.3	32.3	32.3	32.3	32.3
In_Port_Width	mm	26.4	26.4	26.4	26.4	26.4	26.4	26.4	26.4	26.4	26.4	26.4
IN_WTM		10	10	10	10	10	10	10	10	10	10	10
inj_dur	deg	192.2697	184.7141	173.6854	153.4206	141.3331	118.4077	101.6324	86.61179	65.81434	49.87512	17.27269
Inj_P	bar	146.5672	146.3927	146.576	146.1552	144.0524	145.4804	143.7985	145.3234	144.4417	143.2887	127.8519
inj_rate		1	1	1	1	1	1	1	1	1	1	1
inj_Temp	K	285.405	285.579	286.72	288.039	288.131	285.91	284.274	284.411	284.49	284.871	284
Inlet_WHT		1.1	1.1	1.1	1.1	1.1	1.1	1.1	1.1	1.1	1.1	1.1
InMan_T	K	308.828	308.828	309.755	305.523	305.732	303.121	300.568	300.404	299.904	301.265	295.217
INP_WTM		8	7.5	8	8.5	8.5	6.3	7.5	7.5	7.8	8.7	9
Inport_L	mm	90	90	90	90	90	90	90	90	90	90	90
IVP		329.906	329.96	329.927	329.86	319.936	317.281	315.012	315.02	315.001	315.001	314.998
Load		FL	FL	FL	FL	FL	FL	FL	FL	FL	FL	FL
MAF_M		1.308319	1.302077	1.309792	1.239436	1.220906	1.159453	1.177698	1.155191	1.154802	1.149154	0.893472
MAP	bar	1.7674	1.82467	1.86449	1.77654	1.80499	1.72385	1.66331	1.71396	1.77	1.81138	1.09281
MFB10		-0.62518	0.892659	3.40632	2.871112	5.090126	6.008407	6.231099	8.759826	12.22313	15.87599	5.109099
MFB1090	deg	23.162	22.239	21.164	20.682	20.64	19.634	18.573	17.987	18.01	16.479	15.10499
MFB50	deg	8.920028	10.41801	12.93616	12.07913	14.80053	15.41815	15.13043	17.67592	21.28922	24.14585	12.59617
MFB90		23.79013	23.86345	25.79837	24.84659	27.13251	27.09951	25.6887	27.3856	30.83983	32.57202	20.21409
p_amb	bar	1.0183	1.0192	1.019	1.0198	1.0206	1.0238	1.024	1.0259	1.0264	1.0261	1.0273
p_exh_man	bar	3.774666	3.60647	3.46349	3.116704	3.183773	2.99266	3.314162	3.114057	2.882047	2.634246	2.4
p_exh_port	bar	3.774666	3.60647	3.46349	3.116704	3.183773	2.99266	3.314162	3.114057	2.882047	2.634246	2.4
Phi		1.282051	1.282051	1.282051	1.282051	1.273885	1.219512	1.17096	1.119821	1.01833	1	1.003009
PID_Torque_I		0	0	0	0	0	0	0	0	0	0	0
PID_Torque_P		0	0	0	0	0	0	0	0	0	0	0
Pre_Turb_P	bar	2.89343	2.783	2.74062	2.43727	2.43406	2.12298	1.92757	1.98453	1.84031	1.83667	1.15998
Pre_Turb_T	K	1163.461	1154.052	1154.14	1125.633	1124.284	1130.937	1141.037	1125.716	1095.39	1032.698	784.731
QCF	*min^2/m	0.1	0.08	0.085	0.085	0.095	0.06	0.05	0.05	0.05	0.05	0.05
SI1_BDUR_1	deg	0	15.8009	14.1714	16.8416	17.1924	18.0676	15.8679	15.2743	15.9093	15.0922	10.4793
SI1_mf_1		1	1	1	1	1	1	1	1	1	1	1
SI1_MFB50_1	deg	0	11.9622	13.6089	17.8238	22.4518	26.4081	27.5713	26.3741	25.4466	26.9615	15.4937
SI1_thb50_1	deg	9.7825	12.3125	13.47375	19.09625	23.15125	26.78375	27.73875	26.5475	25.69125	27.44375	15.2975
SI1_wexp_1		1.6	2.37996	2.27569	2.52467	2.79674	2.49703	3.13631	3.39956	3.68211	3.178	3.67331
SM_boost_target		1.80673	1.8599	1.89514	1.8082	1.83586	1.75653	1.69607	1.74737	1.79705	1.83803	1.02638
SM_WG_initial		{WG_A}	{WG_A}	{WG_A}	{WG_A}	{WG_A}	{WG_A}	{WG_A}	{WG_A}	{WG_A}	{WG_A}	{WG_A}
SM_WG_max		1017.876	1017.876	1017.876	1017.876	1017.876	1017.876	1017.876	1017.876	1017.876	1017.876	1017.876
SM_WG_min		0	0	0	0	0	0	0	0	0	0	0
SOC	deg	-12	-10	-9	-9	-7	-6	-6	-3	-1	5	-4
SOI	deg	393.479	394.197	395.15	403.632	411.497	416.194	425.716	429.345	441	459.047	461.187
T_amb	K	296.123	296.27	296.997	298.642	297.7	297.964	294.472	295.282	295.8	293.4	292.64
t_exh_man	K	1304	1304.884	1318.746	1313.2	1371.696	1341.398	1176.053	1196.282	1229.118	1092.426	1000
t_exh_port	K	1800	1904.884	1918.746	1913.2	1971.696	1941.398	1776.053	1796.282	1829.118	1692.426	1580
Target_Torque		213	229	240.799	240.877	249.096	246.609	243.266	247.025	245.267	234.89	122.032
Throttle_D	mm	54	54	54	54	54	54	54	54	54	54	54
Turb_Out_P	bar	1.35911	1.33604	1.29935	1.24213	1.21199	1.17588	1.16876	1.14325	1.10741	1.06973	1.03296
Turb_Out_T	K	1067.104	1065.151	1056.133	1031.41	1026.764	1030.917	1065.834	1046.151	1024.355	949.499	723.633
TW_CAC	K	322.9028	322.4422	322.7922	313.1228	313.1661	311.6561	310.3872	310.4506	310.835	311.4244	308
TW_CAT	K	771.92	768.069	757.322	733.034	730.905	748.11	860.547	875.503	903.765	819.465	517.809
WG_A	mm^2	477.3839	478.4017	479.4196	465.1693	478.4017	465.1693	459.0621	488.5805	510.9738	712.5132	823.4617
Wiebe_A		0.757321	0.719511	0.688927	0.765321	0.676864	0.82108	2.231352	2.202509	2.622902	2.489547	2.147857
wt_exh_man	K	364.6456	364.5939	364.5894	364.4817	364.3511	363.7811	364.3511	364.0544	363.485	362.6422	360
wt_exh_port	K	364.6456	364.5939	364.5894	364.4817	364.3511	363.7811	364.3511	364.0544	363.485	362.6422	360

Table 13 Full table of all constants used in the Ricardo model.